NTIA Report 82-114

HF Ground Wave Propagation over Forested and Built-up Terrain

D.A. Hill

U.S. DEPARTMENT OF COMMERCE
Malcolm Baldrige, Secretary

Bernard J. Wunder, Jr., Assistant Secretary
for Communications and Information

December 1982

TABLE OF CONTENTS

	Page
LIST OF FIGURES	iv
LIST OF TABLES	vi
ABSTRACT	1
1. INTRODUCTION	1
2. UNIFORM SLAB MODEL	2
2.1 Integral Representation	3
2.2 The Lateral Wave	6
2.3 Normalized Surface Impedance	6
2.4 Height-Gain Functions	8
2.5 Limit of Vanishing Slab	9
3. INTEGRAL EQUATION APPROACH	10
3.1 Formulation	10
3.2 Integral Equation Solution	13
4. TWO-SECTION PATH	15
4.1 Kirchhoff Theory	15
4.2 Comparison with Integral Equation	20
5. EQUIVALENT SLAB PARAMETERS	22
5.1 Forest Cover	24
5.2 Built-up Areas	24
5.3 Snow Cover	26
6. SPECIFIC PATH CALCULATIONS	30
6.1 Smooth Paths in the Netherlands	30
6.2 Irregular, Forested Terrain in West Germany	35
7. CONCLUSIONS AND RECOMMENDATIONS	50
8. ACKNOWLEDGMENTS	53
9. REFERENCES	53
APPENDIX A: ANTENNA WITHIN THE SLAB	57
REFERENCES	62
APPENDIX B: KIRCHHOFF INTEGRATION	64
REFERENCE	66
APPENDIX C: USER'S GUIDE, LISTING, AND SAMPLE OUTPUT FOR PROGRAM WAGSLAB	67

LIST OF FIGURES

		Page
Figure 1.	Vertical electric dipole over a uniaxial anisotropic slab.	4
Figure 2.	Equivalent geometry for the limit of a free-space slab ($\varepsilon_{hc} = \varepsilon_{vc} = 1$)	11
Figure 3.	Geometry for integral equation. The slab and ground parameters can vary as a function of x, but are constant in y. . .	12
Figure 4.	Geometry for a two-section path with an elevation change D. The section, $x < 0$, has a normalized surface impedance Δ_a, and the section, $x > 0$, has a normalized surface impedance Δ_b.	16
Figure 5.	Propagation from a forest to a clearing for a frequency of 10 MHz.	21
Figure 6.	Propagation from a clearing to a forest for a frequency of 10 MHz.	23
Figure 7.	Relative permittivity ε_v versus building density B.	27
Figure 8.	Magnitude of the spherical earth attenuation function as a function of frequency and snow depth D. Parameters: $\varepsilon_v = \varepsilon_h = 1.55$, $\sigma_v = \sigma_h = 2.5 \times 10^{-5}$ S/m, $\varepsilon_g = 10$, $\sigma_g = 10^{-2}$ S/m	29
Figure 9.	Smooth path in the Netherlands with receiving sites at 60 km and 80 km. The first 70 km has good ground ($\varepsilon_g = 15$ and $\sigma_g = 10^{-2}$ S/m), and the last 10 km has poor ground ($\varepsilon_g = 3$ and $\sigma_g = 10^{-4}$ S/m).	31
Figure 10.	Comparison of measurement with three theories at 2 MHz for a smooth path in the Netherlands. Only the integral equation solution takes into account the poor ground section shown in Figure 9.	32
Figure 11.	Comparison of measurement with three theories at 10 MHz for a smooth path in the Netherlands. Only the integral equation solution takes into account the poor ground section shown in Figure 9	33
Figure 12.	Comparison of measurement with three theories at 30 MHz for a smooth path in the Netherlands. Only the integral equation solution takes into account the poor ground section shown in Figure 9.	34
Figure 13.	Terrain profile for the path from Inneringen to Boblingen . .	37

LIST OF FIGURES (continued)

		Page
Figure 14.	Propagation from Inneringen to Boblingen at 2 MHz. The solid curve is for bare ground, and the dotted curve includes the forest and urban slabs.	38
Figure 15.	Propagation from Inneringen to Boblingen at 5 MHz. The solid curve is for bare ground, and the dotted curve includes the forest and urban slabs. The circles are obtained from multiple knife-edge diffraction theory.	39
Figure 16.	Propagation from Inneringen to Boblingen at 10 MHz. The solid curve is for bare ground, and the dotted curve includes the forest and urban slabs.	40
Figure 17.	Propagation from Inneringen to Boblingen at 20 MHz. The solid curve is for bare ground, and the dotted curve includes the forest and urban slabs.	41
Figure 18.	Propagation from Inneringen to Boblingen at 30 MHz. The solid curve is for bare ground, and the dotted curve includes the forest and urban slabs. The circles are obtained from multiple knife-edge diffraction theory.	42
Figure 19.	Magnitude of height-gain function in forest slab and in air. Parameters: $D = 20$ m, $\varepsilon_v = \varepsilon_h = 1.1$, $\sigma_v = \sigma_h = 10^{-4}$ S/m, $\varepsilon_g = 10$, and $\sigma_g = 10^{-2}$ S/m.	43
Figure 20.	Spherical earth attenuation function for bare ground and with forest cover. Parameters: $D = 20$ m, $\varepsilon_v = \varepsilon_h = 1.1$, $\sigma_v = \sigma_h = 10^{-4}$ S/m, $\varepsilon_g = 10$, and $\sigma_g = 10^{-2}$ S/m	44
Figure 21.	Propagation from Inneringen to Boblingen (solid curve) and in the reverse direction (dotted curve). Both cases are for bare ground, and the frequency is 2 MHz	46
Figure 22.	Propagation from Boblingen to Inneringen (solid curve) and in the reverse direction (dotted curve). Both cases are for bare ground, and the frequency is 5 MHz	47
Figure 23.	Propagation from Inneringen to Boblingen (solid curve) and in the reverse direction (dotted curve). Both cases are for bare ground, and the frequency is 20 MHz.	48
Figure 24.	Terrain profile for the path from Inneringen to Lechfeld. . .	49
Figure 25.	Propagation from Inneringen to Lechfeld (solid) and in the reverse direction (dotted). Both curves are for bare ground, and the frequency is 2 MHz.	51

LIST OF FIGURES (continued)

		Page
Figure 26.	Propagation from Inneringen to Lechfeld (solid) and in the reverse direction (dotted). Both curves are for bare ground, and the frequency is 5 MHz.	52
Figure A.1.	Integration contours in the complex λ plane	60

LIST OF TABLES

Table 1.	Characteristic Parameters of Typical Forests (Dence and Tamir, 1969)	25
Table 2.	Magnitude and Phase of Surface Impedance Δ as a Function of Snow Depth D. Parameters: $\varepsilon_v=\varepsilon_h=1.55$, $\sigma_v=\sigma_h=2.5 \times 10^{-5}$ S/m, $\varepsilon_g=10$, $\sigma_g=10^{-2}$S/m.	28

HF GROUND WAVE PROPAGATION OVER FORESTED AND BUILT-UP TERRAIN

D. A. Hill*

An integral equation method is presented for computing the vertically polarized field strength over irregular terrain which is covered with forest, buildings, or snow. The terrain cover is modeled as an equivalent slab, and a general computer code, WAGSLAB, is developed. Numerous special cases are treated analytically, and comparisons are made with numerical results from WAGSLAB.

Key words: flat earth; HF ground wave propagation; irregular terrain; mixed path; lateral wave, slab model; spherical earth; vertical polarization

1. INTRODUCTION

Integral equations (Hufford, 1952; Ott and Berry, 1970) have been found useful for calculating the ground wave field over irregular, inhomogeneous terrain. More recently Causebrook (1978a) has modified Hufford's integral equation to account for the effect of built-up sections along the path and has been successful in modeling MF propagation in the London vicinity. He assumed that the building heights were small compared to a wavelength, and he did not consider the effect of antenna height.

In this report, we extend Causebrook's general approach upward in frequency to the HF band where the building and forest heights are not necessarily small and the effect of the antenna height is important. The extension utilizes an anisotropic slab to model forest, snow, or buildings along the path. We modify Ott's (1971a) computer program (WAGNER) to include the possibility of a lossy, anisotropic, dielectric slab of arbitrary thickness over the ground. The slab parameters are allowed to vary along the path just as the terrain height and earth conductivity and dielectric constant are allowed to vary in program WAGNER. The source and receiving antennas can be located either within or above the slab, and only vertical polarization is considered. The same technique could be used for horizontal polarization, but the rapid attenuation makes horizontal polarization not useful for ground wave propagation.

---

*The author is with the U.S. Department of Commerce, National Bureau of Standards, Boulder, Colorado 80303.

The integral equation approach that is described in this report is a point-to-point prediction method and should be most useful for frequencies below 30 MHz. For higher frequencies, the variability of the ground wave in time and space becomes large, and an accurate point-to-point prediction becomes difficult. A recent report (Hufford et al., 1982) describes an area prediction model for VHF, UHF, and SHF frequencies.

The organization of this report is as follows: In Section 2, the fields of a vertical electric dipole are analyzed for the dipole either within or above a uniform slab. The effective surface impedance and the height-gain functions are derived. In Section 3, Ott's previous integral equation (1971a) is extended to include a slab above the earth by using surface impedance and height-gain approximations from Section 2. In Section 4, a two-section path is analyzed both by Kirchhoff Theory and by the integral equation method. The analytical result from the Kirchhoff Theory is useful in its own right and also provides a good check for the revised integral equation. In Section 5, the values for the equivalent slab parameters for forests, built-up areas, and snow are discussed. In Section 6, specific path calculations are performed using the integral equation approach. Section 7 includes a summary and recommendations for further work. In Appendix A, both the integral representation and the asymptotic result are derived for the case where the dipole is located within the anisotropic slab. Appendix B includes the rather involved mathematical details of the Kirchhoff integration which is required for the two-section path analysis in Section 4. Finally, Appendix C provides a user's guide, a listing, and a sample output for program WAGSLAB which is essentially an extension of Ott's program WAGNER.

Throughout the report, we present propagation results in terms of a normalized attenuation function f which is the ratio of the actual electric field to twice the free-space field. This is done in order to emphasize propagation effects and to eliminate antenna effects. Thus f is unity for a flat, perfectly conducting ground. If some form of transmission loss is desired, it can be easily computed from the free space transmission loss and the magnitude of f.

2. UNIFORM SLAB MODEL

In this section, we analyze a uniform, anisotropic slab model for a vertical electric dipole source. The asymptotic results for the uniform slab model (Wait, 1967a) can be cast in a very convenient form where the total field can be factored into a product of twice the free space field times a ground-wave attenuation function times the height-gain functions for the source and observer heights. The attenuation function depends on the surface impedance for a layered medium in the

same manner that the flat-earth attenuation function for a homogeneous earth (Wait, 1962) depends on the surface impedance of a homogeneous half-space. We utilize the specific results for the surface impedance and height-gain functions of the uniform slab in Section 3 where the slab parameters are allowed to change along the path.

Although we are primarily interested in the uniform slab model as a starting point for the more general irregular terrain model of Section 3, the uniform slab model is of interest in its own right for modeling uniformly forested paths (Tamir, 1967; Dence and Tamir, 1969; and Gordon and Hoyt, 1982). In this report, we also use a slab to model built-up urban areas or snow accumulation. The specific slab parameters appropriate for forests, urban areas, and snow are discussed in Section 5.

2.1 Integral Representation

We consider first a vertical electric dipole located at a height h over a uniaxial anisotropic slab of thickness D as shown in Figure 1. The dipole has a current moment I ds, and the $\exp(i\omega t)$ time dependence is suppressed. The slab has horizontal and vertical relative permittivities, ε_h and ε_v, respectively, and horizontal and vertical conductivities, σ_h and σ_v, respectively. The region, $z > 0$, is assumed to be free space with permittivity ε_o and zero conductivity. The region, $z < -D$, is ground with relative permittivity ε_g and conductivity σ_g. We assume free space permeability μ_o everywhere. In the following treatment it is convenient to use the following expressions for the various relative complex dielectric constants

$$\varepsilon_{gc} = \varepsilon_g + \sigma_g/(i\omega\,\varepsilon_o) \quad ,$$

$$\varepsilon_{hc} = \varepsilon_h + \sigma_h/(i\omega\,\varepsilon_o) \quad , \tag{1}$$

and

$$\varepsilon_{vc} = \varepsilon_v + \sigma_v/(i\omega\,\varepsilon_o) \quad .$$

The field in air ($z>0$) can be derived from the z component, Π_{oz}, of an electric Hertz vector which has the following integral form (Wait, 1967a):

$$\Pi_{oz} = \frac{I\,ds}{4\pi i\omega\,\varepsilon_o} \int_o^\infty \left[e^{-u_o|z-h|} + R_{||}(\lambda)\, e^{-u_o(z+h)} \right] \frac{\lambda}{u_o} J_o(\lambda\rho)\, d\lambda \quad , \tag{2}$$

where

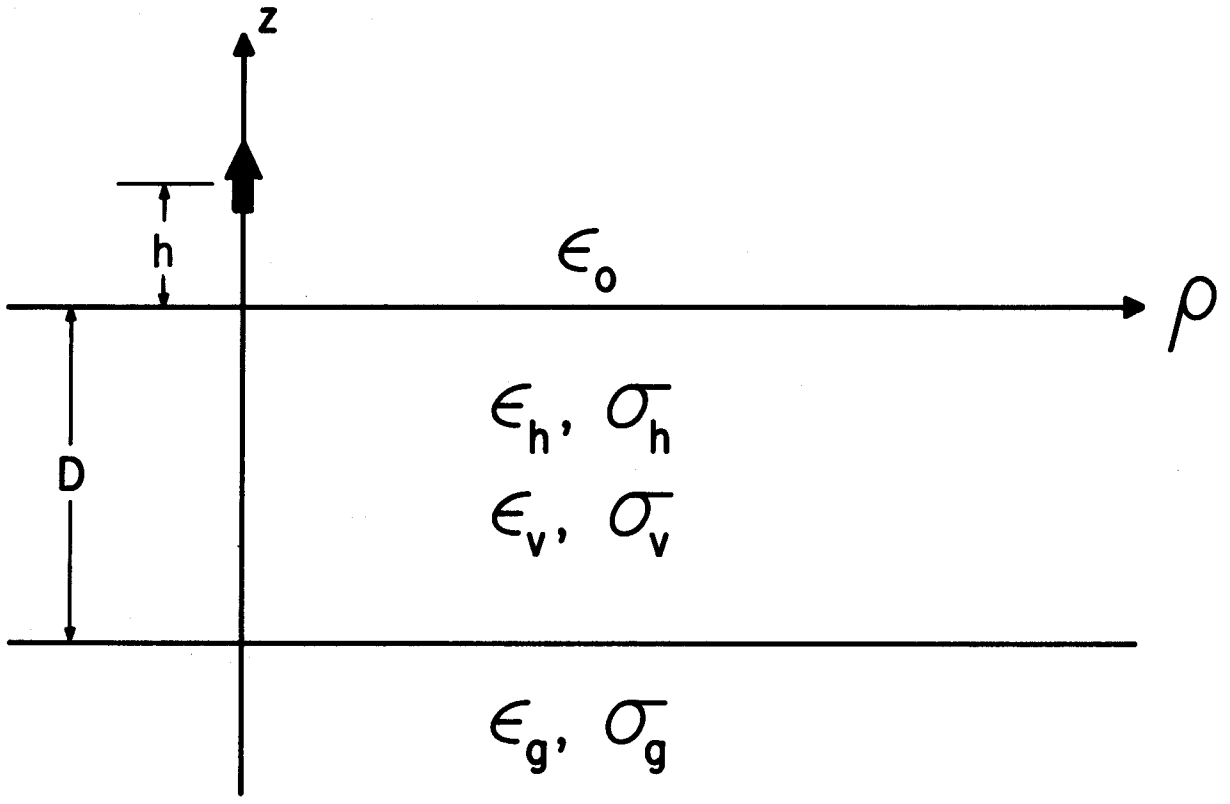

Figure 1. Vertical electric dipole over a uniaxial anisotropic slab.

$$R_{||}(\lambda) = \frac{K_o - Z_1}{K_o + Z_1} \quad , \quad K_o = \frac{u_o}{i\omega \varepsilon_o} \quad ,$$

$$u_o = (\lambda^2 - k^2)^{\frac{1}{2}} \quad , \quad k = \omega/c \quad ,$$

$$Z_1 = K_1 \frac{K_2 + K_1 \tanh(vD)}{K_1 + K_2 \tanh(vD)} \quad ,$$

$$K_1 = v/(i\omega \varepsilon_o \varepsilon_{hc}) \quad , \quad K_2 = u/(i\omega \varepsilon_o \varepsilon_{gc}) \quad ,$$

$$v = (\lambda^2 \kappa + \gamma^2)^{\frac{1}{2}} \quad , \quad \kappa = \varepsilon_{hc}/\varepsilon_{vc} \quad ,$$

$$\gamma^2 = -\omega^2 \mu_o \varepsilon_o \varepsilon_{hc} \quad , \quad u = (\lambda^2 + \gamma_g^2)^{\frac{1}{2}} \quad ,$$

and

$$\gamma_g^2 = -\omega^2 \mu_o \varepsilon_o \varepsilon_{gc} \quad .$$

Cylindrical coordinates (ρ,ϕ,z) are used. The electric and magnetic fields in air $(z>0)$ are given by

$$E_{o\rho} = \frac{\partial^2 \Pi_{oz}}{\partial \rho \partial z} \quad , \quad E_{oz} = (k^2 + \frac{\partial^2}{\partial z^2}) \Pi_{oz} \quad ,$$

$$H_{o\phi} = -i\omega \varepsilon_o \frac{\partial \Pi_{oz}}{\partial \rho} \quad , \tag{3}$$

and

$$E_{o\phi} = H_{o\rho} = H_{oz} = 0 \quad .$$

An integral expression for the fields in the slab $(0 > z > -D)$ can be derived and is similar in form to (2). The fields in the ground $(z < -D)$ are not normally of interest. Expressions for the fields both in air and within the slab when the dipole source is located within the slab are derived in Appendix A.

2.2 The Lateral Wave

In general an evaluation of the fields involves a numerical integration as indicated by (2). However, when $k\rho$ is large and $|z|$ is not large, integrals of the type in (2) can be evaluated asymptotically. The result for the dipole in air ($h>0$) was given by Wait (1967a), and the result for the dipole in the slab ($0 > h > -D$) is derived in Appendix A. In either case, the vertical electric field E_z either in air or in the slab can be cast into the following convenient form

$$E_z \simeq E_o \, f(p) \, G(h) \, G(z) \quad . \tag{4}$$

The result in (4) has the following interpretation. E_o is twice the field of a dipole in free space or by image theory is the field when both the dipole and the observer are located on a flat, perfect conductor:

$$E_o = \frac{-i\omega\mu_o \, I \, ds}{2\pi\rho} \quad . \tag{5}$$

The Sommerfeld attenuation function $f(p)$ accounts for the imperfect conductivity of the ground and the presence of the slab. For a perfectly conducting ground, $p=0$ and $f(0)=1$. In our case, the magnitude of the numerical distance p is large, and $f(p)$ is given by (Wait, 1962)

$$f(p) \simeq -1/(2p) \quad , \tag{6}$$

where

$$p = -ik\rho\Delta^2/2 \quad .$$

The normalized surface impedance Δ will be defined and discussed in the following section. Note that $E_o \, f(p)$ has the expected ρ^{-2} variation which is associated with the "lateral wave" (Tamir, 1967). The point we wish to make here is that the "ground wave" has the same ρ^{-2} variation when $|p|$ is large. The "lateral wave" and the "ground wave" are simply different names for the dominant part of the total field near the ground when the horizontal distance is large. The height gain product, $G(h) \, G(z)$, in (4) is independent of ρ and will be discussed in Section 2.4.

2.3 Normalized Surface Impedance

We define the surface impedance as the ratio of the tangential electric and magnetic fields at the upper surface of the slab ($z=0$). From (2) and (3), we derive the following

$$\left.\frac{-E_{o\rho}}{H_{o\phi}}\right|_{z=0} = Z_1 \tag{7}$$

where Z_1 is given by (2). The surface impedance Z_1 has units of ohms, and from (2) it can be seen that it depends on the horizontal wavenumber λ.

As indicated in Appendix A, the main contribution to the integral comes from the region $\lambda \simeq k$ when ρ is large and the source and observer heights are small. This is equivalent to saying that we can use the surface impedance value for a plane wave at grazing incidence ($\lambda \simeq k$) in ground wave propagation. In addition it is convenient to normalize the surface impedance by dividing by the impedance of free space η_o ($=\sqrt{\mu_o/\varepsilon_o}$). Thus, we define the normalized surface impedance Δ as

$$\Delta = \left. Z_1/\eta_o \right|_{\lambda=k} . \tag{8}$$

From (2) we can write Δ in the following form

$$\Delta = \Delta_1 \frac{\Delta_2 + \Delta_1 \tanh(v_o D)}{\Delta_1 + \Delta_2 \tanh(v_o D)} , \tag{9}$$

where

$$\Delta_1 = \sqrt{\varepsilon_{hc} - \kappa}\,/\varepsilon_{hc} ,$$

$$\Delta_2 = \sqrt{\varepsilon_{gc} - 1}\,/\varepsilon_{gc} ,$$

and

$$v_o = ik\sqrt{\varepsilon_{hc} - \kappa} .$$

Although (9) is derived for the case of a uniform slab, we use the same expression for Δ in Section 3 where the slab parameters are allowed to vary along the path.

There are a number of limiting cases which provide some insight into the dependence of Δ on the various parameters. If the parameters of the slab approach those of the ground ($\varepsilon_{hc} = \varepsilon_{vc} = \varepsilon_{gc}$), then

$$\Delta = \Delta_2 = \sqrt{\varepsilon_{gc} - 1}\,/\varepsilon_{gc} . \tag{10}$$

The same limit (10) is obtained by letting D approach zero. In either case we are back to a homogeneous half-space, and (10) is the known result for a homogeneous half-space.

Another interesting limit is to let the slab thickness D approach infinity. Then if v_o is complex, tanh $(v_o D)$ approaches unity and Δ simplifies:

$$\Delta\Big|_{D=\infty} = \Delta_1 \quad . \tag{11}$$

This is simply the surface impedance for an anisotropic half-space.

In many cases, the slab parameters are close to those of free space. So the limit of ε_{hc} and ε_{vc} approaching unity is also of interest. In this case, the following result is obtained

$$\Delta\Big|_{\varepsilon_{hc}=\varepsilon_{vc}=1} = \Delta_2/(1+ikD\Delta_2) \quad . \tag{12}$$

This limit will be found useful in Section 2.5.

2.4 Height-Gain Functions

The height-gain function G(z) which appears in (4) takes on different forms depending on whether z is positive or negative (Wait, 1967a):

$$G(z) = \begin{cases} G_o(z) \quad , & z \geq 0 \\ G_s(z) \quad , & 0 > z > -D \end{cases} \tag{13}$$

where

$$G_o(z) = 1 + ikz\Delta \quad ,$$

$$G_s(z) = \frac{1}{\varepsilon_{vc}} \frac{e^{v_o z} + R\, e^{-v_o(2D+z)}}{1 + R\, e^{-2v_o D}} \quad ,$$

$$R = \frac{\Delta_1 - \Delta_2}{\Delta_1 + \Delta_2} \quad ,$$

and v_o, Δ_1, and Δ_2 are given by (9). As shown in Appendix A, the same height-gain function applies to both the source and observer locations. This is simply a consequence of reciprocity since even the anisotropic slab is a reciprocal medium (Monteath, 1973).

The limit of $G_o(z)$ as z approaches zero is unity

$$G_o(0) = 1 \quad . \tag{14}$$

However, the limit of $G_s(z)$ as z approaches zero is

$$G_s(0) = 1/\varepsilon_{vc} \quad . \tag{15}$$

This is a consequence of the continuity of normal current density at z=0.

2.5 Limit of Vanishing Slab

In the case of thin forest (Dence and Tamir, 1969), the slab parameters differ only slightly from free space. Thus the limiting case when the slab actually vanishes ($\varepsilon_{hc} = \varepsilon_{vc} = 1$) is of some practical interest as well as being a good check on the asymptotic solution given by (4). By physical reasoning we should recover the result for a dipole at a height D+h and an observer at a height D+z over homogeneous ground when ε_{hc} and ε_{vc} are both equal to unity.

When both h and z are positive, (4) becomes

$$E_z \simeq E_o \left(\frac{-1}{2p}\right) G_o(h)\, G_o(z) \quad . \tag{16}$$

For the case where ε_{hc} and ε_{vc} are unity, Δ reduces to the value in (12). E_o is not a function of ε_{hc} and ε_{vc}. From (6) and (12), the second factor in (16) reduces to

$$\left(\frac{-1}{2p}\right)\Bigg|_{\varepsilon_{hc}=\varepsilon_{vc}=1} = \frac{-(1+ikD\Delta_2)^2}{2\,p_2} \quad , \tag{17}$$

where $p_2=-ik\rho\Delta_2^2/2$.

From (12) and (13), $G_o(h)$ reduces to

$$G_o(h)\Big|_{\varepsilon_{hc}=\varepsilon_{vc}=1} = 1 + \frac{ikh\Delta_2}{(1+ikD\Delta_2)} \quad . \tag{18}$$

By substituting (17) and (18) into (16), the following result is obtained

$$E_z\Big|_{\varepsilon_{hc}=\varepsilon_{vc}=1} = E_o \left(\frac{-1}{2\,p_2}\right) \cdot \left[1+ik\Delta_2(D+h)\right] \cdot \left[1+ik\Delta_2(D+z)\right] \quad . \tag{19}$$

The second factor in (19) is the attenuation function for a homogeneous earth. The third and fourth factors are the height-gain factors for the source and observer

respectively over a homogeneous earth. Thus the slab result reduces to the simpler half-space result as illustrated in Figure 2.

3. INTEGRAL EQUATION APPROACH

For realistic propagation paths, the parameters will vary as a function of position along the path. Analytical methods are not general enough to handle such variations, but the integral equation approach (Hufford, 1952; Ott and Berry, 1970) has been found useful for ground wave propagation over irregular, inhomogeneous terrain. Ott's program WAGNER (Ott, 1971a and 1971b; Ott et al., 1979) has been thoroughly tested and used on a wide variety of propagation paths. In this section we extend Ott's integral equation method to include the presence of a lossy slab over homogeneous earth. As in Ott's method, the properties of the earth (and also the slab) are allowed to change along the path.

3.1 Formulation

A good description of the latest version of program WAGNER and the integral equation on which it is based is given in Ott et al. (1979). The integral equation utilizes the impedance boundary condition which we can generalize from the half-space form to the slab form. The geometry is shown in Figure 3, and the slab and ground parameters are allowed to vary with x but are independent of y.

We consider first the case where both the source and receiver heights are zero. We define the attenuation function f(x) as the ratio of the vertical electric field to E_o, twice the free-space field. The integral equation for f(x) is (Ott et al., 1979):

$$f(x) = W(x,0) - \sqrt{\frac{ik}{2\pi}} \int_0^x f(\xi)\, e^{-ik\phi(x,\xi)} \left\{ y'(\xi)\, W(x,\xi) - \frac{y(x)-y(\xi)}{x-\xi} + (\Delta(\xi)-\Delta_a)\, W(x,\xi) \right\} \left[\frac{x}{\xi(x-\xi)} \right]^{\frac{1}{2}} d\xi \quad , (20)$$

where

$$\phi(x,\xi) = \frac{[y(x)-y(\xi)]^2}{2(x-\xi)} + \frac{y^2(\xi)}{2\xi} - \frac{y^2(x)}{2x} \quad ,$$

$$W(x,\xi) = 1 - i\sqrt{\pi p}\, w(-\sqrt{u}) \quad ,$$

$$p = -ik\Delta^2(\xi)\, (x - \xi)/2 \quad ,$$

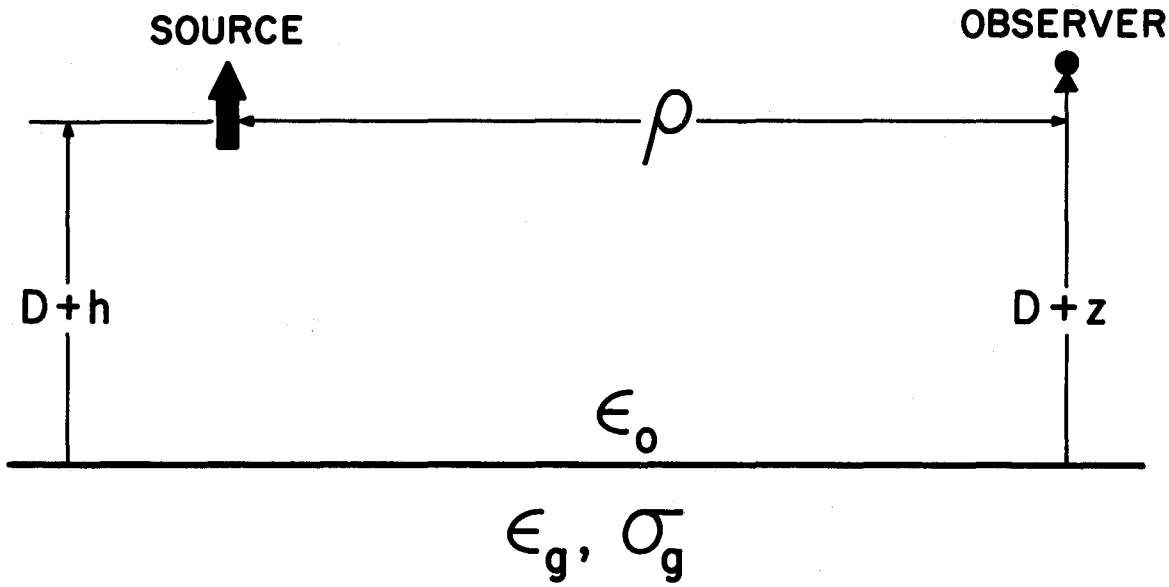

Figure 2. Equivalent geometry for the limit of a free-space slab ($\varepsilon_{hc} = \varepsilon_{vc} = 1$).

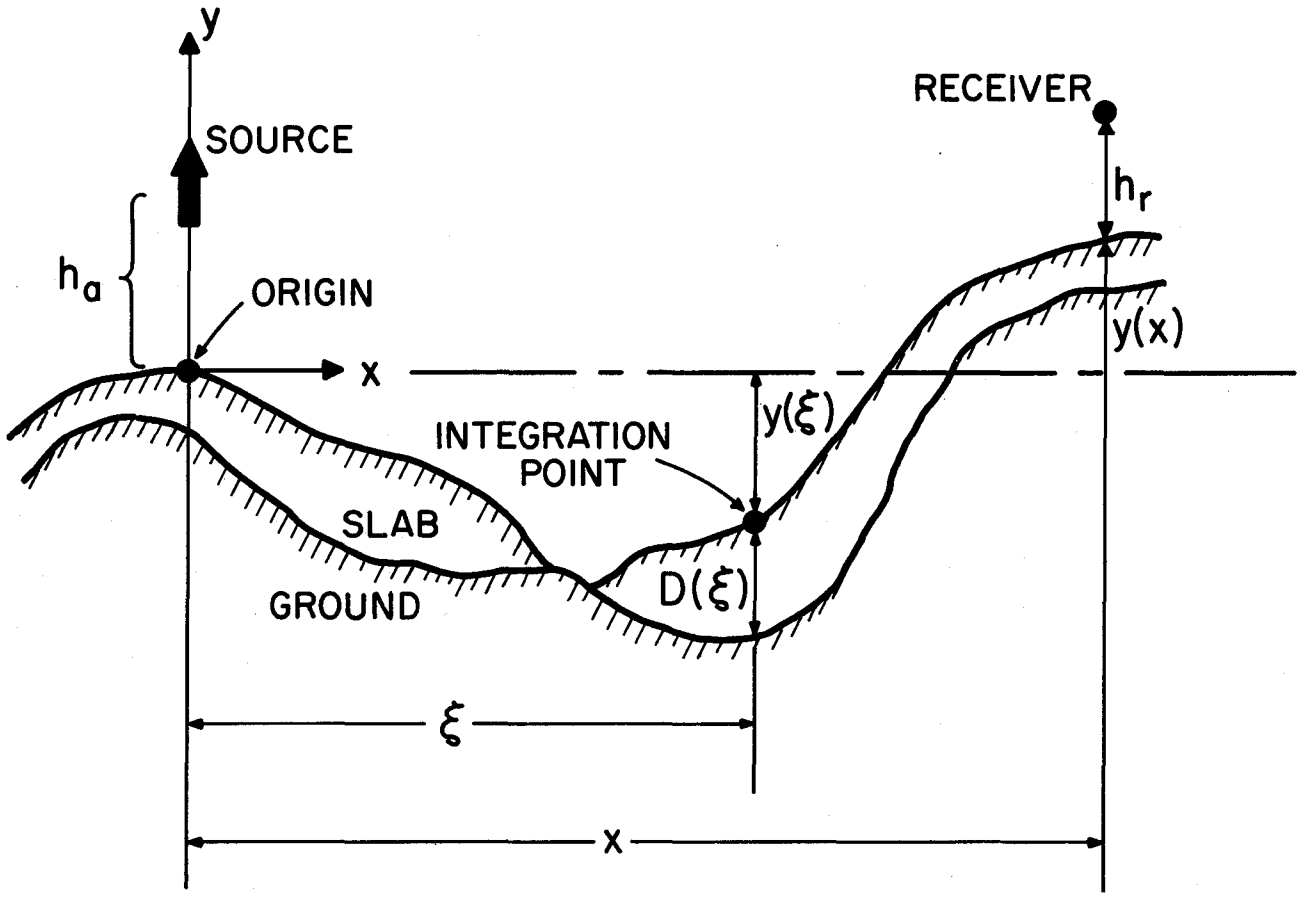

Figure 3. Geometry for integral equation. The slab and ground parameters can vary as a function of x, but are constant in y.

$$u = p\left[1 - \frac{y(x)-y(\xi)}{\Delta(x-\xi)}\right]^2 \quad ,$$

$$w(-\sqrt{u}) = e^{-u}\,\mathrm{erfc}(i\sqrt{u}) = \frac{1}{i\pi}\int_{-\infty}^{\infty}\frac{e^{-t^2}\,dt}{\sqrt{u}+t} \quad ,$$

and the properties of w are discussed by Abramowitz and Stegun (1964). The quantities x, ξ, y(x), and $y(\xi)$ are defined in Figure 3, and $y'(\xi)$ is the slope $dy/d\xi$. The normalized surface impedance $\Delta(\xi)$ is given by (9). As indicated it is a function of distance ξ along the path because it depends on ground constants, ε_g and σ_g, and slab parameters, D, ε_h, σ_h, ε_v, and σ_v, which are a function of distance ξ along the path. The normalized surface impedance Δ_a is evaluated at the source, $\xi=0$.

To account for nonzero source and receiver heights, h_a and h_r, we utilize the height-gain functions discussed in Section 2.4. Thus we define an attenuation function $f_h(x)$ which is the ratio of the vertical electric field to twice the free-space field in terms of the normalized attenuation function f(x) and the height-gain functions:

$$f_h(x) = f(x)\,G(h_a)\,G(h_r) \quad . \tag{21}$$

G is defined in (13), and the heights h_a and h_r must be greater than -D. That is, the source and observer can be either in the slab or in air. $G(h_a)$ is a function of the ground and slab parameters at the source ($\xi=0$), and $G(h_r)$ is a function of the parameters at the observer ($\xi=x$). For the source and observer in air at the surface of the slab ($h_a=h_r=0^+$), both height-gain functions are unity, and the two attenuation functions are equal

$$f_h(x)\Big|_{h_a=h_r=0^+} = f(x) \quad . \tag{22}$$

3.2 Integral Equation Solution

Before discussing the general solution of (20), it is useful to examine the case of a uniform path. In this case, $y(\xi)=y(x)=y'(\xi)=0$ and $\Delta(\xi)=\Delta_a$. Thus the integrand is zero, and f(x) is simply

$$\begin{aligned} f(x) &= W(x,0) \\ &= 1 - i\sqrt{\pi p_a}\; w(-\sqrt{p_a}) \end{aligned} \tag{23}$$

where

$$p_a = -ik\Delta_a^2 x/2 \quad .$$

This result is the expected flat-earth attenuation function (Wait, 1962), and p_a is the numerical distance. When $|p_a|$ is very small, then $f(x) \simeq 1$. For example, p_a is zero for a perfectly conducting upper boundary ($\Delta_a=0$). For large $|p_a|$, the asymptotic form in (6) holds

$$f(x) \simeq \frac{-1}{2\ p_a} \quad . \tag{24}$$

When either y or Δ varies along the path, then the integral equation (20) must be solved numerically. We use the same method of solution as Ott (1971a) which is a forward stepping solution in x (Wagner, 1953). Thus values of f (or f_h) are obtained at discrete values of x along the profile. Since (20) is a Volterra integral equation of the second kind, the value of f(x) depends only on the previously computed values of $f(\xi)$ for $\xi < x$. Physically this means that backscatter is neglected.

For a given path calculation, the computer run time t_r is roughly proportional to the square of the number of x points, N_x. The number of points required to maintain precision along a given path is proportional to length of the path L and the radio frequency. Thus the run time can be written

$$t_r \propto N_x^2 \propto L^2 \cdot \text{freq}^2 \quad . \tag{25}$$

The constant of proportionality depends on how rapidly y and Δ vary along the path and is difficult to quantify.

Appendix C contains a user's guide, a listing, and a sample output for program WAGSLAB. The program is an extension of program WAGNER (Ott et al., 1979). The primary differences are that WAGSLAB requires additional input data for the slab parameters along the path and that the normalized surface impedance Δ is the form for a slab over ground as given by (9) rather than the form for a homogeneous earth given by (10). The slab parameters are allowed to change discontinuously along the path, and as a result Δ will also change discontinuously. However, a linear height interpolation scheme (Ott et al., 1979) is used to determine the height $y(\xi)$ and slope $y'(\xi)$ so that y and y' will be well behaved.

The primary outputs are the magnitude and phase of $f(x)$ and $f_h(x)$. We prefer to use these normalized attenuation functions because the attenuation relative to free space is an easy quantity to interpret and can be separated from the antenna effects. If some form of path loss is preferred, the additional path loss L_a to be added to the free-space path loss is

$$L_a = -20 \log_{10}(2|f_h|) \quad \text{(dB)} \quad .$$

4. TWO-SECTION PATH

The uniform slab model which was discussed in Section 2 has the advantage of yielding a rigorous analytical solution, but has the disadvantage of not providing any information regarding the effects of changes in slab parameters along the path. The integral equation approach described in Section 3 can handle arbitrary changes in slab parameters along the path, but yields only numerical results which are difficult to check. In this section, we treat the two-section path shown in Figure 4. Although this geometry has no exact solution, it is amenable to an approximate analysis which yields a fairly simple analytical result as given in Section 4.1.

The analytical result in Section 4.1 is useful in providing insight into the effect of a forest clearing on propagation. In addition, the analytical result is useful in providing a check for the integral equation method. As seen in Section 4.2, the agreement between the two methods is remarkably good.

4.1 Kirchhoff Theory

The geometry is shown in Figure 4. The section, $x < 0$, has normalized surface impedance Δ_a, and the section, $x > 0$, has normalized surface impedance Δ_b. A jump in surface height of magnitude D occurs at $x=0$. Since we employ the surface impedance boundary condition, there is no need to specify the details of the slab or ground at this point. The region, $x < 0$, could represent a slab of thickness D as in Figure 1 or it could just as well represent elevated ground as in a cliff geometry.

The geometry in Figure 4 has been treated by Monteath (1973) for the case of $D=0$, and here we extend his approach to allow for nonzero D. We take the source and receiving vertical electric dipoles to be located at the surface. The mutual impedance Z_{ab} between the two dipoles can be written as an integral over the vertical aperture S defined by $z > D$. If we make the Kirchhoff approximation that the aperture fields of each dipole are those of a uniform structure ($\Delta_a=\Delta_b$ and $D=0$), then the mutual impedance is given by (Monteath, 1973)

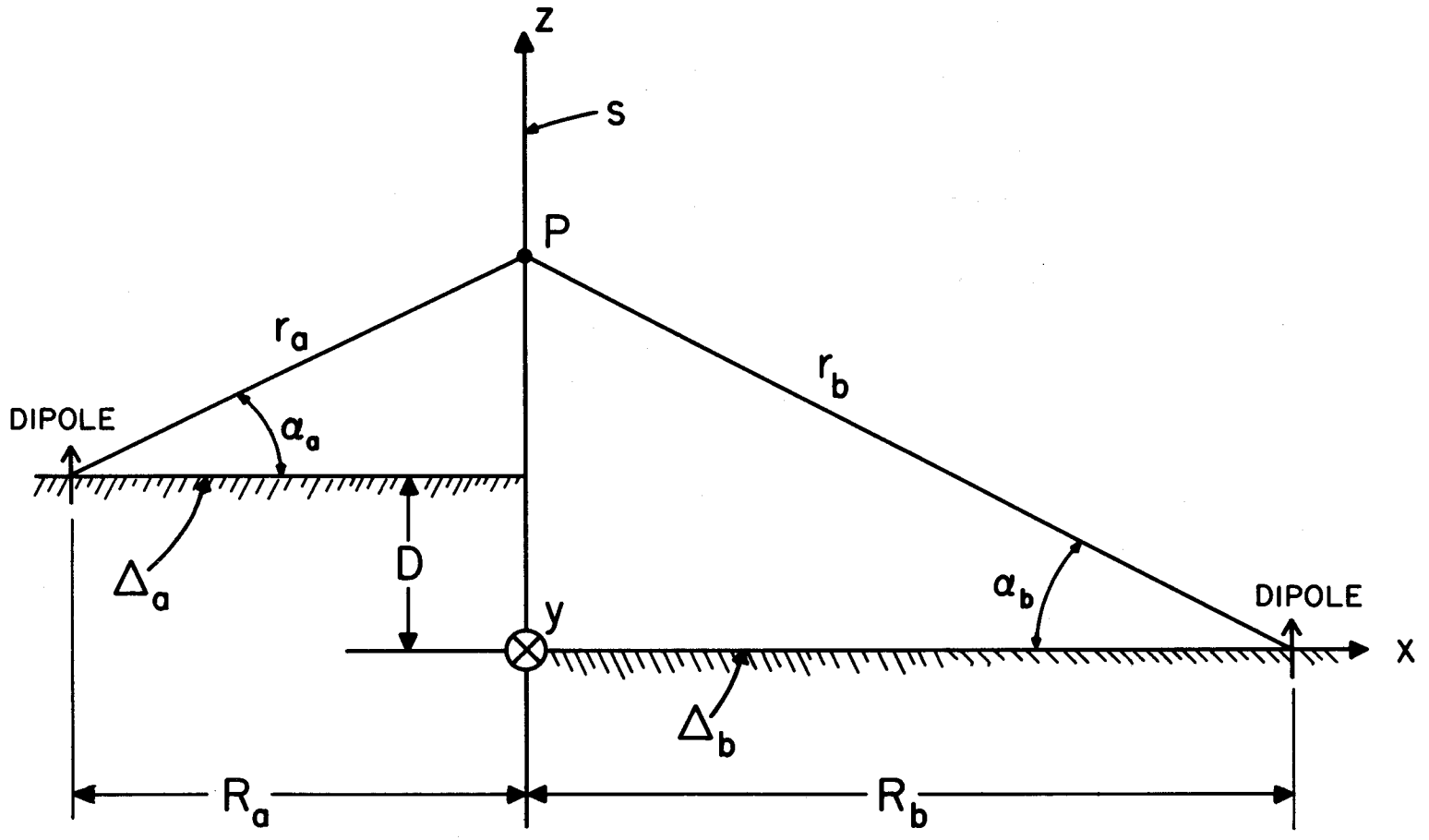

Figure 4. Geometry for a two-section path with an elevation change D. The section, $x < 0$, has a normalized surface impedance Δ_a, and the section, $x > 0$, has a normalized surface impedance Δ_b.

$$Z_{ab} = K_o \int_D^{\infty} dz \int_{-\infty}^{\infty} \frac{(1+\rho_a)\, e^{-ikr_a}}{r_a} \cdot \frac{(1+\rho_b)\, e^{-ikr_b}}{r_b}\, dy \quad , \tag{26}$$

where

$$r_a \simeq R_a + \frac{y^2 + (z - D)^2}{2 R_a} \quad ,$$

$$r_b \simeq R_b + \frac{y^2 + z^2}{2 R_b} \quad ,$$

and ρ_a and ρ_b are reflection coefficients for vertical polarization. K_o is a constant which depends on the dipole lengths, but the final result for the attenuation function is independent of K_o. We make the Fresnel approximation where quadratic terms are kept in the phase but not in the amplitude

$$Z_{ab} = \frac{K_o}{R_a R_b} \int_D^{\infty} dz \int_{-\infty}^{\infty} (1 + \rho_a)(1 + \rho_b) \cdot$$

$$\exp\left\{-ik\left[\frac{y^2}{2}\left(\frac{1}{R_a} + \frac{1}{R_b}\right) + \frac{z^2}{2R_b} + \frac{(z-D)^2}{2 R_a}\right]\right\} dy \quad . \tag{27}$$

The y integration in (27) can be done by stationary phase by using the following result (Monteath, 1973)

$$\int_{-\infty}^{\infty} \exp\left\{-ik\left[\frac{y^2}{2}\left(\frac{1}{R_a} + \frac{1}{R_b}\right)\right]\right\} dy = e^{-i\pi/4} \sqrt{\frac{2\pi}{k\left(\frac{1}{R_a} + \frac{1}{R_b}\right)}} \tag{28}$$

Substituting (28) into (27) and introducing a new constant K_1, we have

$$Z_{ab} = \frac{K_1}{\sqrt{R_a R_b (R_a + R_b)}} \int_D^{\infty} (1+\rho_a)(1+\rho_b) \cdot$$

$$\exp\left\{-ik\left[\frac{z^2}{2 R_b} + \frac{(z - D)^2}{2 R_a}\right]\right\} dz \quad . \tag{29}$$

The reflection coefficients in (29) are given by

$$\rho_a = \frac{\sin \alpha_a - \Delta_a}{\sin \alpha_a + \Delta_a} \text{ and } \rho_b = \frac{\sin \alpha_b - \Delta_b}{\sin \alpha_b + \Delta_b} \quad . \tag{30}$$

A convenient method of normalization is to consider the case of flat perfectly conducting ground ($\Delta_a=\Delta_b=D=0$). In this case, the mutual impedance Z_{abo} is given by (Monteath, 1973)

$$Z_{abo} = \frac{4\ K_1}{\sqrt{R_a R_b (R_a+R_b)}} \int_o^\infty \exp\left[\frac{-ikz^2}{2}\left(\frac{1}{R_a}+\frac{1}{R_b}\right)\right] dz$$

$$= \frac{2\sqrt{2\pi}\ K_1}{(ik)^{\frac{1}{2}}\ (R_a + R_b)} \quad . \tag{31}$$

In a manner consistent with the rest of this report, we define the attenuation function f as the ratio of the mutual impedance Z_{ab} to that for perfect ground Z_{abo}. Thus f is given by

$$f = \frac{Z_{ab}}{Z_{abo}} = \frac{(ik)^{\frac{1}{2}}\sqrt{R_a+R_b}}{2\sqrt{2\pi}\sqrt{R_a R_b}} \int_D^\infty (1+\rho_a)(1+\rho_b) \cdot$$

$$\exp\left\{-ik\left[\frac{z^2}{2\ R_b} + \frac{(z-D)^2}{2\ R_a}\right]\right\} dz \quad . \tag{32}$$

From (30), the reflection coefficient terms in (32) are given by

$$1 + \rho_a = \frac{2 \sin \alpha_a}{\sin \alpha_a + \Delta_a} \simeq \frac{2 \sin \alpha_a}{\Delta_a}$$

and

$$1 + \rho_b = \frac{2 \sin \alpha_b}{\sin \alpha_b + \Delta_b} \simeq \frac{2 \sin \alpha_b}{\Delta_b} \quad , \tag{33}$$

where we have assumed that the angles α_a and α_b are small. Thus we can approximate the sine terms

$$\sin \alpha_a \simeq \frac{z - D}{R_a} \text{ and } \sin \alpha_b \simeq \frac{z}{R_b} \quad . \tag{34}$$

Then (33) becomes

$$1 + \rho_a \simeq \frac{2(z - D)}{\Delta_a R_a} \text{ and } 1 + \rho_b \simeq \frac{2z}{\Delta_b R_b} \quad . \tag{35}$$

Substituting (35) into (32), we have

$$f = \sqrt{\frac{2}{\pi}} \frac{\sqrt{ik(R_a + R_b)}}{\Delta_a \Delta_b (R_a R_b)^{3/2}} \int_D^\infty z(z - D) \cdot$$

$$\exp\left\{-ik\left[\frac{z^2}{2\,R_b} + \frac{(z-D)^2}{2\,R_a}\right]\right\} dz \quad . \tag{36}$$

The evaluation of the integral in (36) is rather tedious and is given in terms of complementary error functions in Appendix B. However, for small values of D, f is given by

$$f \simeq \frac{S\, e^{-H^2}}{ik(R_a+R_b)\ \Delta_a \Delta_b} \quad , \tag{37}$$

where

$$S \simeq 1 + \frac{2H}{\sqrt{\pi}}\left(\frac{1}{\sqrt{A}} - \sqrt{A}\right) + \text{order } H^2$$

$$H = \frac{D\sqrt{ik/2}}{\sqrt{R_a + R_b}} \text{ and } A = \frac{R_a}{R_b} \quad .$$

The leading term in f varies as $(R_a + R_b)^{-1}$ and is independent of D. This is actually the same result which Monteath (1973) obtained for D=0:

$$f\Big|_{D=0} = \frac{1}{ik(R_a+R_b)\Delta_a \Delta_b} \quad . \tag{38}$$

For our purposes of modeling a discontinuous forest region, D is normally on the order of 10 m and $R_a + R_b$ is on the order of kilometers. Thus for the HF band, S in (37) is well approximated by unity, and f is well approximated by (38). This is equivalent to saying that the change in surface impedance has a larger effect on the propagation than does the change in elevation. This is consistent with some recent mode matching calculations for a step change in height over a spherical earth (Hill and Wait, 1982). In the case of $\Delta_a = \Delta_b = \Delta$, (38) reduces to the result for a uniform path as given by (6).

Although the derivation has been carried out for each dipole antenna at the surface as in Figure 4, we can generalize the results to nonzero heights. If the antennas are located at heights h_a and h_b, then a new attenuation function f_h is given by

$$f_h = f\ G(h_a)\ G(h_b) \tag{39}$$

where $G(h_a)$ is the height-gain function for the left section of the path and $G(h_b)$ is the height-gain function for the right section of the path. In either case, the form of G is given by (13).

4.2 Comparison with Integral Equation

In this section, we compare the approximate solution of (39) with the integral equation solution of (21). The same height-gain functions are used in each solution so that the comparison really involves the attenuation function f as calculated by (37) for the aperture solution and by (20) for the integral equation solution. Actually both solutions incorporate a number of approximations, but the approximations employed in the integral equation approach are less severe.

The specific case which we consider involves a forest-to-clearing path. For the ground constants over the entire path, we take the conductivity $\sigma_g = 10^{-2}$ S/m and the relative permittivity $\varepsilon_g = 10$. For the forest slab parameters, we take (Ott and Wait, 1973): $\sigma_h=10^{-4}$ S/m, $\sigma_v=2.5 \times 10^{-4}$ S/m, $\varepsilon_h=1.1$, $\varepsilon_v=1.25$, and D=10 m.

In Figure 5, results are shown for propagation from a forest to a clearing. Both transmitting and receiving antennas are located at the surface of the earth. Results are shown for three theories: the vertical aperture theory of Section 4.1, the integral equation of Section 3, and an analytic continuation method of Tamir (1977). For antenna separations less than 2 km, both antennas are in the forest and the results are those of the uniform slab because all three theories neglect backscatter. In this region, the three theories agree. For the receiving antenna just beyond the forest, the vertical aperture and analytic continuation theories predict a jump in the field strength and are not valid. However, for larger distances, the aperture theory and the integral equation are in good agreement. The Tamir (1977) analytic continuation theory gives a value which is too high. It is possible to show that Tamir's theory is roughly equivalent to replacing f in (37) by

$$f \simeq \frac{1}{ik(R_a+R_b)\ \Delta_b^{\,2}} \quad . \tag{40}$$

In other words the product of the two surface impedances $\Delta_a\ \Delta_b$ is replaced by $\Delta_b^{\,2}$. Since in this case the forest surface impedance Δ_a has a greater magnitude than the ground surface impedance Δ_b, Tamir's result yields a larger field. Only in the limit of a very thin forest does the Tamir result agree with the integral equation and the aperture theory. The increase in field strength in going from forest to clearing was predicted earlier (Office of Telecommunications Technical Memorandum

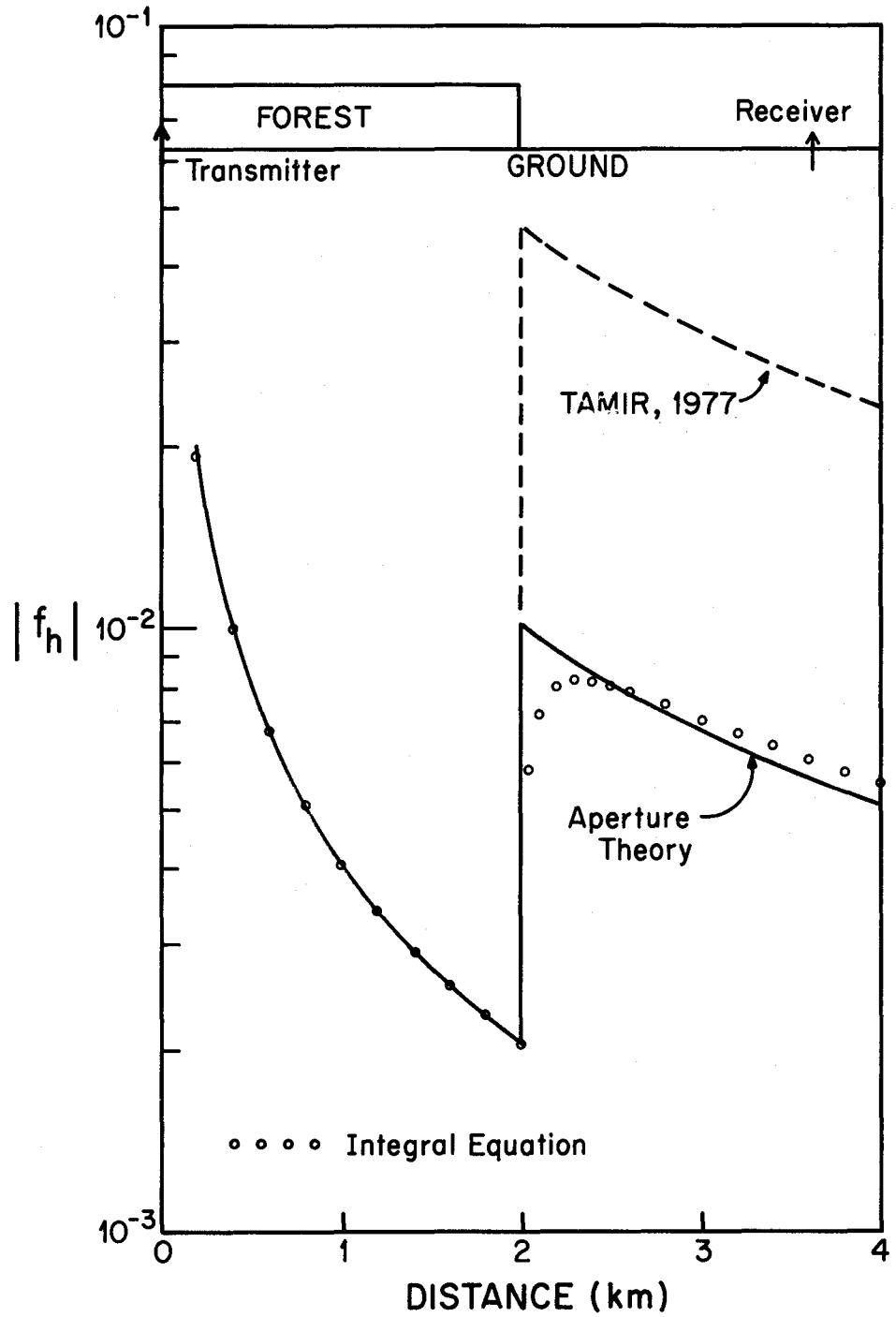

Figure 5. Propagation from a forest to a clearing for a frequency of 10 MHz.

73-154, by Ott and Wait, limited distribution) and is analogous to the "recovery effect" which has been calculated (Wait and Walters, 1963; Hill and Wait, 1981a) and measured (Millington, 1949) for propagation from land to sea.

The problem of propagating from the clearing to the forest is equally interesting, and the three theories are shown in Figure 6. In this case, both antennas are located 10 m above the ground even with the top of the forest. For short distances, the agreement with the integral equation is not perfect because the numerical distance p as defined by (6) is not large. For distances well beyond the forest transition, the aperture and integral equation theories are in good agreement, but the Tamir (1977) analytic continuation result again is high. Actually for the case of the antennas even with the top of the forest, Tamir's analytic continuation result is independent of the forest parameters.

Other cases for various slab parameters and frequencies have been studied, and the trends are qualitatively similar. In order to use the integral equation approach, we actually replace the abrupt height change from the ground to the forest with a linear transition. This is done automatically by program WAGSLAB so that the terrain slope remains finite. A similar linear height interpolation method has been used in program WAGNER (Ott et al., 1979).

5. EQUIVALENT SLAB PARAMETERS

The program WAGSLAB requires the user to supply the slab parameters along the path. The five slab parameters are as pictured in Figure 1: height (D), horizontal conductivity (σ_h), horizontal relative permittivity (ε_h), vertical conductivity (σ_v), and vertical relative permittivity (ε_v). In the HF band, the wavelength ranges from 10 m to 100 m. Consequently, objects such as trees and buildings are not necessarily electrically small. However, the equivalent slab representation seems to be the only tractable model for forests and urban areas at this time.

In this section, we review the literature and make some recommendations regarding the equivalent parameters for forests, urban areas, and snow cover. It is hoped that future comparisons of theory and measurements for propagation through forests and built-up areas will aid in the determination of the appropriate equivalent parameters. It might turn out that a multilayer slab (Ott and Wait, 1973a; Cavalcante et al., 1982) is more appropriate for modeling forests and built-up areas, but it is felt that our knowledge of the equivalent slab parameters is not precise enough to justify such additional complexity at this time. However, such an extension is possible simply by modifying the surface impedance Δ and the height-gain function G.

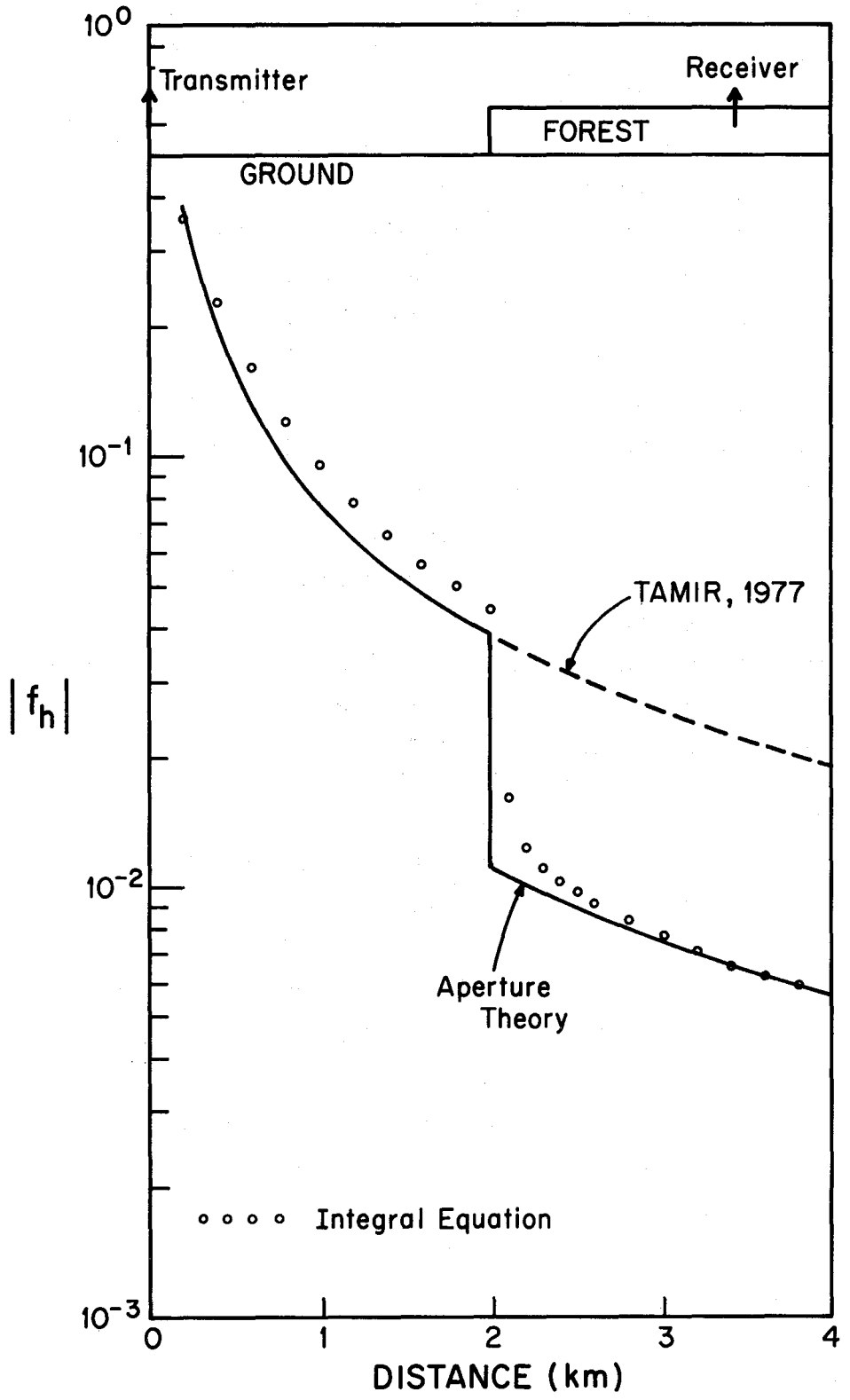

Figure 6. Propagation from a clearing to a forest for a frequency of 10 MHz.

5.1 Forest Cover

During the 1960's there was a great deal of activity in determining the electrical properties of forests in Southeast Asia (Jansky and Bailey, 1966; Parker and Makarabhiromya, 1967). A later workshop (Wait et al., 1974) dealt with many aspects of propagation in forested areas. A general conclusion (Dence and Tamir, 1969) was reached that the equivalent slab model for forests is generally valid for frequencies below about 200 MHz.

Dence and Tamir (1969) refer to three types of forest: "thin," "average," and "dense." The parameters for the slab and the ground for these forest types are given in Table 1. Note that the forest slab is assumed to be isotropic ($\varepsilon_h=\varepsilon_v$ and $\sigma_h=\sigma_v$). The "average" forest is probably most characteristic of Southeast Asia.

A report by the Defense Intelligence Agency (1971) states that the forests of West Germany fall between the "thin" and "average" forests of Dence and Tamir (1969) in Table 1. However, the average tree height is 20 m which corresponds to the "dense" forest of Table 1. Actually the forests of West Germany include both coniferous and deciduous trees, and it seems unlikely that one set of parameters can characterize both types of forests well.

In order to obtain better slab parameters for German forests (or any other forests), two approaches are possible. One is to make ground-wave transmission measurements and to adjust the slab parameters in the theoretical model until a good fit to the measured data is obtained. This is essentially the approach which Causebrook (1978a) used to obtain parameters for the surface impedance of built-up areas in the vicinity of London. A second approach is to attempt to measure the equivalent slab parameters directly (Parker and Hagn, 1966). The first approach has the disadvantage of not yielding any direct information on the slab parameters, but has the advantage of yielding useful transmission results as well as data for fitting slab parameters.

5.2 Built-up Areas

The primary difficulty in characterizing the effect of buildings on HF ground-wave propagation is that the individual buildings are not necessarily small compared to a wavelength. For electrically small hemispherical losses on a perfectly conducting ground, Wait (1959) has shown that an inductive surface impedance results from induced electric and magnetic dipoles in the hemispheres. At MF, Causebrook (1978a) has obtained good agreement between theory and propagation measurements by representing built-up areas by an equivalent surface impedance.

Table 1. Characteristic Parameters of Typical Forests
(Dence and Tamir, 1969)

Parameter		Forest Type		
		"Thin"	"Average"	"Dense"
Tree height	D (m)	5	10	20
Forest	$\varepsilon_v = \varepsilon_h$	1.03	1.1	1.3
	$\sigma_v = \sigma_h$ (S/m)	3×10^{-5}	10^{-4}	3×10^{-4}
Ground	ε_g	5	20	50
	σ_g (S/m)	10^{-3}	10^{-2}	10^{-1}

After attempting a number of approaches which proved to be unsatisfactory at HF, we settled on a fairly simple approach which utilized Causebrook's (1978a) low density theory. We start by taking the low frequency limit of Δ as given by (9). In this case, $v_o D$ is small and we have

$$\tanh (v_o D) \simeq v_o D \quad . \tag{41}$$

Substituting (41) into (9) and keeping only the leading term in $v_o D$, we have

$$\Delta \simeq \Delta_2 + v_o D \Delta_1 \left(1 - \frac{\Delta_2^2}{\Delta_1^2}\right) \quad . \tag{42}$$

For most cases, $|\Delta_2|$ will be much less than $|\Delta_1|$ at low frequencies, and the last term in (42) can be neglected to give the final result

$$\begin{aligned} \Delta &\simeq \Delta_2 + v_o D \Delta_1 \\ &= \Delta_2 + ikD \left(1 - \frac{1}{\varepsilon_{vc}}\right). \end{aligned} \tag{43}$$

Causebrook's (1978a) low density theory gives the following result:

$$\Delta \simeq \Delta(0) + ikD \left[1 - \frac{\ln(1 + 10\ B)}{10\ B}\right] , \tag{44}$$

where B is the fractional building coverage of the ground and $\Delta(0)$ is the impedance at the surface of the ground. Thus we can equate Δ_2 to $\Delta(0)$. The second terms in (43) and (44) can then be equated to yield the following expression for ε_{vc}:

$$\varepsilon_{vc} = \frac{10\ B}{\ln(1 + 10\ B)} \quad . \tag{45}$$

Since B is real and positive and less than one, (45) can be satisfied by the following:

$$\varepsilon_v = \frac{10\ B}{\ln(1 + 10\ B)} \text{ and } \sigma_v = 0 \quad . \tag{46}$$

As the building density B approaches zero, ε_v approaches unity as it should for free space. A plot of ε_v as a function of B is given in Figure 7. Strictly speaking, B should be limited to values much less than unity since (46) was derived on the basis of low density. Although the previous result provides no information on the horizontal parameters of the slab, ε_h and σ_h, it seems reasonable to equate them to the vertical parameters on the assumption of roughly cubic buildings. Thus the final result for the slab parameters is

$$\varepsilon_v = \varepsilon_h = \frac{10\ B}{\ln(1 + 10\ B)} \tag{47}$$

and

$$\sigma_v = \sigma_h = 0 \quad .$$

For cases where built-up areas are mixed with forest, it seems reasonable to increase ε_v, ε_h, σ_v, and σ_h by the appropriate forest values. Also, even though the result in (47) is derived by matching the slab impedance to Causebrook's (1978a) result in the low frequency (small kD) limit, we assume that the slab parameters are frequency independent. This will mean that when kD is no longer small Δ will be different from Causebrook's (1978a) result in (44). However, since we have converted Causebrook's result into equivalent slab parameters, we no longer have the restriction of small kD. Thus we can use (47) at HF. However, improvements in (47) can probably be made once we have propagation measurements through built-up areas at HF.

5.3 Snow Cover

The electrical properties of snow and ice have been reviewed by Evans (1965). For dry snow, the dielectric constant of snow varies almost linearly with density

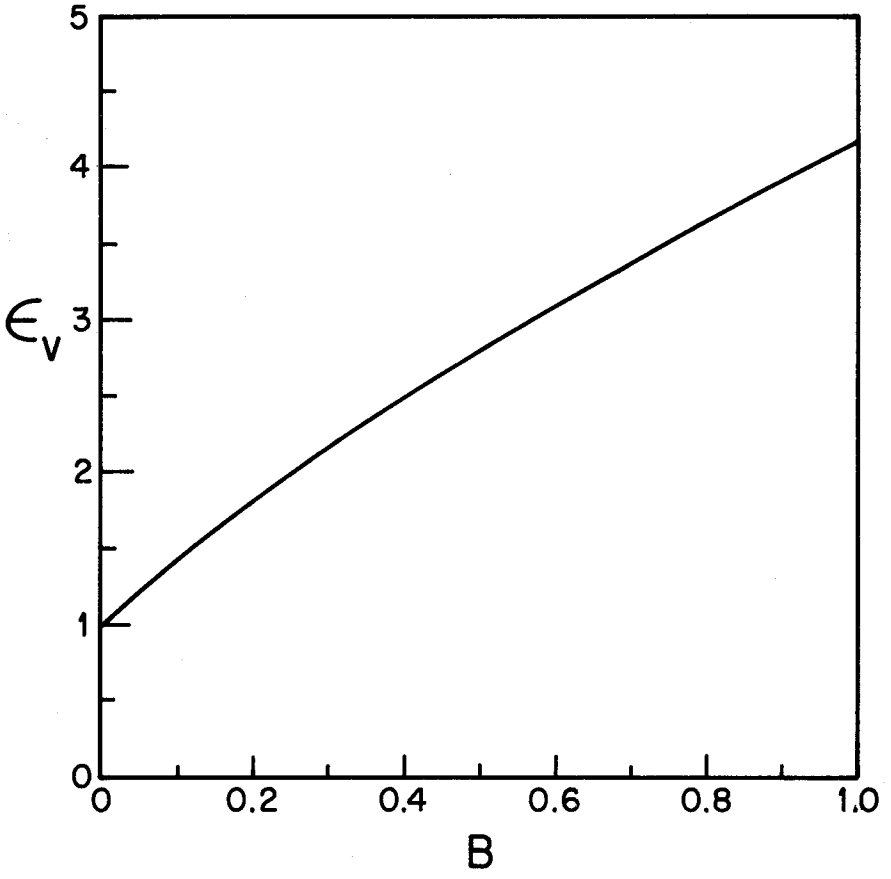

Figure 7. Relative permittivity ε_v versus building density B.

from a value of unity for free space to approximately 3 at the density of ice. The conductivity of dry snow is very small.

The presence of liquid water in snow can raise both the dielectric constant and the conductivity dramatically (Evans, 1965). At a frequency of 1 MHz, Von Hippel (1954) has measured a dielectric constant of 1.2 and a conductivity of 1.85×10^{-6} S/m for freshly fallen snow and a dielectric constant of 1.55 and a conductivity of 2.5×10^{-5} S/m for hard-packed snow followed by light rain. No anisotropy is noted for snow by Evans (1965) or Von Hippel (1954).

To illustrate the effect of snow accumulation on propagation, we show the change in surface impedance as a function of frequency in Table 2. We take the larger value of permittivity for hard-packed, wet snow in order to show the largest effect which is likely for a given snow depth. Although the assumption of a frequency independent conductivity is not correct, the loss tangent for snow is so small that the error in conductivity is unimportant. As seen in Table 1, the effect of increasing snow depth is to increase both the magnitude and phase of Δ, but not greatly. As seen by the flat-earth result in (6), an increase in $|\Delta|$ will result in a decrease in field strength. In Figure 8 we illustrate the effect for a spherical earth. The curves in Figure 8 were computed by a numerically efficient

Table 2. Magnitude and Phase of Surface Impedance Δ as a Function of Snow Depth D. Parameters:

$$\varepsilon_v = \varepsilon_h = 1.55,\ \sigma_v = \sigma_h = 2.5 \times 10^{-5}\ \text{S/m},$$
$$\varepsilon_g = 10,\ \sigma_g = 10^{-2}\ \text{S/m}$$

Frequency \ D	0	0.5 m	1.0 m
3 MHz	$0.128 \angle 39.8°$	$0.138 \angle 42.6°$	$0.147 \angle 45.1°$
10 MHz	$0.218 \angle 29.2°$	$0.244 \angle 34.9°$	$0.274 \angle 39.3°$
30 MHz	$0.282 \angle 14.1°$	$0.338 \angle 25.5°$	$0.427 \angle 30.8°$

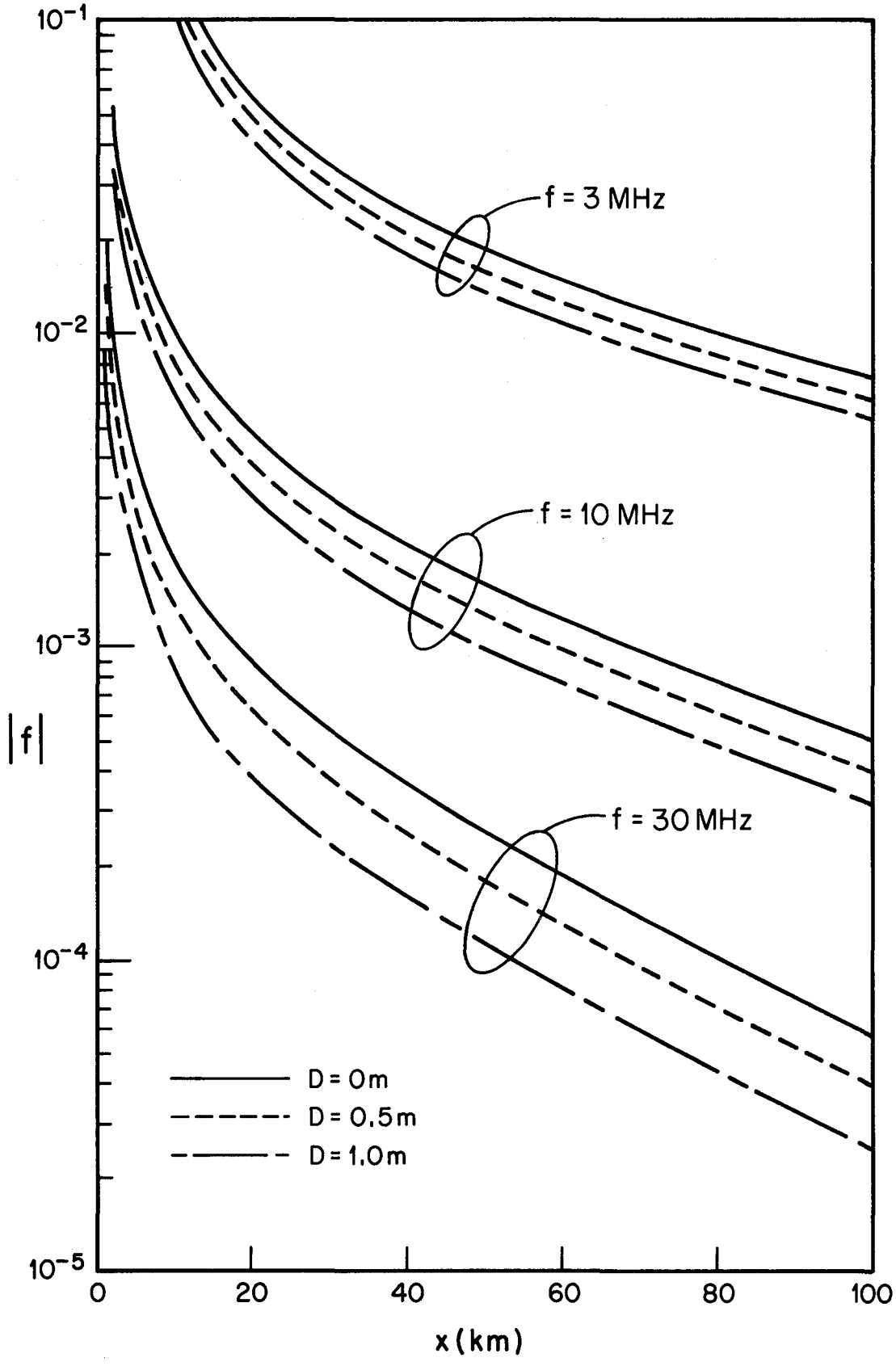

Figure 8. Magnitude of the spherical earth attenuation function as a function of frequency and snow depth D. Parameters: $\varepsilon_v = \varepsilon_h = 1.55$, $\sigma_v = \sigma_h = 2.5 \times 10^{-5}$ S/m, $\varepsilon_g = 10$, $\sigma_g = 10^{-2}$ S/m.

method (Hill and Wait, 1980) which has been used for calculations of ground-wave propagation over sea ice (Hill and Wait, 1981b).

In the case of HF ground-wave propagation over sea ice, a trapped surface wave (Hill and Wait, 1981b) was supported because of the highly inductive surface impedance. As seen in Table 2, a layer of snow over ground does not produce a phase angle of Δ much larger than 45°. Consequently, the main effect of the snow layer is to increase the magnitude of Δ and to decrease the ground-wave field strength. For small depths the effect is small, but for depths of packed snow on the order of a meter the effect becomes significant. As seen in Figure 8, the effect is more prominent at the higher frequencies.

6. SPECIFIC PATH CALCULATIONS

In this section we apply program WAGSLAB to several paths. The smooth paths in the Netherlands are a good check on WAGSLAB because the exact residue series solution for a spherical earth (Hill and Wait, 1980) is available as a check. Both earth curvature and atmospheric refraction are included in WAGSLAB by inputting the appropriate earth radius. In all cases, we used the 4/3 earth radius value ($a \approx 8500$ km) to account for normal atmospheric refraction (Bremmer, 1949; Wait, 1962), but other values could be used for different atmospheric conditions.

The irregular, forested terrain in southern West Germany presents a greater challenge to the integral equation approach. We have no experimental results as checks for these paths, but reciprocity provides a good theoretical check. Also, we have found that the multiple knife-edge model of Vogler (1981) is in reasonably good agreement with the integral equation solution for long, rough paths.

6.1 Smooth Paths in the Netherlands

Measurements of field strength and bit error rate have recently been carried out on paths of 60 km and 80 km in the Netherlands (Van der Vis, 1979). The frequencies range from 2 MHz to 30 MHz, and both vertical and horizontal polarization were transmitted and received. Both paths had the same transmitter, and the two paths were nearly in line. An examination of topographic maps of the area revealed that both paths were over very smooth (less than a few meters in elevation change), unforested terrain with no cities. The main feature of interest was a section of low ground conductivity (dry, sandy soil) at the end of the 80 km path. Consequently, we modeled the path with two smooth sections as shown in Figure 9. Unfortunately, no ground conductivity measurements were made, but we assume the values suggested by Van der Vis (1979): $\varepsilon_g = 15$ and $\sigma_g = 10^{-2}$ S/m for the first

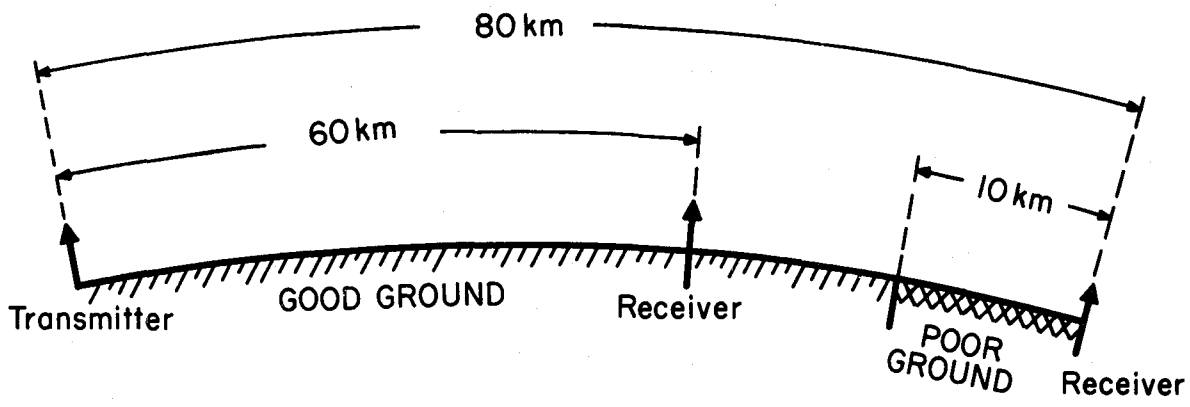

Figure 9. Smooth path in the Netherlands with receiving sites at 60 km and 80 km. The first 70 km has good ground (ε_g = 15 and σ_g = 10^{-2} S/m), and the last 10 km has poor ground (ε_g = 3 and σ_g = 10^{-4} S/m).

70 km of good ground and ε_g=3 and σ_g=10^{-4} S/m for the remaining section of poor ground.

In Figures 10-12, we show the magnitude of the attenuation function f along the path for three different frequencies. As usual, the attenuation function is defined as the ratio of the vertical electric field to that over flat, perfectly conducting ground. Both the transmitting and receiving antennas are assumed to be located at the surface, and the measured data are adjusted to account for the antenna heights by assuming the height-gain function in (13). In each case the integral equation result shows a rapid drop in field strength beyond 70 km because of the decrease in ground constants. The measured data are consistent with this drop, but a detailed comparison is not possible because measurements are available only at 60 km and 80 km. It appears that the ground conductivity and dielectric constant which were suggested by Van der Vis (1979) for the first 70 km were a little too high. Lower values would have provided a better fit with the measurements.

For comparison in Figures 10-12, we also show the spherical earth and flat earth results for a uniform path (Hill and Wait, 1980). Because the integral equation solution assumes no backscatter, it should agree with the spherical earth theory over the first 70 km. The accuracy of the integral equation solution becomes

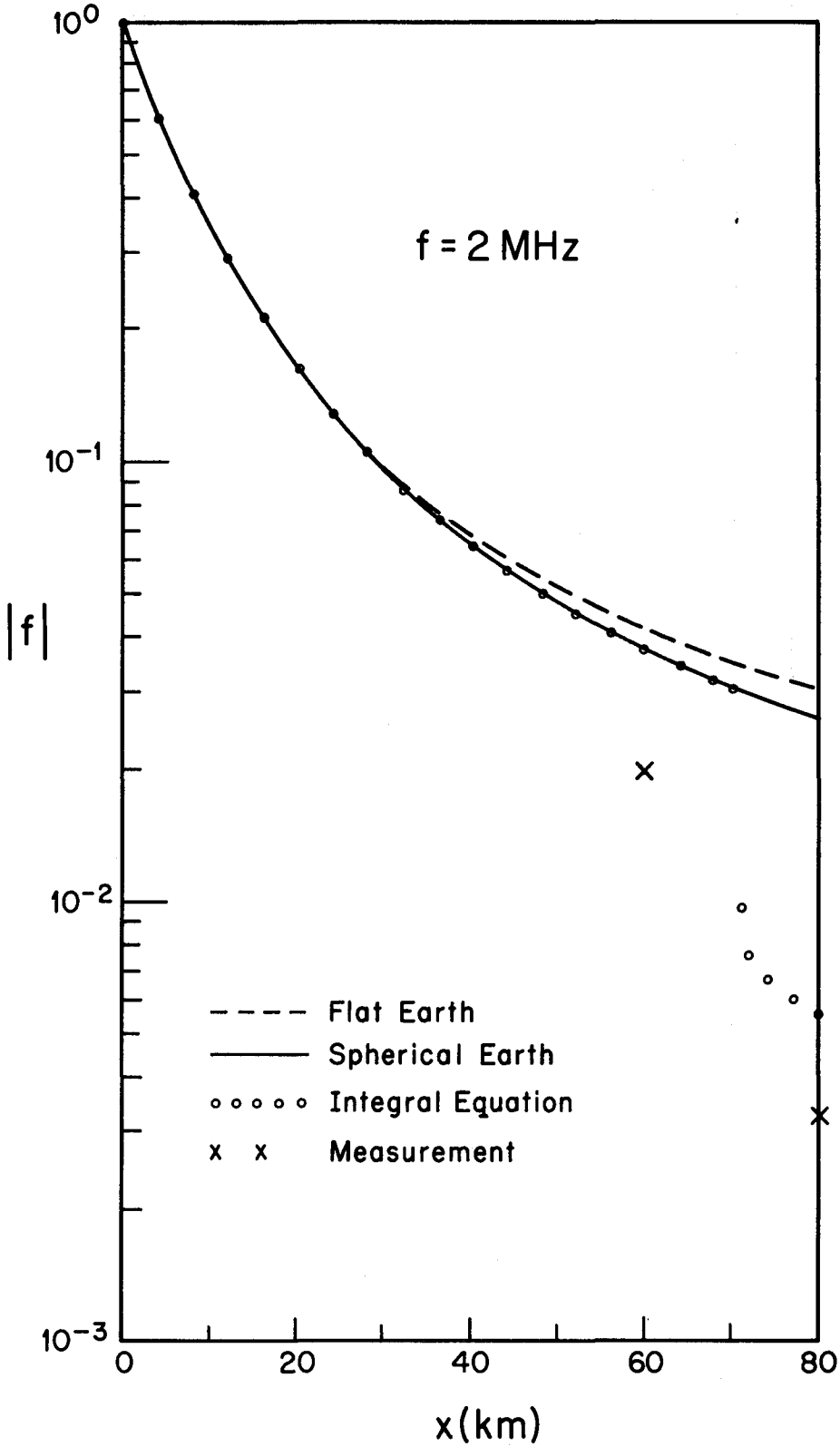

Figure 10. Comparison of measurement with three theories at 2 MHz for a smooth path in the Netherlands. Only the integral equation solution takes into account the poor ground section shown in Figure 9.

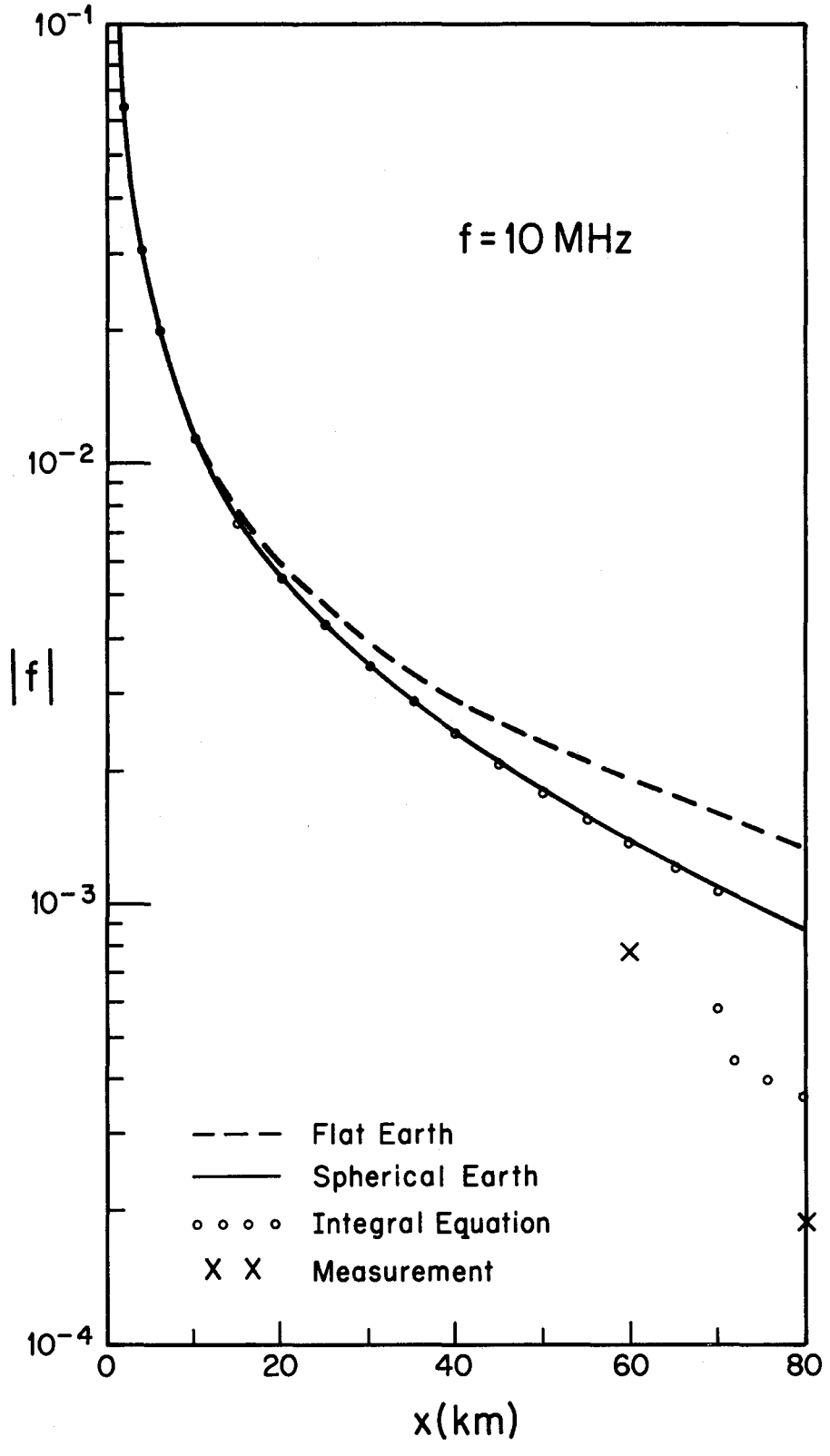

Figure 11. Comparison of measurement with three theories at 10 MHz for a smooth path in the Netherlands. Only the integral equation solution takes into account the poor ground section shown in Figure 9.

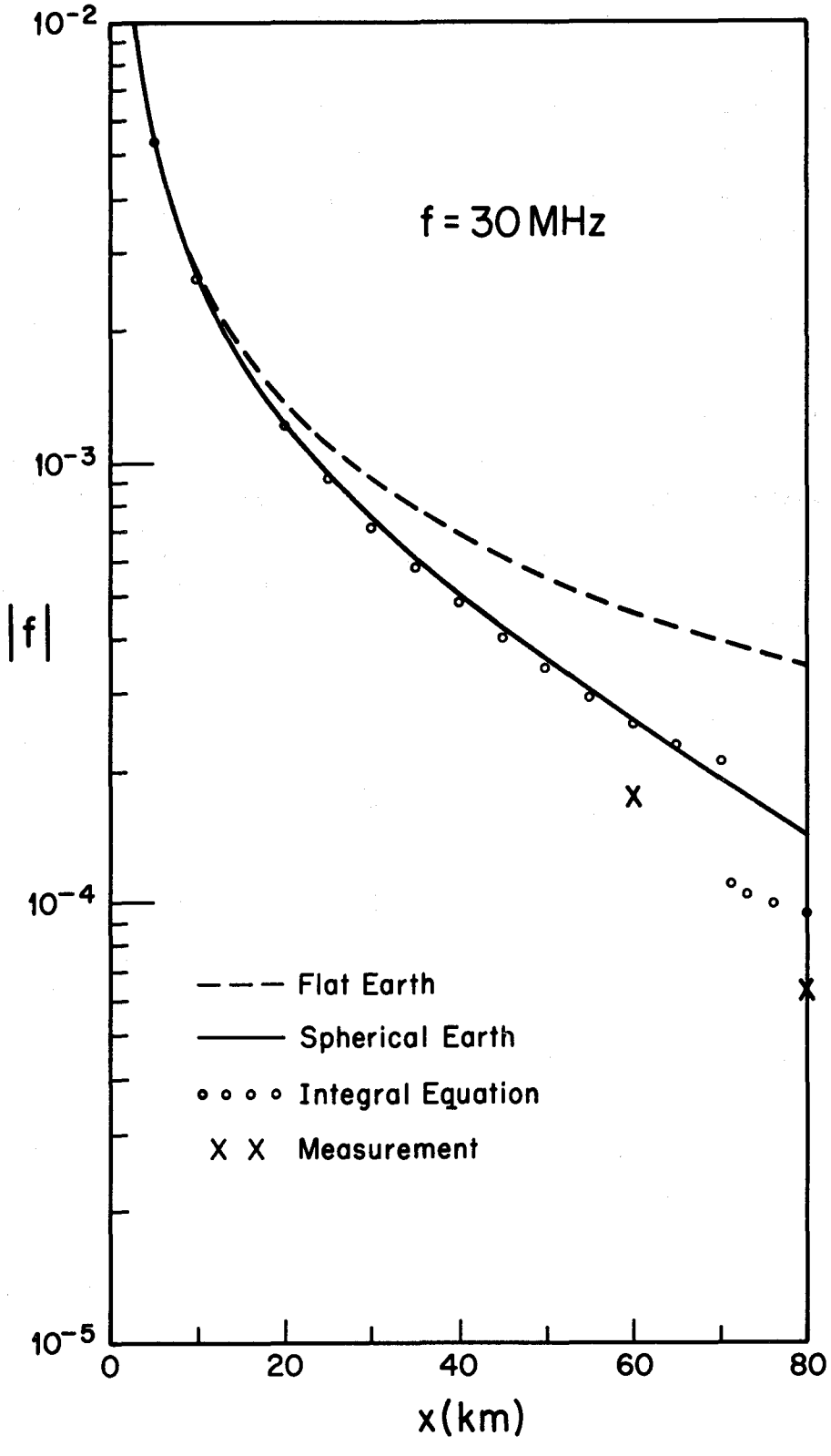

Figure 12. Comparison of measurement with three theories at 30 MHz for a smooth path in the Netherlands. Only the integral equation solution takes into account the poor ground section shown in Figure 9.

harder to maintain at higher frequencies and longer paths. At 30 MHz, it was necessary to sample approximately every 40 m (equals 4 wavelengths) along the path to obtain the agreement (which is not perfect) in Figure 12. This resulted in 2000 sample points along the path and an execution time of approximately 15 min on a large mainframe computer. This rather long run time decreases rapidly as the frequency is decreased as indicated by (25). Thus program WAGSLAB can be considered very efficient for the lower portion of the HF band but only marginally efficient at 30 MHz. It should probably not be used above 30 MHz except for very short paths.

Also shown for comparison in Figures 10-12 is the flat earth result for a uniform path. It is easy to see that earth curvature is not particularly important at 2 MHz but is quite important at 30 MHz. An approximate upper bound in path length and frequency for the validity of flat earth theory can be obtained from examining the spherical earth theory. The earth curvature can normally be neglected when the following inequality is satisfied

$$\left(\frac{ka}{2}\right)^{1/3}\left(\frac{x}{a}\right) << 1 \quad . \tag{48}$$

From examination of numerical results (Hill and Wait, 1980), we can set the right-hand side of (48) equal to 0.2. If we assume a = 8500 km (= 4/3 earth radius), then the maximum path length x_{max} for good agreement between flat and spherical earth theory is given by

$$x_{max} \simeq \frac{38.1}{f_{MHz}^{1/3}} \text{ (km)} \quad , \tag{49}$$

where f_{MHz} is the frequency in megahertz. From (49), x_{max} = 30.2 km at 2 MHz, and x_{max} = 12.3 km at 30 MHz. For x greater than x_{max}, the flat earth theory predicts a field strength which is too high as seen in Figures 10-12. For example, in Figure 12 at a frequency of 30 MHz and a distance of 80 km, the flat earth field strength is a factor of 2.43 greater (= 7.7 dB) than the spherical earth result.

6.2 Irregular, Forested Terrain in West Germany

In order to provide a more demanding test for program WAGSLAB, we examined two paths over irregular, forested terrain in southern West Germany. We have no experimental data for these paths at this time, but there has been some planning for future HF ground wave measurements in the area (NTIA Technical Memorandum 82-80 by Kissick and Adams, limited distribution).

The path which we considered in most detail is a 56.6 km path from Inneringen to Boblingen. The terrain profile shown in Figure 13 was generated from the files of the Defense Mapping Agency. The terrain profile checks very well with the profile which we obtained by hand from 1:50,000 scale maps of the area. The path contains numerous forested sections and three short sections with buildings. For the forested sections, we chose a height D of 20 m and the "average" electrical properties of Table 1. For the urban areas we did not have available information on building height and density. We chose a building height D of 10 m and a building density B of 0.2 (Causebrook, 1978a). From (47), this yields dielectric constants of $\varepsilon_v=\varepsilon_h=1.82$. For conductivity we took the value for "thin" forest, $\sigma_v=\sigma_h=3 \times 10^{-5}$ S/m, rather than $\sigma_v=\sigma_h=0$ as given by (47) because it seems likely that some trees are present in the urban areas. The actual locations of the forest and urban slabs are given by the input data in the sample computer run in Appendix C. We also had to guess at the ground parameters and chose the following values for fairly good ground over the entire path: $\varepsilon_g=10$ and $\sigma_g=10^{-2}$ S/m.

In Figures 14-18, we show propagation from Inneringen to Boblingen both with and without the forest and building slabs at five frequencies from 2 MHz to 30 MHz. In all cases, both the transmitting and receiving antennas are located at the surface of the ground ($h_a=h_r=-D$). As a result, the dotted curves which include the slabs are more irregular because the height-gain function $G(h_r)$ is discontinuous as the receiving antenna moves from bare ground into a slab. This results in a discontinuous value of f_h which is proportional to $G(h_r)$ as shown by (21). The dependence of G on height both in and above the forest slab is shown in Figure 19. In most cases, $|G(h_r)|$ is less than unity in the slab and increases from unity above the slab.

The height-gain effect can be considered a local effect on the field, but the normalized surface impedance $\Delta(\xi)$ influences the field at all points for $x > \xi$ as seen by (20). In most cases, $|\Delta|$ is greater in the forest region than over bare ground. Consequently, the dotted curves in Figures 14-18 which include the forest and urban slabs generally lie below the solid curves for bare ground. At the higher frequencies where the terrain roughness is more important, the effect of the slabs is less dominant. The analytical solution for a spherical earth (Hill and Wait, 1981b) is shown in Figure 20 for both bare ground and forest slab cover. The forest cover has a large effect at 5 MHz, but a much smaller effect at 20 MHz and 30 MHz where diffraction loss becomes important.

Two difficulties with the integral equation approach are that computation time becomes large for long, rough paths at high frequencies as indicated by (25) and

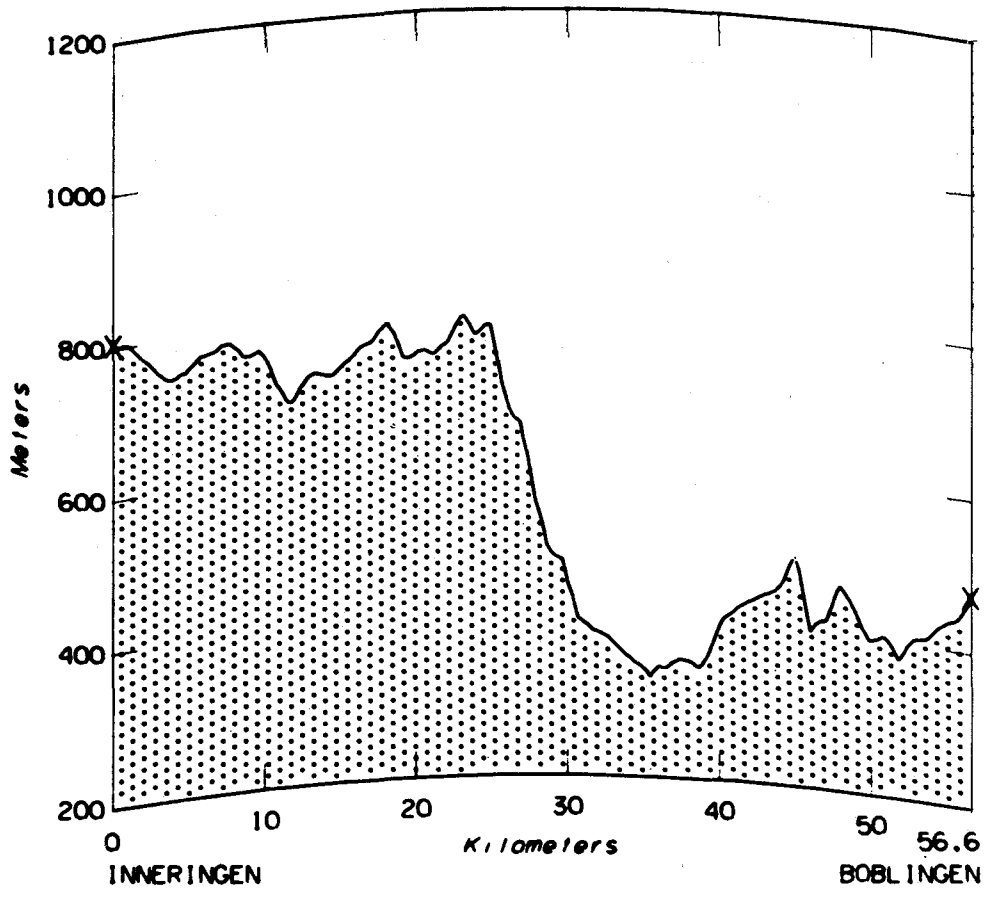

Figure 13. Terrain profile for the path from Inneringen to Boblingen.

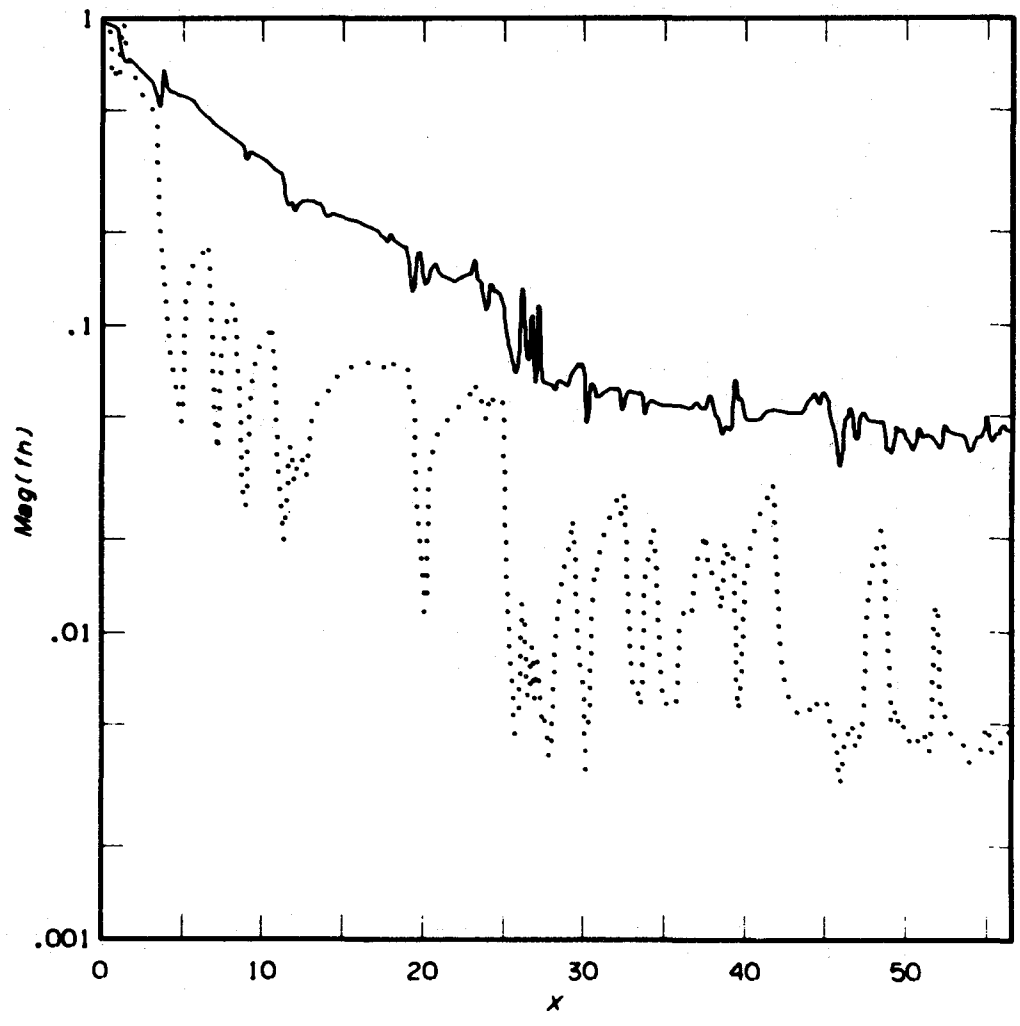

Figure 14. Propagation from Inneringen to Boblingen at 2 MHz. The solid curve is for bare ground, and the dotted curve includes the forest and urban slabs.

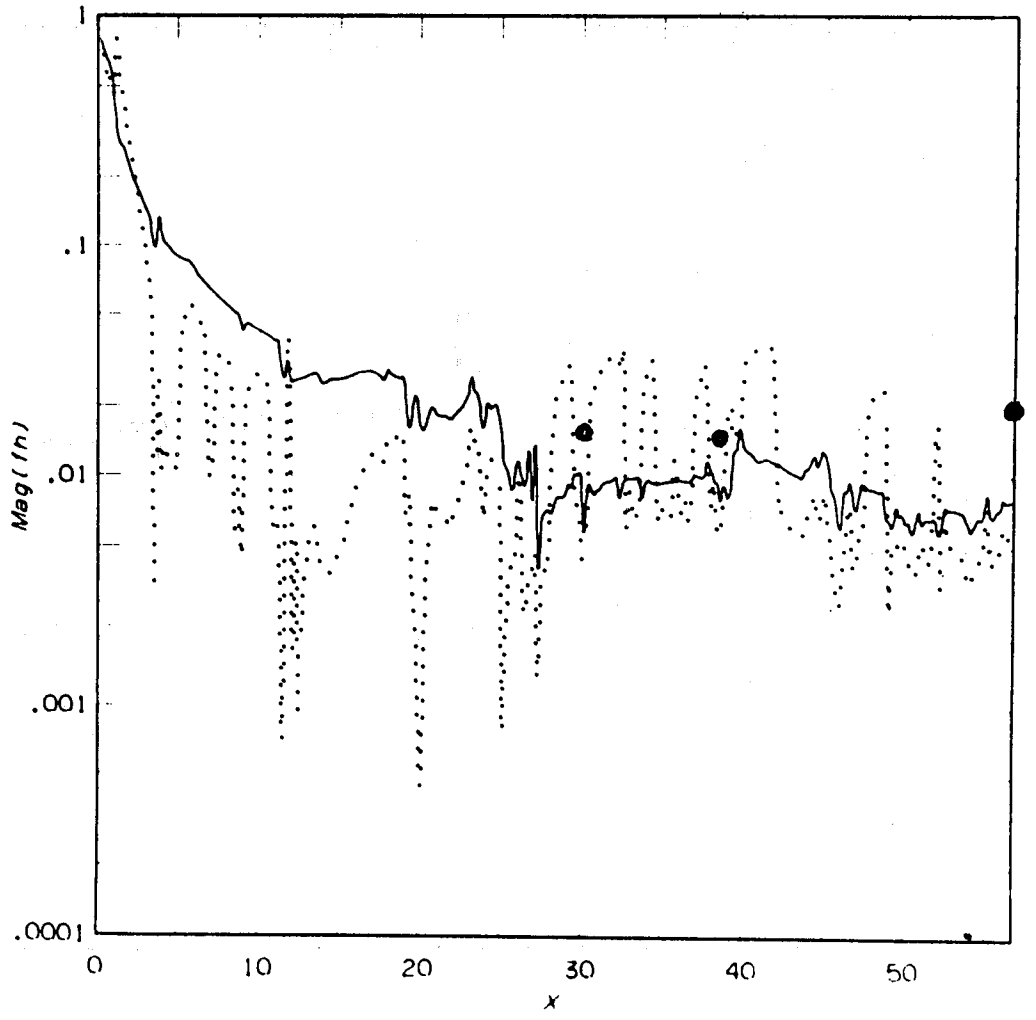

Figure 15. Propagation from Inneringen to Boblingen at 5 MHz. The solid curve is for bare ground, and the dotted curve includes the forest and urban slabs. The circles are obtained from multiple knife-edge diffraction theory.

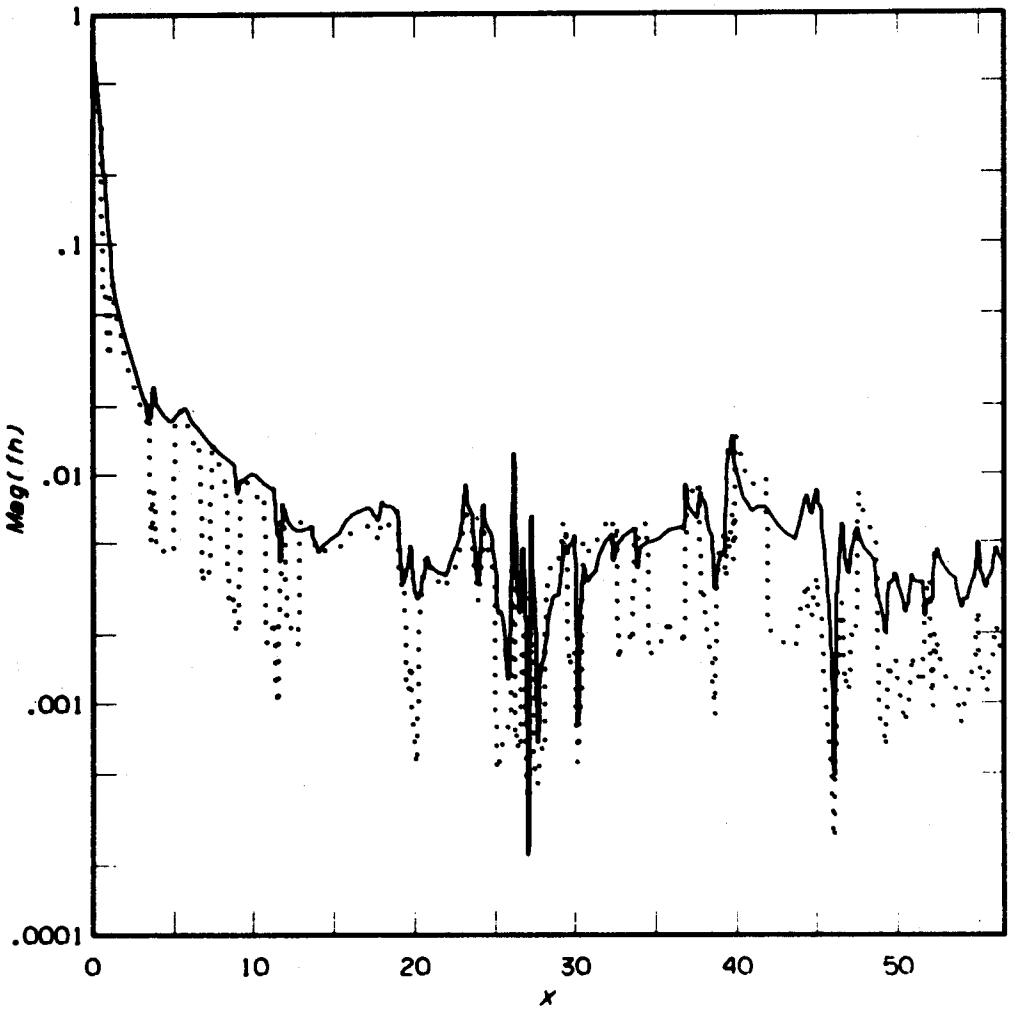

Figure 16. Propagation from Inneringen to Boblingen at 10 MHz. The solid curve is for bare ground, and the dotted curve includes the forest and urban slabs.

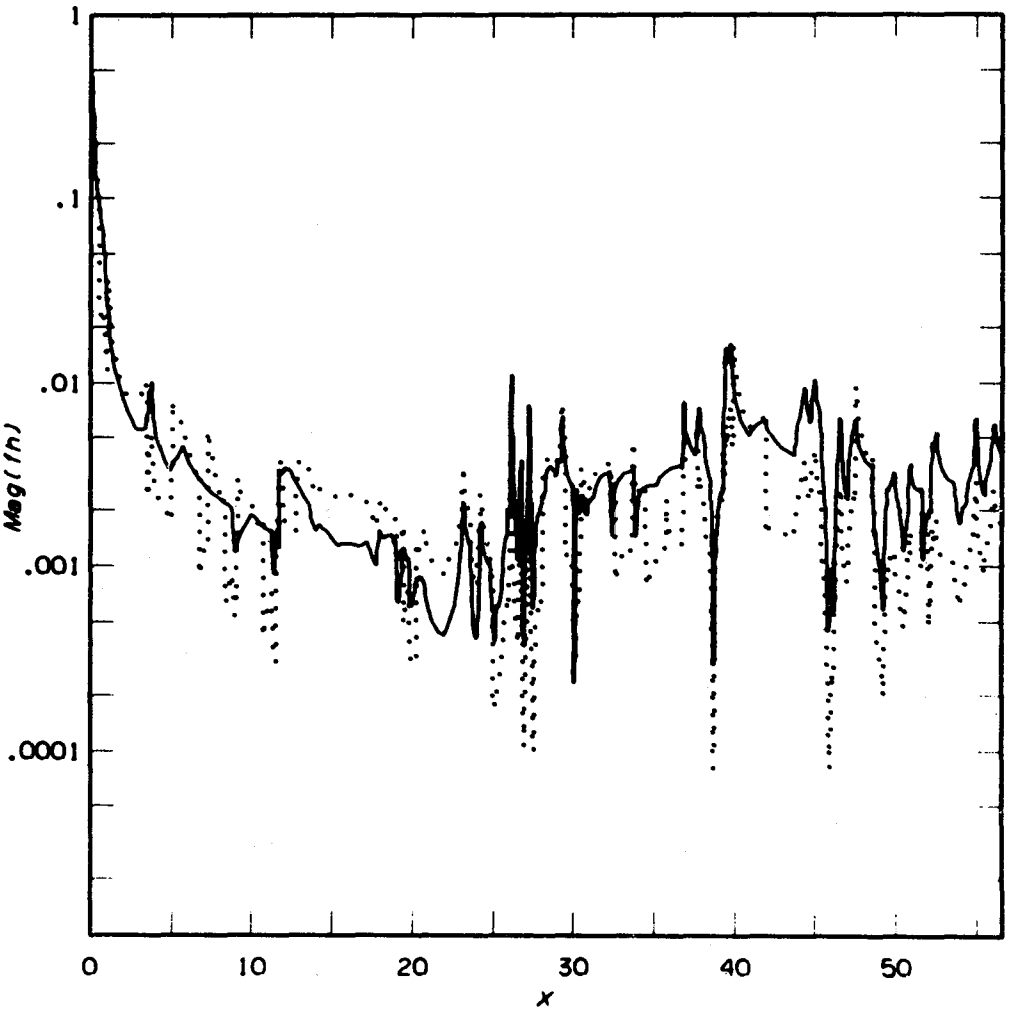

Figure 17. Propagation from Inneringen to Boblingen at 20 MHz. The solid curve is for bare ground, and the dotted curve includes the forest and urban slabs.

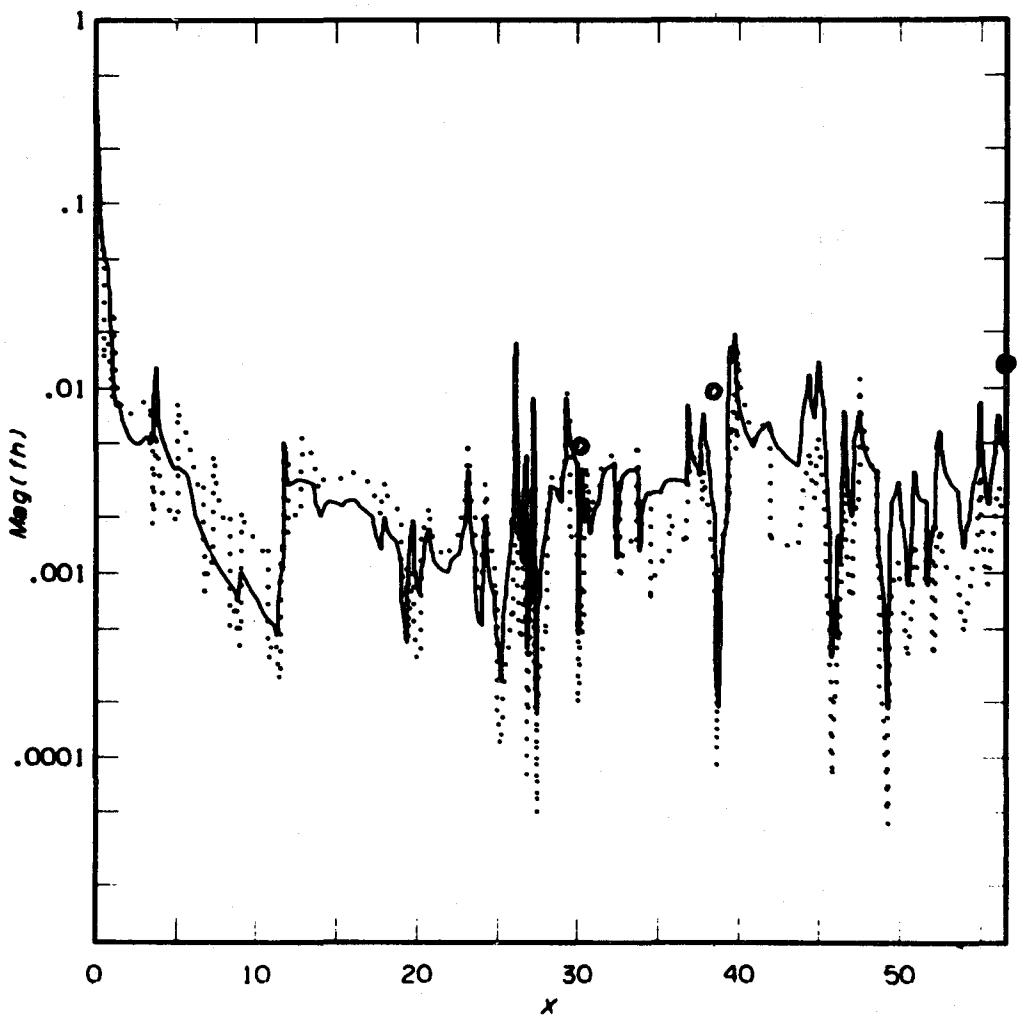

Figure 18. Propagation from Inneringen to Boblingen at 30 MHz. The solid curve is for bare ground, and the dotted curve includes the forest and urban slabs. The circles are obtained from multiple knife-edge diffraction theory.

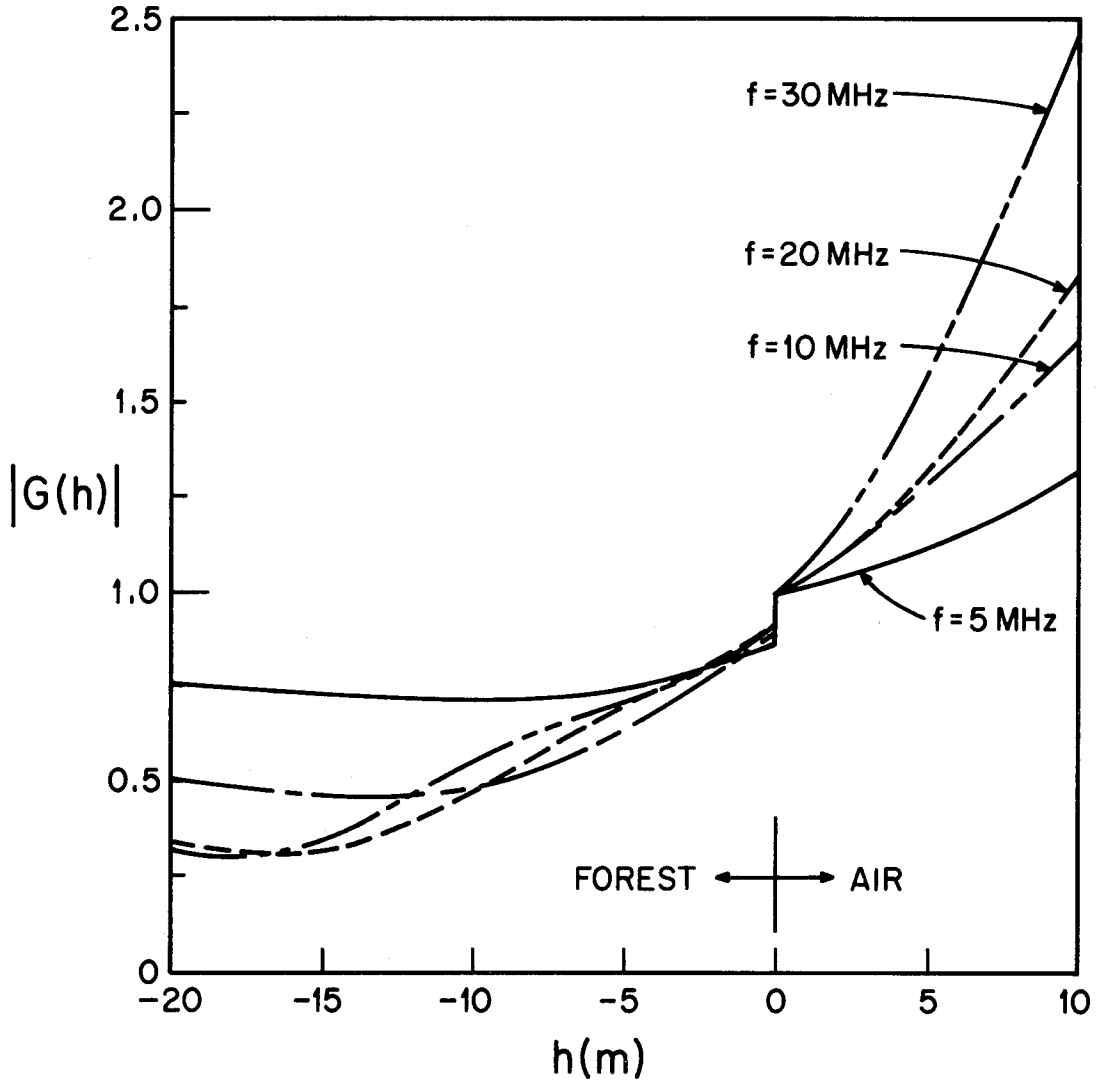

Figure 19. Magnitude of height-gain function in forest slab and in air. Parameters: D = 20 m, $\varepsilon_v = \varepsilon_h = 1.1$, $\sigma_v = \sigma_h = 10^{-4}$ S/m, $\varepsilon_g = 10$, and $\sigma_g = 10^{-2}$ S/m.

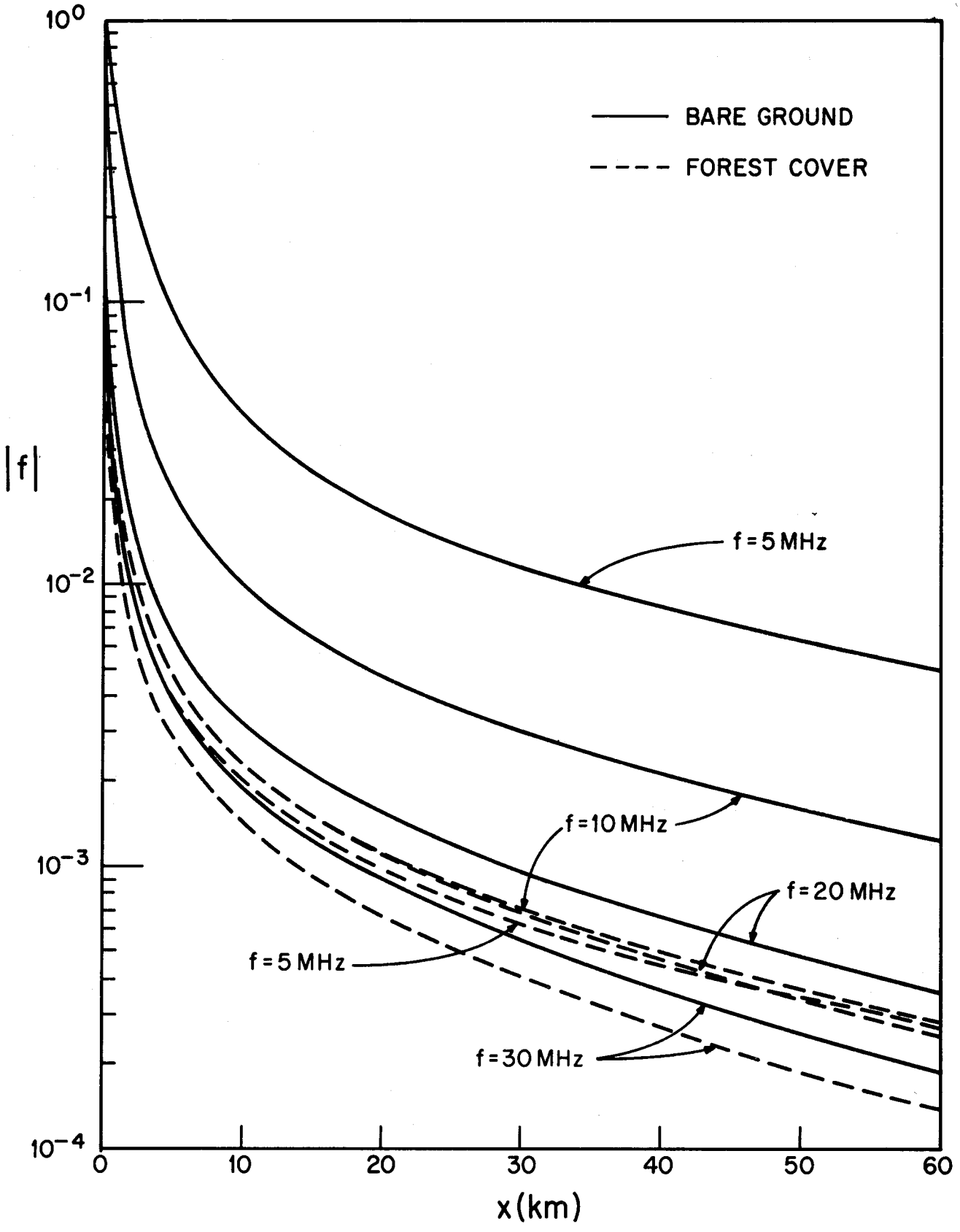

Figure 20. Spherical earth attenuation function for bare ground and with forest cover. Parameters: D = 20 m, $\varepsilon_v = \varepsilon_h = 1.1$, $\sigma_v = \sigma_h = 10^{-4}$ S/m, $\varepsilon_g = 10$, and $\sigma_g = 10^{-2}$ S/m.

also precision loss occurs for long rough paths. It is generally difficult to predict the precise limitations of the integral equation approach (Ott, 1971b), but generally the results start to appear noisy with large oscillations when the integral equation approach starts to fail. This behavior is difficult to identify because the actual field variation for rough paths at high frequencies contains oscillations due to multipath. A good example is the change in character of the Inneringen to Bollingen results as the frequency is increased in Figures 14-18. The 30 MHz curve is much noisier than the 2 MHz curve. Also the average signal level does not continue to drop for large distances. To check the behavior, we compared the integral equation result with Vogler's (1981) multiple knife edge calculation for the same path. Vogler's results are shown at 5 MHz in Figure 15 and at 30 MHz in Figure 18, and each point was obtained by fitting the terrain profile with ten equivalent knife edges. The agreement is slightly better at 30 MHz, but is fairly good even at 5 MHz. Vogler's results at 30 MHz actually predict a higher field strength at 56.6 km than at 30 km because of the shadowing which occurs from the steep terrain slope between 25 km and 30 km.

A second check for the integral equation solution is reciprocity. If we reverse the transmitting and receiving points (Monteath, 1973), the results should be unchanged. In Figures 21-23 we show the integral equation result for propagation in both directions over the Inningen to Boblingen path. If reciprocity is satisfied, then the two results at the end of the path (x=56.6 km) should be identical. Because of the way the terrain profile is handled, we would actually expect some small differences. It is clear that reciprocity is very well satisfied at 2 MHz and 5 MHz, but that some difference occurs at 20 MHz. We can conclude that some accuracy is lost at 20 MHz. Perhaps agreement could be improved by increasing the number of sample points, but we did not attempt this. The good agreement with the multiple knife edge results at 30 MHz in Figure 18 indicates that the integral equation solution can produce useful results at the upper end of the HF band even if some accuracy is lost.

A second terrain profile which runs from Inneringen to Lechfeld is shown in Figure 24. This path is longer (116.5 km), but much smoother than the Inneringen to Boblingen path in Figure 13. Also this path is less heavily forested than the Inneringen to Boblingen path and runs through a great deal of farm and pasture land. Consequently, we did not consider any forest or building effects and used $\varepsilon_g=10$ and $\sigma_g=10^{-2}$ S/M for the ground parameters over the entire path. Again we set both antenna heights h_a and h_r equal to zero.

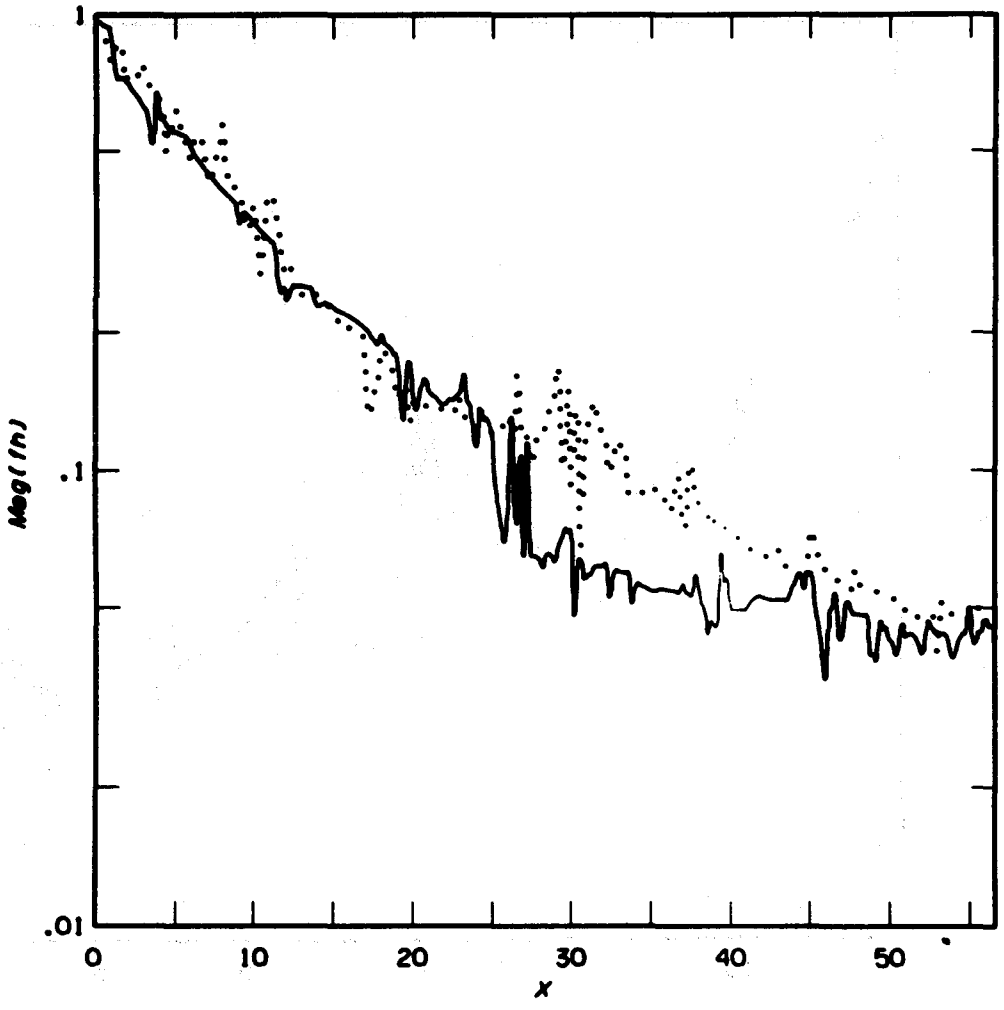

Figure 21. Propagation from Inneringen to Boblingen (solid curve) and in the reverse direction (dotted curve). Both cases are for bare ground, and the frequency is 2 MHz.

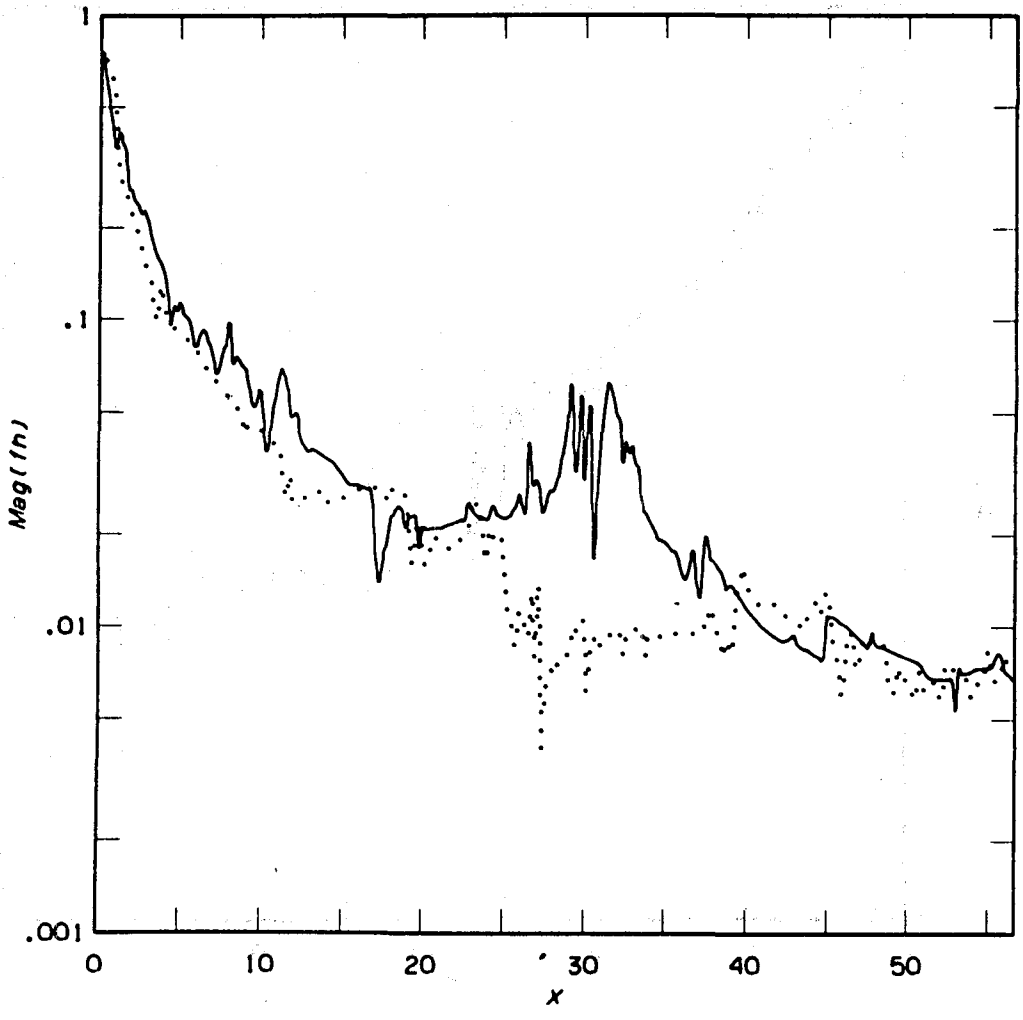

Figure 22. Propagation from Boblingen to Inneringen (solid curve) and in the reverse direction (dotted curve). Both cases are for bare ground, and the frequency is 5 MHz.

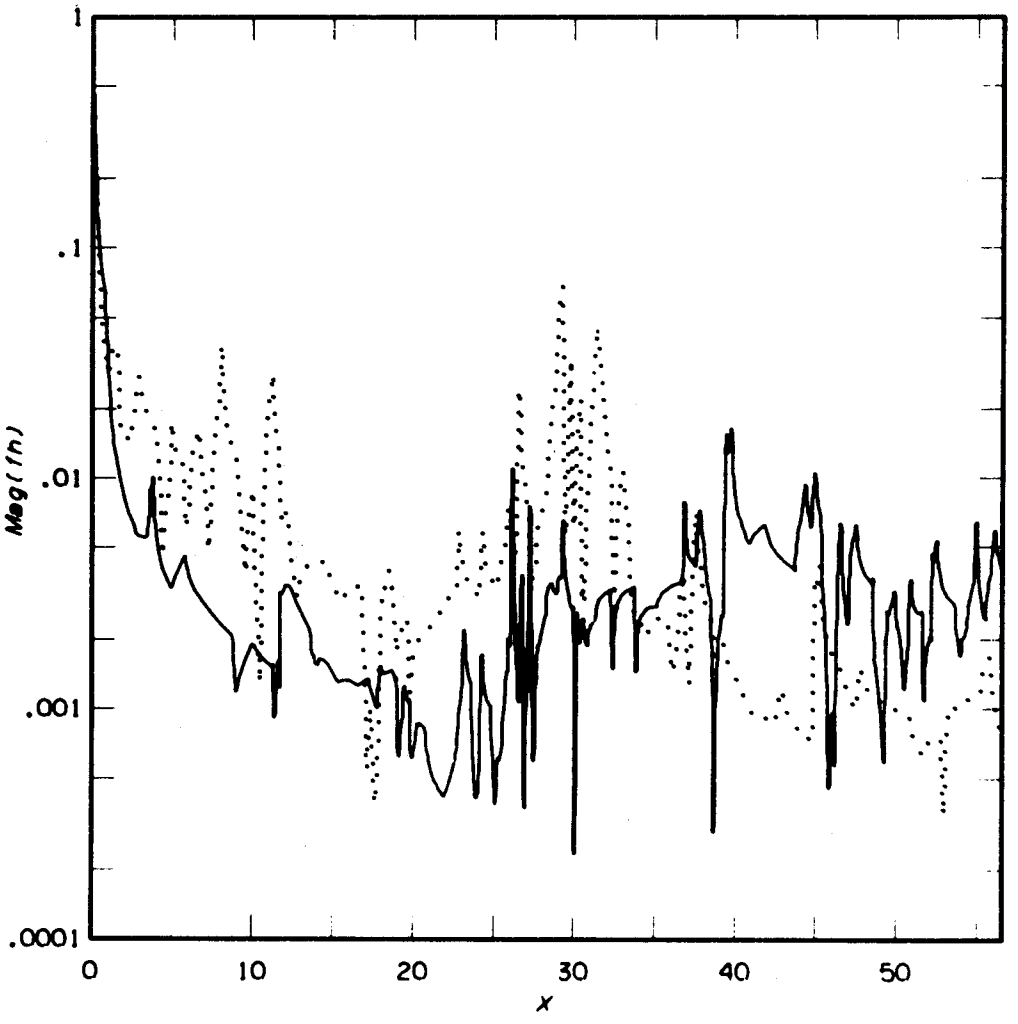

Figure 23. Propagation from Inneringen to Boblingen (solid curve) and in the reverse direction (dotted curve). Both cases are for bare ground, and the frequency is 20 MHz.

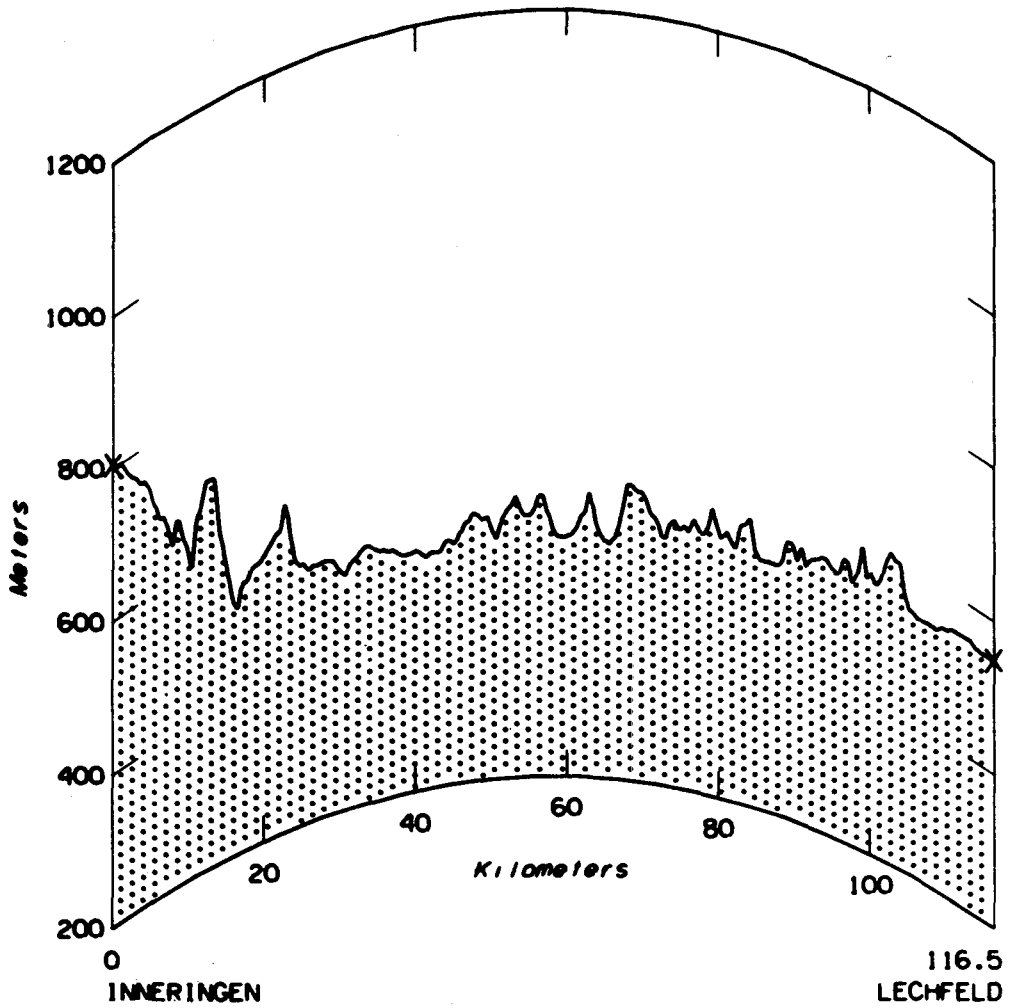

Figure 24. Terrain profile for the path from Inneringen to Lechfeld.

In Figures 25 and 26, we show propagation in both directions at frequencies of 2 MHz and 5 MHz. Since the results are in close agreement at the ends of the paths, reciprocity is well satisfied and the accuracy is probably quite good. We did not run WAGSLAB for higher frequencies over such a long path because of the large computer time which would have been required.

7. CONCLUSIONS AND RECOMMENDATIONS

The main purpose of this report is to describe a theoretical method for predicting HF ground wave propagation over irregular terrain with forest, building, or snow cover. The only method that appears to be general enough for detailed predictions over arbitrary paths is the integral equation method (Ott, 1971a). The approach which was adopted and described in Section 3 was to generalize Ott's program WAGNER (Ott et al., 1979) to allow for the effect of a lossy, anisotropic slab over the earth. The slab parameters can be chosen to match those of forest, snow, or buildings as discussed in Section 5. Although the approach was applied to the HF band (3 MHz - 30 MHz), it actually becomes more efficient as the frequency is decreased. For frequencies above HF, it is probably only useful for short, relatively smooth paths. The new computer code is called WAGSLAB and a user's guide, listing, and sample output are given in Appendix C.

Numerous special cases were considered in this report because they are good checks for WAGSLAB and because they are amenable to analytical solution. For uniform paths which are short enough to neglect earth curvature, the uniform slab model (Tamir, 1967; Wait, 1967a) is adequate. This model is described in Section 2, and the results are cast into a form convenient for ground wave propagation. When the path has two sections as in a forest-to-clearing case, an approximate analytical solution can be derived. This solution is derived and compared with the integral equation solution in Section 4. When the path is uniform, but is long enough for curvature to be important, then spherical earth theory (Hill and Wait, 1981b) can be used. It is compared with the integral equation solution in Section 6.1.

Two long, rough paths were analyzed by program WAGSLAB in Section 6.2. No experimental results were available, but some comparisons were made with multiple knife edge diffraction (Vogler, 1981). Also, reciprocity was checked by running the terrain profiles in each direction. This appears to provide an excellent check for asymmetric paths.

This report represents only a first attempt at ground wave prediction over irregular, forested, and built-up terrain. Numerous improvements and extensions are probably possible, but we recommend the following: (1) detailed comparisons

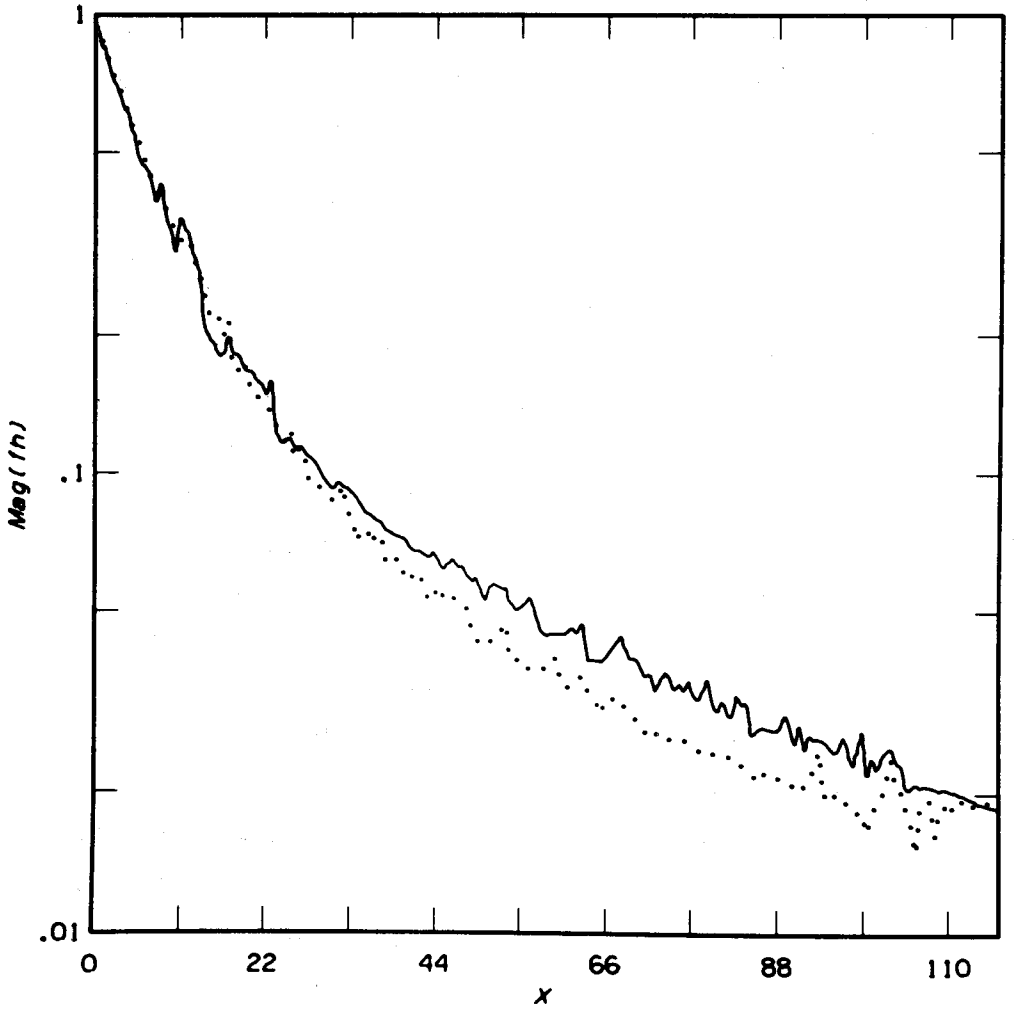

Figure 25. Propagation from Inneringen to Lechfeld (solid) and in the reverse direction (dotted). Both curves are for bare ground, and the frequency is 2 MHz.

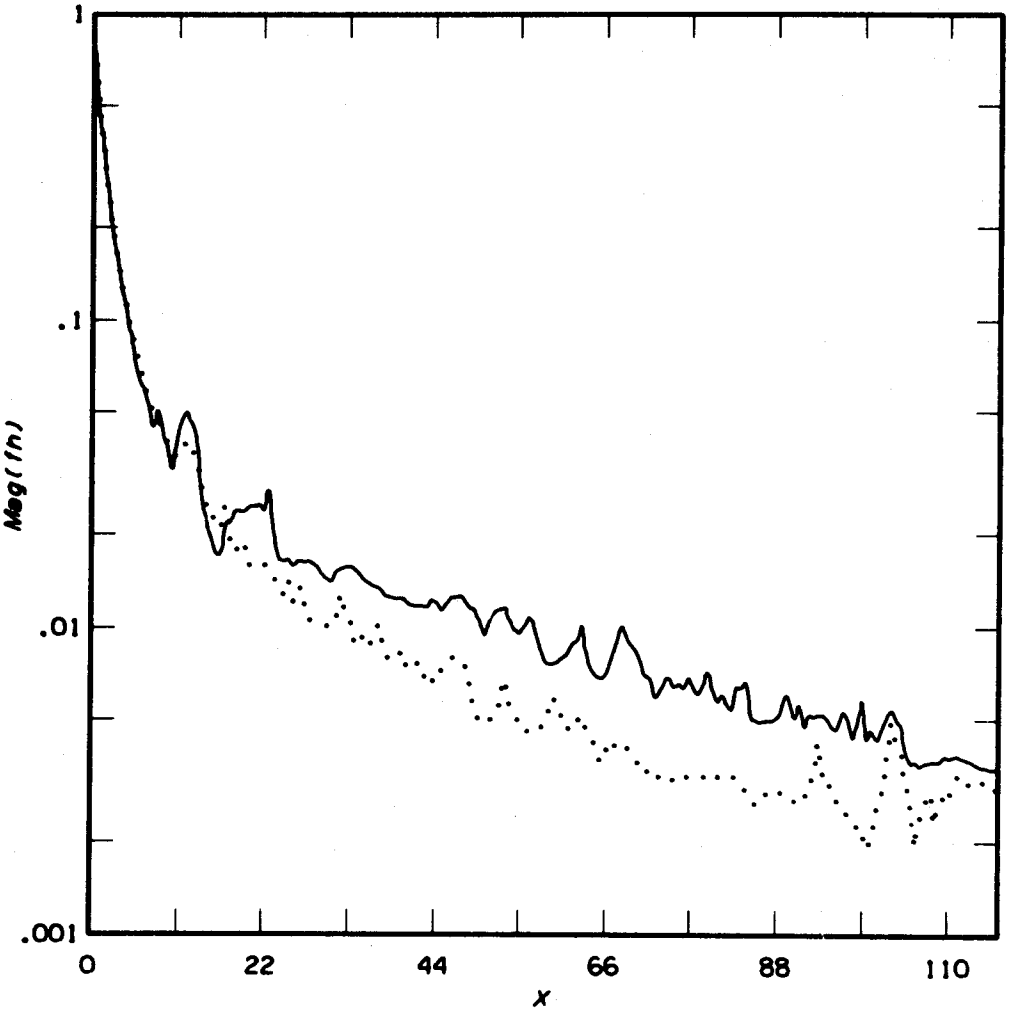

Figure 26. Propagation from Inneringen to Lechfeld (solid) and in the reverse direction (dotted). Both curves are for bare ground, and the frequency is 5 MHz.

with measurements over a variety of radial paths containing forest, building, and snow cover (NTIA Technical Memorandum 82-80 by Kissick and Adams, limited distribution); (2) a complete study of the limits of WAGSLAB for long paths and high frequencies; (3) consideration of a switch from the integral equation approach to multiple knife-edge diffraction for long, rough paths; and (4) the addition of an additional height-gain function for the magnetic field which would be applicable to reception with loop antennas. The height-gain functions for the vertical electric field and the horizontal magnetic field are equal in free space, but are different within the slab medium. This difference has been observed experimentally in cities and forests at MF by Causebrook (1978b). In addition it might be possible after a comparison with measurements to improve the theory for the equivalent slab parameters for cities or to infer the equivalent parameters directly from measurements.

8. ACKNOWLEDGMENTS

The Defense Nuclear Agency (DNA) supported the research described in this report. Major Bernard Romanik and Dr. Patrick Crowley of DNA initiated the idea to develop a prediction program for HF ground wave propagation over irregular terrain with forest, building, or snow cover. Mrs. Rita Reasoner of ITS provided invaluable computer programming assistance. Mr. Lewis Vogler of ITS provided the multiple knife-edge diffraction calculations. Discussions with Dr. William Kissick of ITS and Dr. Randolph Ott of COMSAT were very helpful.

9. REFERENCES

Abramowitz, M., and I. A. Stegun (1964), Handbook of Mathematical Functions, National Bureau of Standards, AMS 55.

Bremmer, H. (1949), Terrestrial Radio Waves (Elsevier Publishing Company, Amsterdam).

Causebrook, J. H. (1978a), Medium-wave propagation in built-up areas, Proc. IEE 125, pp. 804-808.

Causebrook, J. H. (1978b), Electric/magnetic field ratios of ground waves in a realistic terrain, Electronics Letters 14, pp. 614-615.

Cavalcante, G. P. D. S., D. A. Rogers, and A. J. Giarola (1982), Analysis of electromagnetic wave propagation in multilayered media using dyadic Green's functions, Radio Sci. 17, pp. 503-508.

Defense Intelligence Agency (1971), Basic phenomena involved in MF and HF radio communications, ST-CS-06-13-71, Appendix III.

Dence, D., and T. Tamir (1969), Radio loss of lateral waves in forest environments, Radio Sci. 4, pp. 307-318.

Evans, S. (1965), Electrical properties of ice and snow--a review, J. Glaciology 42, pp. 773-792.

Gordon, G. A., and E. Hoyt (1982), An estimate of HF/VHF surface-wave communication link reaches in the West German forest environment, RDA-TR-119930-001, R & D Associates, Marina del Rey, California.

Hill, D. A., and J. R. Wait (1980), Ground wave attenuation function for a spherical earth with arbitrary surface impedance, Radio Sci. 15, pp. 637-643.

Hill, D. A., and J. R. Wait (1981a), HF ground wave propagation over mixed land, sea, and sea-ice paths, IEEE Trans. Geosci. Remote Sensing GE-19, pp. 210-216.

Hill, D. A., and J. R. Wait (1981b), HF radio wave transmission over sea ice and remote sensing possibilities, IEEE Trans. Geosci. Remote Sensing GE-19, pp. 204-209.

Hill, D. A., and J. R. Wait (1982), Ground wave propagation over a mixed path with an elevation change, IEEE Trans. Ant. Prop. AP-30, pp. 139-141.

Hufford, G. A. (1952), An integral equation approach to the problem of wave propagation over an irregular terrain, Quart. J. Appl. Math. 9, pp. 391-404.

Hufford, G. A., A. G. Longley, and W. A. Kissick (1982), A guide to the use of the ITS irregular terrain model in the area prediction mode, NTIA Report 82-100.

Jansky and Bailey Research and Engineering Department (1966), Tropical propagation research, final report, Vol. 1, Atlantic Research Corp., Alexandria, Virginia.

Millington, G. (1949), Ground wave propagation over an inhomogeneous smooth earth, Pt. 1, Proc. IEE 96, pp. 53-64.

Monteath, G. D. (1973), Applications of the Electromagnetic Reciprocity Principle (Pergamon Press, Oxford).

Ott, R. H. (1971a), An alternative integral equation for propagation over irregular terrain, 2, Radio Sci. 6, pp. 429-435.

Ott, R. H. (1971b), A new method for predicting HF ground wave attenuation over inhomogeneous, irregular terrain, U.S. Dept. of Commerce, Res. Rept. No. OT/TRER 7, January (NTIS Accession No. AB721179).

Ott, R. H., and L. A. Berry, (1970), An alternative integral equation for propagation over irregular terrain, Radio Sci. 5, pp. 767-771.

Ott, R. H., L. E. Vogler, and G. A. Hufford (1979), Ground wave propagation over irregular, inhomogeneous terrain: comparison of calculations and measurements, NTIA Report 79-20 (NTIS Accession No. PB 298668/AS).

Ott, R. H., and J. R. Wait (1973), Excitation mechanisms for transmission through forest-covered and vegetated media, U.S. Department of Commerce, Office of Telecommunications, Boulder, Colorado, Technical Report No. ACC-ACO-8-73 prepared for U.S. Army Communications Command, Ft. Huachuca, Arizona (NTIS Accession No. AD 771-915).

Parker, H. W., and G. H. Hagn (1966), Feasibility study of the use of open-wire transmission lines capacitors and cavities to measure the electrical properties of vegetation, Stanford Res. Inst., Special Tech. Rept. 29, Menlo Park, CA.

Parker, H. W., and W. Makarabhiromya (1967), Electric constants measured in vegetation and in earth at five sites in Thailand, Stanford Res. Inst., Special Technical Report 43, Menlo Park, California.

Tamir, T. (1967), On radio-wave propagation in forest environments, IEEE Trans. Ant. Prop. AP-15, pp. 806-817.

Tamir, T. (1977), Radio wave propagation along mixed paths in forest environments, IEEE Trans. Ant. Prop. AP-25, pp. 471-477.

Van der Vis (1979), Measurements on short distance HF data links, National Defense Research Organization TNO, Report IR 1979-72.

Vogler, L. E. (1981), The attenuation of electromagnetic waves by multiple knife-edge diffraction, NTIA Report 81-86 (NTIS Accession No. PB 82-139239).

Von Hippel, A. (1954), Dielectric Materials and Applications (Technology Press of MIT, Cambridge).

Wagner, C. (1953), On the numerical solution of volterra integral equations, J. Math. Phys. 32, pp. 289-401.

Wait, J. R. (1959), Guiding of electromagnetic waves by uniformly rough surfaces, Pts. 1 and 2, IEEE Trans. Ant. Prop. AP-7, pp. 5154-5168.

Wait, J. R. (1962), Electromagnetic Waves in Stratified Media (Pergamon Press, New York).

Wait, J. R. (1967a), Radiation from dipoles in an idealized jungle environment, Radio Sci. 2, pp. 747-750.

Wait, J. R. (1967b), Asymptotic theory for dipole radiation in the presence of a lossy slab lying on a conducting half-space, IEEE Trans. Ant. Prop. AP-15, pp. 645-648.

Wait, J. R., R. H. Ott, and T. Telfer (1974), Workshop on radio systems in forested and or vegetated environments, Technical Report No. ACC-ACO-1-74, U.S. Army Communications Command, Fort Huachuca, Arizona.

Wait, J. R., and L. C. Walters (1963), Curves for ground wave propagation over mixed land and sea paths, IEEE Trans. Ant. Prop. AP-11, pp. 38-45.

APPENDIX A: ANTENNA WITHIN THE SLAB

In this appendix, we consider the case where the vertical electric dipole source is located within the slab. The geometry is shown in Figure 1, but the antenna height h is now negative: $0 > h > -D$.

Following the notation in Section 2.1, the fields in air ($z > 0$) can be derived from the z component, Π_{oz}, of an electric Hertz vector of the following form:

$$\Pi_{oz} = \frac{I\ ds}{4\pi i\omega\epsilon_o} \int_o^\infty T_o(\lambda)\ e^{-u_o z}\ \frac{\lambda}{u_o}\ J_o(\lambda\rho)\ d\lambda \quad , \tag{A-1}$$

where $T_o(\lambda)$ is an unknown transmission coefficient and all other symbols are defined in Section 2.1. The three nonzero field components, $E_{o\rho}$, E_{oz}, and $H_{o\phi}$, are given by (3).

In the ground ($z < -D$), the z component, Π_{gz}, of the Hertz vector can be written

$$\Pi_{gz} = \frac{I\ ds}{4\pi i\omega\epsilon_o\epsilon_{gc}} \int_o^\infty T_g(\lambda)\ e^{u(z+D)}\ \frac{\lambda}{u}\ J_o(\lambda\rho)\ d\lambda \quad , \tag{A-2}$$

where $T_g(\lambda)$ is an unknown transmission coefficient and all other symbols are defined in Section 2.1. The three nonzero field components, $E_{g\rho}$, E_{gz}, and $H_{g\phi}$, are given by

$$E_{g\rho} = \frac{\partial^2 \Pi_{gz}}{\partial\rho\ \sigma z} \quad , \quad E_{gz} = \left(-\gamma_g^2 + \frac{\partial^2}{\partial\ z^2}\right)\Pi_{gz} \quad , \tag{A-3}$$

and

$$H_{g\phi} = -i\omega\epsilon_o\epsilon_{gc}\ \frac{\partial\ \Pi_{gz}}{\partial\rho} \quad .$$

Within the anisotropic slab ($-D < z < o$), it is most convenient to work directly with the azimuthal magnetic field, H_ϕ. Clemmow (1966) has given the expression for the field in an infinite medium which we can generalize to the appropriate form within a slab:

$$H_\phi = \frac{I\ ds\ \kappa}{4\pi} \int_o^\infty J_1(\lambda\rho)\left[e^{-v|z-h|} + A(\lambda)\ e^{vz} + B(\lambda)\ e^{-vz}\right]\left(\frac{\lambda^2}{v}\right) d\lambda \quad , \tag{A-4}$$

where $A(\lambda)$ and $B(\lambda)$ are unknown coefficients and all other symbols are defined in Section 2.1. From Maxwell's curl equation, the two nonzero components of the electric field, E_ρ and E_z, can be written

$$E_\rho = \frac{-1}{i\omega\varepsilon_o\varepsilon_{hc}} \frac{\partial H_\phi}{\partial z}$$

and

$$E_z = \frac{\kappa}{i\omega\varepsilon_o\varepsilon_{hc}\rho} \frac{\partial}{\partial\rho} (\rho H_\phi) \quad . \tag{A-5}$$

The four unknowns, $T_o(\lambda)$, $T_g(\lambda)$, $A(\lambda)$, and $B(\lambda)$, can be determined from the continuity of tangential electric and magnetic fields at the interfaces:

$$(E_{o\rho} - E_\rho)\Big|_{z=0} = 0 \quad ,$$

$$(H_{o\phi} - H_\phi)\Big|_{z=0} = 0 \quad ,$$

$$(E_\rho - E_{g\rho})\Big|_{z=-D} = 0 \quad ,$$

and

$$(H_\phi - H_{g\phi})\Big|_{z=-D} = 0 \quad . \tag{A-6}$$

By substituting the field expressions into (A6) and performing some algebra, we obtain the following expressions for the unknowns:

$$A(\lambda) = R_o\, e^{vh} \left[1 + R_g\, e^{-v(2D+2h)}\right] /S \quad ,$$

$$B(\lambda) = R_g\, e^{-v(2D+h)} \left[1 + R_o\, e^{2vh}\right] /S \quad ,$$

$$T_o(\lambda) = \frac{\kappa\, u_o(1+R_o)\, e^{vh}}{v\, S} \left[1 + R_g\, e^{-v(2D+2h)}\right] \quad , \tag{A-7}$$

$$T_g(\lambda) = \frac{\kappa\, u\, e^{-v(D+h)}}{v\, S} \left[1 + R_o\, e^{2vh}\right] \quad ,$$

where $S = 1 - R_o R_g\, e^{-2vD}$,

$$R_o = \frac{K_1 - K_o}{K_1 + K_o} \quad , \quad R_g = \frac{K_1 - K_2}{K_1 + K_2} \quad ,$$

and all other symbols are defined in Section 2.1. This completes the formal integral representation of the fields in all three regions.

The integral forms for the fields can be evaluated asymptotically when the horizontal distance ρ is large. We are primarily interested in the vertical electric field, and from (A-1) and (3), the vertical electric field in air ($z > 0$) can be written

$$E_{oz} = \frac{I\ ds}{4\pi i\omega\varepsilon_o} \int_o^\infty T_o(\lambda)\ e^{-u_o z} \left(\frac{\lambda^3}{u_o}\right) J_o(\lambda\rho)\ d\lambda \quad . \qquad \text{(A-8)}$$

The Bessel function in (A-8) can be replaced by Hankel functions (Abramowitz and Stegun, 1964), and the integration range in (A-8) can be extended to $-\infty$ to yield the following form (Wait, 1967b):

$$E_{oz} = \frac{I\ ds}{4\pi i\omega\varepsilon_o} \int_{-\infty}^\infty \frac{T_o(\lambda)}{2}\ e^{-u_o z} \left(\frac{\lambda^3}{u_o}\right) H_o^{(2)}(\lambda\rho)\ d\lambda \quad . \qquad \text{(A-9)}$$

We follow the method which Wait (1967b) used for a dipole above an isotropic dielectric slab. The integral in (A-9) can be deformed around the branch cuts which result from branch points at k and $k_g (= -i\ \gamma_g)$ as shown in Figure A.1. In addition, there may be one or more surface wave poles at $\lambda = k_s$ which result from poles of $T_o(\lambda)$ (= zeros of S) as given by (A-6). The contributions from the contour C_g and any surface wave poles are exponentially attenuated for large ρ, and we keep only the branch cut integral C_o:

$$E_{oz} \simeq \frac{I\ ds}{4\pi i\omega\varepsilon_o} \int_{C_o} \frac{T_o(\lambda)}{2}\ e^{-u_o z}\ \frac{\lambda^3}{u_o}\ H_o^{(2)}(\lambda\rho)\ d\lambda \quad . \qquad \text{(A-10)}$$

In order to evaluate (A-10), we first rewrite $T_o(\lambda)$ in a form which is equivalent to that in (A-7):

$$T_o(\lambda) = \frac{2\ K_o}{K_o + Z_1}\ \frac{e^{vh}[1 + R_g\ e^{-v(2D+2h)}]}{\varepsilon_{vc}[1+R_g\ e^{-2vD}]} \quad . \qquad \text{(A-11)}$$

Near $\lambda = k$, (A-11) can be approximated

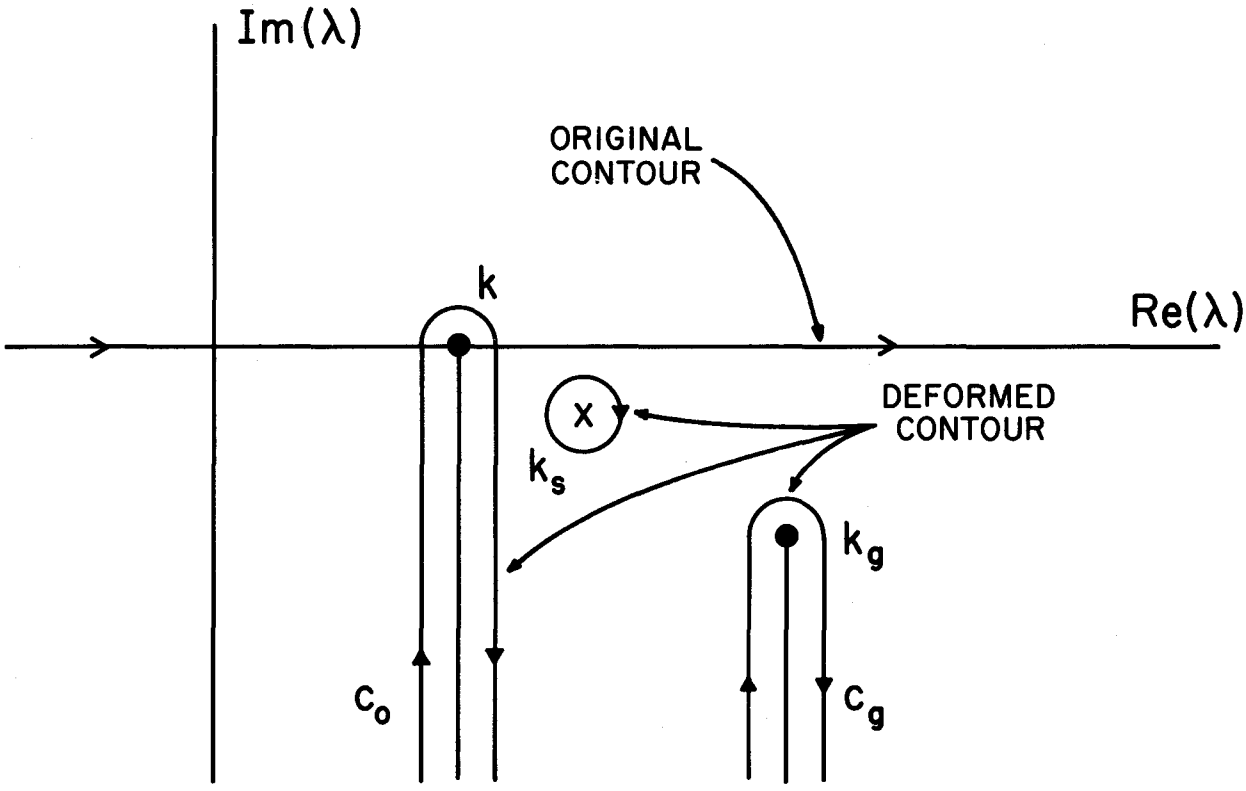

Figure A.1. Integration contours in the complex λ plane.

$$\frac{T_o(\lambda)}{2} \simeq \frac{1}{\varepsilon_{vc}} \left. \frac{e^{vh}[1+R_g\, e^{-v(2D+2h)}]}{1 + R_g\, e^{-2vD}} \right|_{\lambda=k} \cdot \frac{K_o}{K_o + Z_1} \quad . \tag{A-12}$$

The first factor in (A-12) is identically equal to $G_s(h)$ as given by (13). Thus, (A-12) can be written

$$\frac{T_o(\lambda)}{2} \simeq \frac{K_o}{K_o + Z_1} G_s(h) \quad . \tag{A-13}$$

Substituting (A-13) into (A-10) and approximating λ^2 by k^2, we have

$$E_{oz} \simeq \frac{I\, ds\, k^2\, G_s(h)}{4\pi i\omega\varepsilon_o} \int_{C_o} \frac{K_o\, e^{-u_o z}}{K_o + Z_1} \frac{\lambda}{u_o} H_o^{(2)}(\lambda\rho)\, d\lambda \quad . \tag{A-14}$$

Wait (1967b) has evaluated the integral over C_o:

$$\int_{C_o} \simeq \frac{1 + ik\Delta z}{ik_o\Delta^2\rho^2} e^{-ik\rho} \quad . \tag{A-15}$$

Substituting (A-15) into (A-14), we can write E_{oz} in the final form

$$E_{oz} = E_o\, f(p)\, G_s(h)\, G_o(z) \quad , \tag{A-16}$$

where E_o is given by (5), $f(p)$ is given by (6), and G_s and G_o are given by (13). This form is consistent with the result in (4),, but disagrees with the result for the dipole in the slab given by Wait (1967a). He has an extra factor of $\kappa^{\frac{1}{2}}$ multiplying $G_s(h)$ which leads to a height-gain function which is different for the source and observer in the slab. More recently, Wait (private communication) has agreed that the factor $\kappa^{\frac{1}{2}}$ is spurious and that (A-16) is the correct result. Thus the height-gain function in (13) applies to both the source and observer, and reciprocity is satisfied.

For the case of both the dipole and the observer located within the slab, E_z is obtained from (A-4) and (A-5):

$$E_z = \frac{I\,ds}{4\pi i\omega\varepsilon_o\varepsilon_{vc}} \int_o^\infty J_o(\lambda\rho) \left[e^{-v|z-h|} + A(\lambda)\, e^{vz} + B(\lambda)\, e^{-vz}\right] \frac{\lambda^3}{v}\, d\lambda \qquad \text{(A-17)}$$

$$= \frac{I\,ds}{\pi i\omega\varepsilon_o\varepsilon_{vc}} \int_{-\infty}^\infty H_o^{(2)}(\lambda\rho) \left[e^{-v|z-h|} + A(\lambda)\, e^{vz} + B(\lambda)\, e^{-vz}\right] \frac{\lambda^3}{v}\, d\lambda \quad .$$

For large ρ, we again include only the C_o contour in Figure 27. Also, the first factor in (A-17) does not contribute, and E_z is approximately given by

$$E_z \simeq \frac{I\,ds}{8\pi i\omega\varepsilon_o\varepsilon_{vc}} \int_{C_o} H_o^{(2)}(\lambda\rho) \left[A(\lambda)\, e^{vz} + B(\lambda)\, e^{-vz}\right] \frac{\lambda^3}{v}\, d\lambda \quad . \qquad \text{(A-18)}$$

By expanding $A(\lambda)$ and $B(\lambda)$ about $\lambda=k$, (A-18) can be put into a form similar to (A-14):

$$E_z \simeq \frac{I\,ds\, k^2\, G_s(h)\, G_s(z)}{4\pi i\omega\varepsilon_o} \int_{C_o} \frac{K_o}{K_o + Z_1} \frac{\lambda}{u_o} H_o^{(2)}(\lambda\rho)\, d\lambda \quad . \qquad \text{(A-19)}$$

In this case, the integral over C_o is given by

$$\int_{C_o} \simeq \frac{e^{-ik\rho}}{i\, k_o\, \Delta^2\rho^2} \quad . \qquad \text{(A-20)}$$

From (A-19) and (A-20), E_z can be written

$$E_z \simeq E_o\, f(p)\, G_s(h)\, G_s(z) \quad .$$

As expected, the same height-gain function G_s appears for both the dipole height h and observer height z since both are located in the slab.

REFERENCES

Abramowitz, M., and I. A. Stegun (1964), Handbook of Mathematical Functions, National Bureau of Standards, AMS 55.

Clemmow, P. C. (1966), The Pland Wave Spectrum of Electromagnetic Fields (Pergamon Press, Oxford), Section 8.1.5.

Wait, J. R. (1967a), Radiation from dipoles in an idealized jungle environment, Radio Sci. 2, pp. 747-750.

Wait, J. R. (1967b), Asymptotic theory for dipole radiation in the presence of a lossy slab lying on a conducting half-space, IEEE Trans. Ant. Prop., AP-15, pp. 645-648.

APPENDIX B. KIRCHHOFF INTEGRATION

In order to evaluate (36), we first rewrite f in the following manner:

$$f = \sqrt{\frac{2}{\pi}} \frac{\sqrt{ik(R_a + R_b)}}{\Delta_a \Delta_b (R_a R_b)^{3/2}} I \quad , \tag{B-1}$$

where

$$I = \int_D^\infty z(z - D) \exp\left\{-ik\left[\frac{z^2}{2 R_b} + \frac{(z - D)^2}{2 R_a}\right]\right\} dz \quad .$$

The problem now is to evaluate I.

We first make the substitution, $z' = z - D$:

$$I = \int_o^\infty (z' + D)\, z' \exp\left\{-ik\left[\frac{(z' + D)^2}{2 R_b} + \frac{z'^2}{2 R_a}\right]\right\} dz' \quad . \tag{B-2}$$

By completing the square in the exponent, (B-2) can be rewritten:

$$I = \exp\left[\frac{-ik D^2}{2(R_a + R_b)}\right] \int_o^\infty (z' + D) z' \cdot$$

$$\cdot \exp\left\{-\frac{ik}{2}\left[\frac{1}{R_a} + \frac{1}{R_b}\right]\left[z' + \frac{D}{R_b\left(\frac{1}{R_b} + \frac{1}{R_a}\right)}\right]^2\right\} dz' \tag{B-3}$$

We now make a second substitution:

$$u = \sqrt{\frac{ik}{2}\left(\frac{1}{R_a} + \frac{1}{R_b}\right)}\left[z' + \frac{D}{R_b\left(\frac{1}{R_b} + \frac{1}{R_a}\right)}\right] \quad . \tag{B-4}$$

After some algebra, this allows (B-3) to be written

$$I = \frac{\exp\left[-i\,\frac{k D^2}{2(R_a + R_b)}\right]}{\left[\frac{ik}{2}\left(\frac{1}{R_b} + \frac{1}{R_a}\right)\right]^{3/2}} I_u \quad , \tag{B-5}$$

where

$$I_u = \int_{u_\ell}^{\infty} (u^2 + a_1 u + a_o)\, e^{-u^2}\, du \quad ,$$

$$u_\ell = \frac{D}{R_b} \sqrt{\frac{ik}{2\left(\frac{1}{R_a} + \frac{1}{R_b}\right)}} \quad ,$$

$$a_1 = \frac{D\sqrt{ik/2}\,\left(\frac{1}{R_a} - \frac{1}{R_b}\right)}{\sqrt{\frac{1}{R_a} + \frac{1}{R_b}}} \quad ,$$

and

$$a_o = \frac{D^2(ik/2)}{R_a + R_b} \quad .$$

The integral in (B-5) can be evaluated in terms of the complementary error function (Abramowitz and Stegun, 1964):

$$\mathrm{erfc}(u_\ell) = \frac{2}{\sqrt{\pi}} \int_{u_\ell}^{\infty} e^{-u^2}\, du \quad . \tag{B-6}$$

Using (B-6) and doing one integration by parts, we can write (B-5) as

$$I_u = \frac{a_o\sqrt{\pi}}{2}\,\mathrm{erfc}(u_\ell) + \frac{a_1}{2}\, e^{-u_\ell^2} + \frac{1}{2}\left[\frac{\sqrt{\pi}}{2}\,\mathrm{erfc}(u_\ell) + u_\ell\, e^{-u_\ell^2}\right]$$

$$= \frac{\sqrt{\pi}}{2}\,(a_o + \tfrac{1}{2})\,\mathrm{erfc}(u_\ell) + \frac{a_1 + u_\ell}{2}\, e^{-u_\ell^2} \tag{B-7}$$

For the special case of D=0, we have $u_\ell = a_o = a_1 = 0$, and I_u is given by

$$I_u\Big|_{D=0} = \frac{\sqrt{\pi}}{4}\,\mathrm{erfc}(0) = \frac{\sqrt{\pi}}{4} \quad . \tag{B-8}$$

This result leads us to rewrite I_u:

$$I_u = \frac{\sqrt{\pi}}{4}\, S \quad , \tag{B-9}$$

$$S = (1 + 2\,a_o)\ \mathrm{erfc}(u_\ell) + \frac{2(a_1 + u_\ell)}{\sqrt{\pi}}\, e^{-u_\ell^2} \quad .$$

Using (B-1), (B-5), and (B-9), we can now obtain the following final result for f:

$$f = \frac{S\, e^{-H^2}}{ik(R_a + R_b)\ \Delta_a \Delta_b} \quad , \tag{B-10}$$

where

$$S = (1 + 2\,H^2)\ \mathrm{erfc}(\sqrt{A}\,H) + \frac{2}{\sqrt{\pi}}\,\frac{H}{\sqrt{A}}\, e^{-A\,H^2} \quad ,$$

$$H = \frac{D\sqrt{ik/2}}{\sqrt{R_a + R_b}} \quad ,$$

and

$$A = R_a/R_b \quad .$$

The exponential factor, $\exp(-H^2)$, has magnitude unity and only results in a phase delay. All of the dependence of the magnitude of f on D is contained in S. For most cases, $|H|$ is small. In this case we can expand S in a power series in H by using the small argument expansion of the complementary error function (Abramowitz and Stegun, 1964)

$$S \simeq 1 + \frac{2H}{\sqrt{\pi}}\left(\frac{1}{\sqrt{A}} - \sqrt{A}\right) + \text{order } H^2 \quad . \tag{B-11}$$

The magnitude of S is then approximated by

$$|S| \simeq 1 + \sqrt{\frac{2}{\pi}}\,|H|\left(\frac{1}{\sqrt{A}} - \sqrt{A}\right) + \text{order } |H^2| \quad . \tag{B-12}$$

REFERENCE

Abramowitz, M., and I. A. Stegun (1964), Handbook of Mathematical Functions, National Bureau of Standards, AMS 55.

APPENDIX C. USER'S GUIDE, LISTING, AND SAMPLE OUTPUT FOR PROGRAM WAGSLAB

The input data are described as follows. Most quantities are pictured in Figure 3 (or 1). Note on Card 3 that the antenna heights are referred to the ground, not the top of the slab.

Card 1: KIND, TD (I10, F10.0)
KIND = beginning type of distance at which F(x) will be evaluated.
1 is specified on next cards
0 is equidistant
TD = total distance in kilometers

Card 2A: X(I) (8F10.5)
X(I) = specific distances in kilometers at which F(x) will be evaluated.
IF KIND = 1 use these cards to begin giving specific distances until you are done or want to change to equidistant points.
Terminate this set of distances with a 0.

Card 2B1: NED (I2)
NED = number (limited to 50) of consecutive sections with F(x) evaluated at equidistant points. (This should agree with the number of pairs of DEP and FINT).

Card 2B2: (DEP(I), FINT(I), I = 1,NED) (8F10.0)
DEP(I) = distance in kilometers at which this set of equidistant points ends.
FINT(I) = interval of these equidistant points in kilometers.
If KIND = 0, use these cards to begin.

Note: There may be a series of 2A and 2B cards to reach the total distance given on card 1.

Card 3: HA, FREQ, HAR, AKM (4F10.5)
HA = transmitter antenna height in kilometers = h_a-D
FREQ = frequency in MHz
HAR = receiver antenna height in kilometers = h_r-D
AKM = effective earth radius in kilometers

Card 4: ID (8A10)
ID = path identification.

Card 5: N, IXUNITS, IZUNITS, REFEL (3I10,F10.1)
N = number of points on terrain profile
IXUNITS = 0, distance input in kilometers
= 1, distance input in statute miles
IZUNITS = 0, height input in meters
= 1, height input in feet
REFEL = reference elevation in IZUNITS(=height at d=0)

Card 6 to M: (X(I), I = 1,N) (4(F10.2,F10.0))
X(I) = terrain distances in IXUNITS
Z(I) = terrain heights in IZUNITS

Card M+1: NGC (I10)
NGC = number of sets of ground constants
(limited to 50).

Card M+2 to end: (DX(I), SIGX(I), EPSX(I), ISLAB, T(I), EH(I), EV(I), SH(I), SV(I), I = 1,NGC) (F8.2,F8.6,F8.2,I2,3F8.2,2F8.6)
DX(I) = maximum distance in kilometers for given set of ground constants
SIGX(I) = conductivity of ground = σ_g (S/m)
EPSX(I) = relative permittivity of ground = ε_g
ISLAB = 0 is no slab in this section
= 1 slab ground constants to follow
T(I) = thickness of slab in meters = D
EH(I) = horizontal relative permittivity for slab = ε_h
EV(I) = vertical relative permittivity for slab = ε_v
SH(I) = horizontal conductivity for slab = σ_h (S/m)
SV(I) = vertical conductivity for slab = σ_v (S/m)

A listing of program WAGSLAB and all subroutines is given below. Program WAGSLAB is essentially a modification of program WAGNER (Ott et al., 1979) to allow for the effect of a slab over the ground.

```
      PROGRAM WAGSLAB(INPUT,OUTPUT,TAPE60=INPUT,TAPE2)
C
C     MODIFICATION OF WAGNER FOR DAVE HILL, 5/82, TO ACCOMMODATE SLABS OF
C     SNOW ,BUILDINGS, AND VEGETATION.  MAIN CHANGES IN SUBROUTINE IN
C     USING GROUND CONSTANTS TO COMPUTE DELTA (IMPEDANCE).  GHA(1)
C     AND GHR(NGC) (DEPENDENT ON PARTICULAR SETS OF GROUND CONSTANTS)
C     ARE COMPUTED IN IN AND USED IN FH(X) WHICH IS COMPUTED IN WAGSLAB.
C     H AND HP ARE MODIFIED IN TERRANE WHEN A SLAB IS PRESENT.
C     VERTICAL POLARIZATION IS SET CONSTANT.  PREVIOUS REFERENCES TO
C     HA ARE ELIMINATED.
C
      DIMENSION IPOL(2)
      DIMENSION ADAB(3),ADGH(3)
      DIMENSION F(2000),R13(2000),R14(2000),R15(2000),R16(2000),
     CR17(2000),R18(2000),R19(2000),R20(2000),R21(2000)
      COMMON /1/ HA,HAR,AKM
      COMMON /2/ D,H,HP
      COMMON /3/ DELTAR,WAVE
      COMMON /4/ FREQ,POL
      COMMON /5/ NG,AB(48),GH(48)
      COMMON /6/ N,X(2001),INDEX
      COMMON /INPUT/ DUMM(10320),ID(8),REFEL
      COMMON /GCX/ NGC,DX(50),ETAX(50),DELTAX(50),SIGX(50),EPSX(50),
     CT(50),SH(50),SV(50),EH(50),EV(50),GHA,GHR(50)
      COMMON/PMF/FLDS(2000),DKM(2000)
      DOUBLE PRECISION DAB,DGH
      COMPLEX FEWH,F,ALAMZ,SUM,DELTAR,ETAR
      COMPLEX KERNL,P0,P1,P2,P3,P4,CTMP
      COMPLEX ETA,DELTA
      COMPLEX GHA,GHR,ETAX,DELTAX,FH
      DATA (NG=5)
      DATA (ADAB=.9061798459,.5384693101,0.)
      DATA (ADGH=.2369268851,.4786286704,.56888888888)
      CANG(Z)=ATAN2(AIMAG(Z),REAL(Z))
      IPOL(1)=8H  VERTIC$IPOL(2)=8HHORIZONT
C
C     READ GAUSSIAN QUADRATURE ABCISSAS AND WEIGHTS
C
      NR=(NG+1)/2
      DO 1 L=1,NR
      DAB=ADAB(L)
      DGH=ADGH(L)
      J=NG-L+1
      AB(L)=DAB
      AB(J)=-AB(L)
      GH(L)=DGH
1     GH(J)=GH(L)
C
C     CALL SUBROUTINE DISTX TO SET UP DISTANCE ARRAY X IN METERS.
C     START WITH X(2).  X(1)=0. HAS ALREADY BEEN SET.
C     THE DISTANCES DO NOT HAVE TO BE EQUALLY SPACED.
C     SUBROUTINE DISTX SHOULD TEST N TO BE LESS THAN OR EQUAL TO 2000.
C
4     X(1)=0.
      F(1)=(1.,0.)
      CALL DISTX
C
C     MAKE SURE THERE ARE AT LEAST 4 DISTANCES.
C
      IF (N.GE.4) GO TO 2
      PRINT 18
      CALL EXIT
C
2     SQRTX2=SQRT(X(2))
      SQRTX3=SQRT(X(3))
      SQRTX4=SQRT(X(4))
```

```
      D1=SQRT(X(2)*X(3)*X(4))*(X(2)*(SQRTX4-SQRTX3)+X(3)*(SQRTX2-SQRTX4)
     1+X(4)*(SQRTX3-SQRTX2))
      R1=X(3)*X(4)*(SQRTX4-SQRTX3)/D1
      R2=X(2)*X(4)*(SQRTX2-SQRTX4)/D1
      R3=X(2)*X(3)*(SQRTX3-SQRTX2)/D1
      R4=(X(2)*(SQRTX4**3-SQRTX3**3)+X(3)*(SQRTX2**3-SQRTX4**3)+X(4)*(SQ
     1RTX3**3-SQRTX2**3))/D1
      R5=SQRT(X(3)*X(4))*(X(3)-X(4))/D1
      R6=SQRT(X(2)*X(4))*(X(4)-X(2))/D1
      R7=SQRT(X(2)*X(3))*(X(2)-X(3))/D1
      R8=(SQRTX2*(SQRTX3**3-SQRTX4**3)+SQRTX3*(SQRTX4**3-SQRTX2**3)+SQRT
     1X4*(SQRTX2**3-SQRTX3**3))/D1
      R9=SQRT(X(3)*X(4))*(SQRTX4-SQRTX3)/D1
      R10=SQRT(X(2)*X(4))*(SQRTX2-SQRTX4)/D1
      R11=SQRT(X(2)*X(3))*(SQRTX3-SQRTX2)/D1
      R12=(SQRTX2*(X(4)-X(3))+SQRTX3*(X(2)-X(4))+SQRTX4*(X(3)-X(2)))/D1
      DO 3 M=5,N
      M1=M-1
      M2=M-2
      DELTA1=X(M)-X(M1)
      DELTA2=X(M)-X(M2)
      D2=(DELTA1-DELTA2)*DELTA1*DELTA2
      R13(M)=X(M1)*X(M2)*(X(M2)-X(M1))/D2
      R14(M)=X(M)*X(M2)*(X(M)-X(M2))/D2
      R15(M)=X(M)*X(M1)*(X(M1)-X(M))/D2
      R16(M)=(X(M1)**2-X(M2)**2)/D2
      R17(M)=(X(M2)**2-X(M)**2)/D2
      R18(M)=(X(M)**2-X(M1)**2)/D2
      R19(M)=(X(M2)-X(M1))/D2
      R20(M)=(X(M)-X(M2))/D2
3     R21(M)=(X(M1)-X(M))/D2
C
C     READ TRANSMITTER HEIGHT, FREQUENCY, RECEIVER HEIGHT AND EARTH RADIUS.
C     COL       DESCRIPTION
C     1-10      TRANSMITTER HEIGHT, KM
C     11-20     FREQUENCY, MHZ
C     21-30     RECEIVER HEIGHT, KM
C     31-40     EARTH RADIUS, KM
C
      READ 19, HA,FREQ,HAR,AKM
      POL=1.
C
C     NOTE THAT VERTICAL POLARIZATION IS NOW CONSTANT.
C
      HAR=HAR*1.E+3
      HA=HA*1.E3
      KPOL=POL
      ALAM=2.997925E2/FREQ
      WAVE=6.283185307/ALAM
      ALAMZ=((0.7071067812,0.7071067812)/SQRT (ALAM))
      TO=SECOND(DUM)
C
C     LOOP ON DISTANCE
C
      DO 14 I=1,N
      INDEX=I
      IF (I .NE. 1) GO TO 51
      CALL TERRAN2(X(I),H,HP,ETA,DELTA,ETAR,DELTAR,COND,EPS)
      PRINT 20, FREQ,IPOL(KPOL),AKM,HA,HAR
      GO TO 52
51    CALL TERRANE (X(I),H,HP,ETA,DELTA,ETAR,DELTAR,COND,EPS)
52    CONTINUE
      IF (I.EQ.1) GO TO 33
      D=X(I)+(H**2)/(2.*X(I))
      F(I)=FEWH(H,X(I))
      IF (I.LE.6) GO TO 13
C
C     J = 2 THROUGH 4
C
      SUM=(0.,0.)
      DO 9 J=2,4
      P0=P1=P2=P3=(0.,0.)
      K=J-1
      XP2=0.5*(X(J)+X(K))
      XM2=0.5*(X(J)-X(K))
```

```
      DO 7 M=1,NG
      XO=XP2+AB(M)*XM2
      CTMP=KERNL(XO)*GH(M)
      P1=P1+CTMP*SQRT(XO)
      P2=P2+CTMP*XO
      P3=P3+CTMP*SQRT(XO)**3
      IF (K.NE.1) GO TO 6
      XO=0.25*X(J)*(1.+AB(M))**2
      PO=PO+SQRT(XO)*KERNL(XO)*GH(M)
      GO TO 7
6     PO=PO+CTMP
7     CONTINUE
      P1=P1*XM2
      P2=P2*XM2
      P3=P3*XM2
      IF (K.NE.1) GO TO 8
      PO=PO*SQRT(X(J))
      GO TO 9
8     PO=PO*XM2
9     SUM=SUM+PO*R4*P1+R8*P2+R12*P3+F(2)*(R1*P1+R5*P2+R9*P3)+F(3)*(R2*P1
     1+R6*P2+R10*P3)+F(4)*(R3*P1+R7*P2+R11*P3)
C
C     J = 5 THROUGH I-1
C
      I1=I-1
      DO 11 J=5,I1
      PO=P2=P4=(0.,0.)
      XP2=0.5*(X(J)+X(J-1))
      XM2=0.5*(X(J)-X(J-1))
      DO 10 M=1,NG
      XO=XP2+AB(M)*XM2
      CTMP=KERNL(XO)*GH(M)
      PO=PO+CTMP
      P2=P2+CTMP*XO
10    P4=P4+CTMP*XO**2
      PO=PO*XM2
      P2=P2*XM2
      P4=P4*XM2
11    SUM=SUM+F(J-2)*(R15(J)*PO+R18(J)*P2+R21(J)*P4)+F(J-1)*(R14(J)*PO+R
     117(J)*P2+R20(J)*P4)+F(J)*(R13(J)*PO+R16(J)*P2+R19(J)*P4)
C
C     J=1
C
      THETA=ASIN (SQRT(X(I1)/X(I)))
      CTHETA=COS (THETA)
      PO=P2=P4=(0.,0.)
      DO 12 M=1,NG
      TEMP=1.-0.25*CTHETA**2*(1.+AB(M))**2
      XO=X(I)*TEMP
      CTMP=SQRT(X(I)-XO)*KERNL(XO)*GH(M)
      PO=PO+CTMP
      P2=P2+CTMP*TEMP
12    P4=P4+CTMP*TEMP**2
      PO=PO*CTHETA*SQRT(X(I))
      P2=P2*CTHETA*SQRT(X(I))**3
      P4=P4*CTHETA*SQRT(X(I))**5
      F(I)=(F(I)-ALAMZ*(SUM+F(I-2)*(R15(I)*PO+R18(I)*P2+R21(I)*P4)+F(I1)
     1*(R14(I)*PO+R17(I)*P2+R20(I)*P4)))/(1.+ALAMZ*(R13(I)*PO+R16(I)*P2+.
     2R19(I)*P4))
13    AMP=CABS(F(I))
      PHA=CANG(F(I))
      IGCD=1
      DO 30 IGC=1,NGC
      IF (X(I) .LE. DX(IGC)) GO TO 32
      IGCD=IGC+1
30    CONTINUE
32    CONTINUE
      FH=F(I)*GHA*GHR(IGCD)
      AMPH=CABS(FH)
      PHAH=CANG(FH)
      RR2=20.*ALOG10(WAVE*X(I)/AMPH)
      BTL=RR2
      FLDS(I)=139.37+20.*ALOG10(FREQ)-RR2
      DKM(I)=X(I)*.001
      TIME=SECOND(DUM)-TO
      GO TO 34
```

```
33     PRINT 24
       PRINT 26, (DX(IGC),SIGX(IGC),EPSX(IGC),T(IGC),SH(IGC),SV(IGC),
      CEH(IGC),EV(IGC),DELTAX(IGC),GHR(IGC), IGC=1,NGC)
       PRINT 23, GHA
       PRINT 21
       GO TO 14
34     CONTINUE
       PRINT 22, X(I),H,AMP,PHA,AMPH,PHAH,TIME,FLDS(I),BTL
       WRITE (2,*) X(I)/1000.,AMPH
14     CONTINUE
       GO TO 4
C
18     FORMAT (*ONUMBER OF DISTANCES < 4*)
19     FORMAT (4F10.5)
20     FORMAT (*OFREQUENCY =*,F10.2,10X,A8,*AL POLARIZATION*,8X,*EARTH RA
      CDIUS =*F10.0,* KM*/
      C1X,*TRANSMITTER ANTENNA HEIGHT =*F7.3,* METERS*,10X,*RECEIVER ANTE
      CNNA HEIGHT =*F7.3,* METERS*)
21     FORMAT (//9X,*X*,10X,*Z*,16X,*F(X)*,
      C24X,*FH(X)*,13X,*TIMING*,2X,*FIELD STR*,3X,*BTL*/
      C8X,*(M)*,8X,*(M)*,6X,*MAG*,
      C10X,*ARG*,12X,*MAG*,10X,*ARG*,12X,*(SEC)*,4X,*(DBU)*)
22     FORMAT (*0*,F12.2,F10.1,E15.5,E13.5,
      CE15.5,E13.5,F10.3,F10.2,F8.2)
23     FORMAT (/1X,*GHA=*2F8.4)
24     FORMAT (//1X,*DISTANCE SIGMA  EPSILON SLAB     SH      *,
      C*  SV           EH      EV          IMPEDANCE    *,
      C*         GHR*/)
26     FORMAT (1X,F7.0,F9.6,F7.2,F5.0,2X,2F9.6,2X,2F7.2,2X,2F8.4,
      C2X,2F8.4)
       END




       COMPLEX FUNCTION KERNL(XO)
       COMMON /1/ HA,HAR,AKM
       COMMON /2/ D,H,HP
       COMMON /3/ DELTAR,WAVE
       COMMON /4/ FREQ,POL
       COMMON /5/ NG,AB(48),GH(48)
       COMMON /6/ NX,X(2001),I
       COMPLEX FEWH,DELTA,DELTAR,ETA,ETAR
       CALL TERRANE (XO,HO,HPO,ETA,DELTA,ETAR,DELTAR,COND,EPS)
       XMS=X(I)-XO
       HD=H-HO
       R1=SQRT(XO**2)
       RW=WAVE*(XO+((HO**2)/(2.*XO))+XMS+((HD**2)/(2.*XMS))-D)
       KERNL=CMPLX(COS (RW),-SIN (RW))*SQRT(X(I)/(R1*XMS))*((HPO+DELTA-DE
      1LTAR)*FEWH(HD,XMS)-(HD/XMS))
       RETURN
       END
```

```
      COMPLEX FUNCTIONWERF(ZZZ)
      COMPLEX Z,ZZZ,ZV,V,Z2,C,W,S
      DIMENSION C(12), W(5,4)
      EQUIVALENCE (S,C(12))
      LOGICAL LZ2
      DATA (C(1)=(.0,-.5641895835))
      DATA (((W(I,J),I=1,5),J=1,4)=(1.,.0),
     X (3.678794411714423E-01,6.071577058413937E-01),
     X (1.831563888873418E-02,3.400262170660662E-01),
     X (1.234098040866788E-04,2.011573170376004E-01),
     X (1.125351747192646E-07,1.459535899001528E-01),
     X (4.275835761558070E-01,0.000000000000000E+00),
     X (3.047442052569126E-01,2.082189382028316E-01),
     X (1.402395813662779E-01,2.222134401798991E-01),
     X (6.531777728904697E-02,1.739183154163490E-01),
     X (3.628145643998864E-02,1.358389510006551E-01),
     X (2.553956763105058E-01,0.000000000000000E+00),
     X (2.184926152748907E-01,9.299780939260186E-02),
     X (1.479527595120158E-01,1.311797170842178E-01),
     X (9.271076642644332E-02,1.283169622282615E-01),
     X (5.968692961044590E-02,1.132100561244882E-01),
     X (1.790011511813930E-01,0.000000000000000E+00),
     X (1.642611363929861E-01,5.019713513524966E-02),
     X (1.307574696698522E-01,8.111265047745472E-02),
     X (9.640250558304439E-02,9.123632600421258E-02),
     X (6.979096164964750E-02,8.934000024036461E-02))
      XX=REAL(ZZZ)
      YY=AIMAG(ZZZ)
      X=ABS (XX)
      Y=ABS (YY)
      Z=CMPLX(X,Y)
      LZ2=.FALSE.
      IF (X.GE.4.5.OR.Y.GE.3.5) GO TO 6
      I=X+.5
      J=Y+.5
      V=CMPLX(FLOAT(I),FLOAT(J))
      ZV=Z-V
      C(2)=W(I+1,J+1)
      AI=0.
      DO 1 I=3,12
      AI=AI-.5
      C(I)=(V*C(I-1)+C(I-2))/AI
1     CONTINUE
      J=12
      DO 2 I=2,11
      J=J-1
2     S=S*ZV+C(J)
3     IF (YY.GE.0.) GO TO 4
      IF (.NOT.LZ2) Z2=Z*Z
      S=2.*CEXP(-Z2)-S
      IF (XX.GT.0.) S=CONJG(S)
      GO TO 5
4     IF (XX.LT.0.) S=CONJG(S)
5     WERF=S
      RETURN
6     LZ2=.TRUE.
      Z2=Z*Z
      S=Z*((0.,0.4613135279)/(Z2-0.1901635092)+(0.,0.09999216168)/
     1(Z2-1.7844927485)+(0.,0.002889389748)/(Z2-5.525343743791)
      GO TO 3
      END
```

```
      COMPLEX FUNCTIONFEWH(HD,XD)
      COMMON /3/ DELTAR,WAVE
      COMPLEX TEMP,Q,Z,Z2,ZZ,HWERF,WERFZ,WERF,ZWERF,DELTAR
      TEMP=(0.7071067812,-0.7071067812)*SQRT(.5*WAVE)
      XD2=SQRT(XD)
      Q=-TEMP*HD/XD2
      Z=TEMP*DELTAR*XD2+Q
      ZZ=-Z
      ZI=AIMAG(ZZ)
      IF (ZI.LT.0..OR.(ABS(REAL(ZZ)).LT.6..AND.ZI.LT.6.)) GO TO 1
      Z2=ZZ**2
      HWERF=(Z2-2.)/(ZZ*(Z2-3.5))
      GO TO 2
1     WERFZ=WERF(ZZ)
      HWERF=ZZ-0.5*WERFZ/(ZZ*WERFZ+(0.,-0.56418958))
2     ZWERF=Z+HWERF
      FEWH=(Q*ZWERF-0.5)/(Z*ZWERF-0.5)
      RETURN
      END




      SUBROUTINE TERRANE (X,H,HP,ETA,DELTA,ETAR,DELTAR,COND,EPS)
      COMMON/INPUT/ TD(5000),THT(5000)
      COMMON /GCX/ NGC,DX(50),ETAX(50),DELTAX(50),SIGX(50),EPSX(50),
     CT(50),SH(50),SV(50),EH(50),EV(50),GHA,GHR(50)
      COMMON /1/ HA,HAR,AKM
      COMPLEX ETAX,DELTAX,ETAR,DELTAR,ETA,DELTA
C
C     COMPUTE HEIGHT, SLOPE, CONDUCTIVITY AND DIELECTRIC CONSTANT AT X.
C
7     CONTINUE
      IF (X .GT. TD(N)) X=TD(N)
      A=1000.*AKM
      HP=-X/A
      H=.5*X*HP
      DO 6 I=2,N
      IF (X .GT. TD(I)) GO TO 6
      H=H+THT(I-1)+((X-TD(I-1))/(TD(I)-TD(I-1)))*(THT(I)-THT(I-1))
      HP=HP+(THT(I)-THT(I-1))/(TD(I)-TD(I-1))
      GO TO 9
6     CONTINUE
9     CONTINUE
      DO 2 I=1,50
      IF (X .LE. (DX(I)+.0001)) GO TO 4
2     CONTINUE
4     ETA=ETAX(I)
      DELTA=DELTAX(I)
      COND=SIGX(I)
      EPS=EPSX(I)
C
C     MODIFICATION OF H AND HP FOR PRESENCE OF SLAB.
C
      IF (I .EQ. 1) GO TO 10
      H=H+T(I-1)+((X-DX(I-1))/(DX(I)-DX(I-1)))*(T(I)-T(I-1))
      HP=HP+(T(I)-T(I-1))/(DX(I)-DX(I-1))
      GO TO 12
10    CONTINUE
      H=H+T(1)
12    CONTINUE
      RETURN
      ENTRY TERRAN2
      CALL IN(N)
      ETAR=ETAX(1)
      DELTAR=DELTAX(1)
      GO TO 7
      END
```

```
      SUBROUTINE DISTX
C
C     SUBROUTINE TO FILL DISTANCE ARRAY.  USE EITHER SPECIFIC
C     DISTANCES (KIND = 1) OR COMPUTE DISTANCES AT EQUIDISTANT
C     POINTS (KIND = 0).  A COMBINATION OF THE TWO KINDS CAN BE
C     USED.  ALL VARIABLES ARE READ IN IN KILOMETERS AND THE
C     DISTANCE ARRAY IS FILLED IN METERS.
C
      COMMON /6/ N,X(2001),INDEX
      DIMENSION DEP(50),FINT(50)
      N=2
      READ 100, KIND,TD
      IF (EOF(60)) 8,2
2     CONTINUE
      TDM=TD*1.E+3
      IF (KIND) 4,12
4     DO 6 L=N,2001,8
      K=L+7
      READ 101, (X(I), I=L,K)
      DO 6 J=1,8
      N=L+J-1
      IF (X(N) .LE. 0.) GO TO 10
      X(N)=X(N)*1.E+3
6     CONTINUE
7     PRINT 102
8     CALL EXIT
10    IF (X(N-1) .LT. TDM) GO TO 12
      N=N-1
      RETURN
12    READ 103, NED,(DEP(I),FINT(I), I=1,NED)
      DO 20 I=1,NED
      DEPM=DEP(I)*1.E+3
      FINTM=FINT(I)*1.E+3
      SV=.1*FINTM
      DO 14 J=N,2001
      JS=J
      X(J)=FINTM+X(J-1)
      IF (X(J) .GE. (TDM-SV)) GO TO 16
      IF (X(J) .GE. (DEPM-SV)) GO TO 18
14    CONTINUE
      GO TO 7
16    X(JS)=TDM
      N=JS
      RETURN
18    X(JS)=DEPM
      N=JS+1
20    CONTINUE
      GO TO 4
100   FORMAT (I10,F10.0)
101   FORMAT (8F10.5)
102   FORMAT (*0NUMBER OF DISTANCES EXCEEDS DIMENSION*)
103   FORMAT (I2/(8F10.0))
      END
```

```
      SUBROUTINE IN(N)
      COMMON /INPUT/X(5000), Z(5000), A(120), B(120), AA(40), AB(40), ID
     1(8),REFEL
      COMMON /CCX/ NGC,DX(50),ETAX(50),DELTAX(50),SIGX(50),EPSX(50),
     CT(50),SH(50),SV(50),EH(50),EV(50),GHA,GHR(50)
      COMMON /1/ HA,HAR,AKM
      COMMON /4/ FREQ,POL
      COMPLEX ETAX,EHC,EVC,AK,V,D1,D2,TVT,DELTAX,CTANH
      COMPLEX GHA,GHR,R,FH,FHT,EI
      DATA EI/(0.,1.)/
      FH(ANT)=1.+EI*WN*DELTAX(I)*(ANT-T(I))
      FHT(ANT)=(CEXP(-V*(T(I)-ANT))+R*CEXP(-V*(T(I)+ANT)))/
     C(EVC*(1.+R*CEXP(-2.*V*T(I))))
C
C     INPUT
C
C     ID = IDENTIFICATION
C     N = NUMBER OF DATA POINTS
C     IXUNITS =0, DISTANCES INPUT IN KILOMETERS
C     IXUNITS =1, DISTANCES INPUT IN MILES
C     IZUNITS = 0, HEIGHTS INPUT IN METERS
C     IZUNITS = 1, HEIGHTS INPUT IN FEET
C     REFEL = REFERENCE ELEVATION IN METERS
C
1502  FORMAT (8A10)
1503  FORMAT (2X,8A10)
1504  FORMAT  (4(F10.5,F10.1))
1505  FORMAT(4(F10.2,F10.0))
1506  FORMAT  (10X,I10,2F15.5)
1510  FORMAT (3I10,F10.1)
1511  FORMAT (2X,*NUMBER OF PROFILE DATA POINTS IS*I10/
     C2X,*REFERENCE ELEVATION IS*F10.2,* METERS*/
     C2X,*PATH PROFILE AS PUT IN FOLLOWS*/)
1512  FORMAT (//* THE NUMBER OF SCALED DATA POINTS HAS EXCEEDED 5000 OR
     1THE NUMBER OF GROUND CONSTANT PAIRS HAS EXCEEDED 50*)
1513  FORMAT (*0ADJUSTED PATH PROFILE FOLLOWS*/23X,* D IN METERS*,3X,
     1*HT IN METERS*)
1514  FORMAT  (1H1)
1515  FORMAT (*0*I2,* DISTANCE AND GROUND CONSTANT PAIRS FOLLOW*/
     111X,*D IN KM*,3X,*SIGMA*,2X,*EPSILON*/
     C(10X,F8.3,F8.4,F9.0))
1516  FORMAT (F8.2,F8.6,F8.2,I2,3F8.2,2F8.6)
      FTOM = .3048
      READ 1502, ID
      PRINT 1514
      PRINT 1503, ID
      READ 1510, N,IXUNITS,IZUNITS,REFEL
      IF (IZUNITS .EQ. 1) REFEL=REFEL*FTOM
      IF (N .GT. 5000) GO TO 110
      PRINT 1511, N,REFEL
      READ 1505, (X(I),Z(I), I=1,N)
      PRINT 1504, (X(I), Z(I), I = 1, N)
      IF (N .LT. 1) GO TO 120
      PRINT 1513
      XCONST=1000.
      IF (IXUNITS .EQ. 1) XCONST=1609.3
      ZCONST=1.
      IF (IZUNITS .EQ. 1) ZCONST=FTOM
      DO 105 I = 1, N
      Z(I)=Z(I)*ZCONST-REFEL
      X(I)=X(I)*XCONST
      PRINT 1506, I, X(I), Z(I)
 105  CONTINUE
 120  CONTINUE
      READ 1510, NGC
      IF (NGC .GT. 50) GO TO 110
      WN=2.*3.141592654*FREQ/299.7925
      DO 130 I=1,NGC
      READ 1516, DX(I),SIGX(I),EPSX(I),ISLAB,T(I),EH(I),EV(I),SH(I),
     CSV(I)
      ETAX(I)=CMPLX(EPSX(I),-17975.*SIGX(I)/FREQ)
      IF (ISLAB .NE. 0) GO TO 125
      DELTAX(I)=CSQRT(ETAX(I)-1.)
      DELTAX(I)=DELTAX(I)/ETAX(I)
      IF (I .EQ. 1) GHA=FH(HA)
      GHR(I)=FH(HAR)
```

```
      GO TO 130
125   CONTINUE
      EHC=CMPLX(EH(I),-17975.*SH(I)/FREQ)
      EVC=CMPLX(EV(I),-17975.*SV(I)/FREQ)
      AK=EHC/EVC
      V=CMPLX(0.,WN)*CSQRT(EHC-AK)
      D1=CSQRT(EHC-AK)/EHC
      D2=CSQRT(ETAX(I)-1.)/ETAX(I)
      TVT=CTANH(V*T(I))
      DELTAX(I)=D1*((D2+D1*TVT)/(D1+D2*TVT))
      IF (I .NE. 1) GO TO 127
      IF (T(I) .GT. HA) GO TO 126
      GHA=FH(HA)
      GO TO 127
126   CONTINUE
      R=(D1-D2)/(D1+D2)
      GHA=FHT(HA)
127   CONTINUE
      IF (T(I) .GT. HAR) GO TO 128
      GHR(I)=FH(HAR)
      GO TO 130
128   CONTINUE
      R=(D1-D2)/(D1+D2)
      GHR(I)=FHT(HAR)
130   DX(I)=DX(I)*1000.
      RETURN
110   CONTINUE
      PRINT 1512
      END



      COMPLEX FUNCTION CTANH(Z)
      COMPLEX Z,U
      U=CEXP(2.*Z)
      CTANH=(U-1.)/(U+1.)
      END
```

A sample output for program WAGSLAB is given below:

```
INNERINGEN TO BORLINGEN
NUMBER OF PROFILE DATA POINTS IS       115
REFERENCE ELEVATION IS    810.00 METERS
PATH PROFILE AS PUT IN FOLLOWS

 0.00000     810.0     .53000     820.0     .80000     827.0    1.00000     820.0
 1.40000     800.0    2.55000     780.0    3.35000     760.0    3.60000     735.0
 3.80000     760.0    4.95000     760.0    5.80000     780.0    6.20000     780.0
 8.80000     780.0    9.00000     768.0   10.05000     780.0   11.30000     780.0
11.65000     740.0   11.75000     700.0   11.95000     700.0   13.10000     720.0
13.60000     730.0   14.10000     720.0   15.40000     740.0   16.20000     760.0
17.25000     780.0   17.80000     780.0   18.00000     790.0   18.75000     800.0
19.00000     800.0   19.40000     740.0   19.80000     770.0   20.20000     740.0
20.40000     740.0   20.80000     760.0   22.00000     760.0   22.70000     780.0
23.05000     800.0   23.20000     820.0   23.60000     820.0   24.08000     780.0
24.30000     820.0   24.85000     820.0   25.15000     800.0   25.90000     640.0
26.05000     640.0   26.20000     720.0   26.60000     670.0   26.80000     705.0
27.10000     620.0   27.30000     700.0   27.70000     600.0   28.30000     520.0
28.70000     500.0   29.00000     480.0   29.25000     480.0   29.35000     500.0
30.00000     500.0   30.20000     440.0   30.60000     440.0   30.85000     420.0
31.35000     400.0   32.30000     400.0   32.45000     380.0   33.75000     380.0
33.90000     360.0   35.20000     340.0   36.80000     340.0   36.90000     360.0
37.60000     360.0   37.85000     380.0   38.10000     380.0   38.50000     360.0
38.65000     340.0   38.75000     320.0   39.30000     320.0   39.50000     380.0
39.80000     420.0   41.00000     420.0   41.93000     440.0   43.75000     440.0
44.10000     460.0   44.40000     480.0   44.75000     480.0   45.00000     500.0
45.35000     500.0   45.65000     460.0   45.95000     400.0   46.10000     370.0
46.60000     440.0   47.05000     420.0   47.25000     440.0   47.55000     460.0
48.60000     460.0   48.65000     440.0   49.30000     380.0   49.50000     400.0
49.95000     415.0   50.30000     400.0   50.55000     380.0   50.75000     380.0
50.95000     400.0   51.65000     400.0   51.75000     380.0   52.20000     380.0
52.30000     400.0   52.55000     420.0   53.65000     420.0   54.00000     400.0
54.35000     400.0   54.85000     420.0   55.00000     440.0   55.55000     425.0
55.90000     440.0   56.15000     460.0   56.63000     465.0

ADJUSTED PATH PROFILE FOLLOWS
                    D IN METERS    HT IN METERS
                1       0.00000        0.00000
                2     530.00000       10.00000
                3     800.00000       17.00000
                4    1000.00000       10.00000
                5    1400.00000      -10.00000
                6    2550.00000      -30.00000
                7    3350.00000      -50.00000
                8    3600.00000      -75.00000
                9    3800.00000      -50.00000
               10    4950.00000      -50.00000
               11    5800.00000      -30.00000
               12    6200.00000      -30.00000
               13    8800.00000      -30.00000
               14    9000.00000      -42.00000
               15   10050.00000      -30.00000
               16   11300.00000      -30.00000
               17   11650.00000      -70.00000
               18   11750.00000     -110.00000
               19   11950.00000     -110.00000
               20   13100.00000      -90.00000
               21   13600.00000      -80.00000
               22   14100.00000      -90.00000
               23   15400.00000      -70.00000
               24   16200.00000      -50.00000
               25   17250.00000      -30.00000
               26   17300.00000      -30.00000
               27   18000.00000      -20.00000
               28   18750.00000      -10.00000
               29   19000.00000      -10.00000
               30   19400.00000      -70.00000
```

31	19800.00000	-40.00000
32	20200.00000	-70.00000
33	20400.00000	-70.00000
34	20800.00000	-50.00000
35	22000.00000	-50.00000
36	22700.00000	-30.00000
37	23050.00000	-10.00000
38	23200.00000	10.00000
39	23600.00000	10.00000
40	24080.00000	-30.00000
41	24300.00000	10.00000
42	24850.00000	10.00000
43	25150.00000	-10.00000
44	25900.00000	-170.00000
45	26050.00000	-170.00000
46	26200.00000	-90.00000
47	26600.00000	-140.00000
48	26800.00000	-105.00000
49	27100.00000	-190.00000
50	27300.00000	-110.00000
51	27700.00000	-210.00000
52	28300.00000	-290.00000
53	28700.00000	-310.00000
54	29000.00000	-330.00000
55	29250.00000	-330.00000
56	29350.00000	-310.00000
57	30000.00000	-310.00000
58	30200.00000	-370.00000
59	30600.00000	-370.00000
60	30850.00000	-390.00000
61	31350.00000	-410.00000
62	32300.00000	-410.00000
63	32450.00000	-430.00000
64	33750.00000	-430.00000
65	33900.00000	-450.00000
66	35200.00000	-470.00000
67	35800.00000	-470.00000
68	36900.00000	-450.00000
69	37600.00000	-450.00000
70	37850.00000	-430.00000
71	38100.00000	-430.00000
72	38500.00000	-450.00000
73	38650.00000	-470.00000
74	38750.00000	-490.00000
75	39300.00000	-490.00000
76	39500.00000	-430.00000
77	39800.00000	-390.00000
78	41000.00000	-390.00000
79	41930.00000	-370.00000
80	43750.00000	-370.00000
81	44100.00000	-350.00000
82	44400.00000	-330.00000
83	44750.00000	-330.00000
84	45000.00000	-310.00000
85	45350.00000	-310.00000
86	45650.00000	-350.00000
87	45950.00000	-410.00000
88	46100.00000	-440.00000
89	46600.00000	-370.00000
90	47050.00000	-390.00000
91	47250.00000	-370.00000
92	47550.00000	-350.00000
93	48600.00000	-350.00000
94	48650.00000	-370.00000
95	49300.00000	-430.00000
96	49500.00000	-410.00000
97	49950.00000	-395.00000
98	50300.00000	-410.00000
99	50550.00000	-430.00000
100	50750.00000	-430.00000
101	50950.00000	-410.00000
102	51650.00000	-410.00000
103	51750.00000	-430.00000
104	52200.00000	-430.00000
105	52300.00000	-410.00000

106	52550.00000	-390.00000
107	53650.00000	-390.00000
108	54000.00000	-410.00000
109	54350.00000	-410.00000
110	54850.00000	-390.00000
111	55000.00000	-370.00000
112	55550.00000	-385.00000
113	55900.00000	-370.00000
114	56150.00000	-350.00000
115	56630.00000	-345.00000

FREQUENCY = 2.00 VERTICAL POLARIZATION EARTH RADIUS = 8500. KM
TRANSMITTER ANTENNA HEIGHT = 0.000 METERS RECEIVER ANTENNA HEIGHT = 0.000 METERS

DISTANCE	SIGMA	EPSILON	SLAB	SH	SV	EH	EV	IMPEDANCE		GHR	
500.	.010000	10.00	0.	0.000000	0.000000	0.00	0.00	.0787	.0697	1.0000	0.0000
1080.	.010000	10.00	20.	.000100	.000100	1.10	1.10	.5442	.2888	.6644	.1684
3510.	.010000	10.00	0.	0.000000	0.000000	0.00	0.00	.0787	.0697	1.0000	0.0000
5080.	.010000	10.00	20.	.000100	.000100	1.10	1.10	.5442	.2888	.6644	.1684
6750.	.010000	10.00	0.	0.000000	0.000000	0.00	0.00	.0787	.0697	1.0000	0.0000
7320.	.010000	10.00	20.	.000100	.000100	1.10	1.10	.5442	.2888	.6644	.1684
8400.	.010000	10.00	0.	0.000000	0.000000	0.00	0.00	.0787	.0697	1.0000	0.0000
9110.	.010000	10.00	20.	.000100	.000100	1.10	1.10	.5442	.2888	.6644	.1684
10770.	.010000	10.00	0.	0.000000	0.000000	0.00	0.00	.0787	.0697	1.0000	0.0000
11560.	.010000	10.00	20.	.000100	.000100	1.10	1.10	.5442	.2888	.6644	.1684
11980.	.010000	10.00	0.	0.000000	0.000000	0.00	0.00	.0787	.0697	1.0000	0.0000
12820.	.010000	10.00	10.	.000030	.000030	1.82	1.82	.1435	.2748	.6104	.0286
19460.	.010000	10.00	0.	0.000000	0.000000	0.00	0.00	.0787	.0697	1.0000	0.0000
20280.	.010000	10.00	20.	.000100	.000100	1.10	1.10	.5442	.2888	.6644	.1684
25030.	.010000	10.00	0.	0.000000	0.000000	0.00	0.00	.0787	.0697	1.0000	0.0000
28100.	.010000	10.00	20.	.000100	.000100	1.10	1.10	.5442	.2888	.6644	.1684
29540.	.010000	10.00	0.	0.000000	0.000000	0.00	0.00	.0787	.0697	1.0000	0.0000
30460.	.010000	10.00	20.	.000100	.000100	1.10	1.10	.5442	.2888	.6644	.1684
32630.	.010000	10.00	0.	0.000000	0.000000	0.00	0.00	.0787	.0697	1.0000	0.0000
33680.	.010000	10.00	20.	.000100	.000100	1.10	1.10	.5442	.2888	.6644	.1684
34550.	.010000	10.00	0.	0.000000	0.000000	0.00	0.00	.0787	.0697	1.0000	0.0000
35750.	.010000	10.00	20.	.000100	.000100	1.10	1.10	.5442	.2888	.6644	.1684
36920.	.010000	10.00	10.	.000030	.000030	1.82	1.82	.1435	.2748	.6104	.0286
37700.	.010000	10.00	0.	0.000000	0.000000	0.00	0.00	.0787	.0697	1.0000	0.0000
38750.	.010000	10.00	10.	.000030	.000030	1.82	1.82	.1435	.2748	.6104	.0286
39360.	.010000	10.00	0.	0.000000	0.000000	0.00	0.00	.0787	.0697	1.0000	0.0000
39920.	.010000	10.00	20.	.000100	.000100	1.10	1.10	.5442	.2888	.6644	.1684
41960.	.010000	10.00	0.	0.000000	0.000000	0.00	0.00	.0787	.0697	1.0000	0.0000
47500.	.010000	10.00	20.	.000100	.000100	1.10	1.10	.5442	.2888	.6644	.1684
48800.	.010000	10.00	0.	0.000000	0.000000	0.00	0.00	.0787	.0697	1.0000	0.0000
51670.	.010000	10.00	20.	.000100	.000100	1.10	1.10	.5442	.2888	.6644	.1684
52080.	.010000	10.00	0.	0.000000	0.000000	0.00	0.00	.0787	.0697	1.0000	0.0000
56630.	.010000	10.00	20.	.000100	.000100	1.10	1.10	.5442	.2888	.6644	.1684

GHA= 1.0000 0.0000

X (M)	Z (M)	F(X) MAG	F(X) ARG	FH(X) MAG	FH(X) ARG	TIMING (SEC)	FIELD STR (DBU)	BTL
200.00	3.8	.96930E+00	-.38983E+00	.96930E+00	-.38983E+00	.180	126.65	18.74
400.00	7.5	.95300E+00	-.55580E+00	.95300E+00	-.55580E+00	.184	120.48	24.91
600.00	15.2	.95266E+00	-.69678E+00	.65300E+00	-.44850E+00	.185	113.68	31.71
800.00	27.3	.97126E+00	-.83019E+00	.66575E+00	-.58191E+00	.187	111.35	34.04
1000.00	27.2	.94560E+00	-.91492E+00	.64816E+00	-.66664E+00	.189	109.18	36.21

1200.00	18.9	.96455E+00	-.25896E+01	.96455E+00	-.25896E+01	.200	111.05	34.34
1400.00	7.3	.84870E+00	-.26652E+01	.84870E+00	-.26652E+01	.211	108.60	36.80
1600.00	2.1	.76305E+00	-.26492E+01	.76305E+00	-.26492E+01	.224	106.51	38.88
1800.00	-3.1	.69663E+00	-.26693E+01	.69663E+00	-.26693E+01	.237	104.70	40.69
2000.00	-8.2	.64871E+00	-.26960E+01	.64871E+00	-.26960E+01	.253	103.16	42.23
2200.00	-13.4	.61157E+00	-.27255E+01	.61157E+00	-.27255E+01	.269	101.82	43.57
2400.00	-18.6	.58130E+00	-.27562E+01	.58130E+00	-.27562E+01	.285	100.63	44.76
2600.00	-24.2	.55178E+00	-.27955E+01	.55178E+00	-.27955E+01	.304	99.48	45.91
2800.00	-30.9	.53034E+00	-.28323E+01	.53034E+00	-.28323E+01	.325	98.49	46.90
3000.00	-37.6	.51095E+00	-.28676E+01	.51095E+00	-.28676E+01	.345	97.57	47.82
3200.00	-44.3	.49379E+00	-.29009E+01	.49379E+00	-.29009E+01	.367	96.71	48.68
3400.00	-54.8	.44438E+00	-.30159E+01	.44438E+00	-.30159E+01	.391	95.27	50.12
3600.00	-74.6	.29656E+00	.26569E+01	.20328E+00	.29052E+01	.418	87.98	57.41
3800.00	-47.2	.22414E+00	.30071E+01	.15363E+00	-.30278E+01	.446	85.08	60.31
4000.00	-44.7	.16306E+00	.27201E+01	.11177E+00	.29684E+01	.474	81.87	63.52
4200.00	-42.2	.11980E+00	.27928E+01	.82119E-01	.30411E+01	.505	78.77	66.62
4400.00	-39.8	.10462E+00	.28246E+01	.71714E-01	.30729E+01	.536	77.19	68.20
4600.00	-37.4	.90031E-01	.28520E+01	.61712E-01	.31002E+01	.570	75.50	69.90
4800.00	-34.9	.80126E-01	.28926E+01	.54922E-01	.31409E+01	.605	74.11	71.28
5000.00	-31.3	.73901E-01	.29486E+01	.50655E-01	-.30863E+01	.641	73.06	72.33
5200.00	-27.1	.11860E+00	-.27635E+01	.11860E+00	-.27635E+01	.680	80.10	65.29
5400.00	-25.0	.13901E+00	-.26952E+01	.13901E+00	-.26952E+01	.721	81.16	64.23
5600.00	-22.8	.15515E+00	-.26678E+01	.15515E+00	-.26678E+01	.764	81.79	63.60
5800.00	-20.6	.16575E+00	-.26612E+01	.16575E+00	-.26612E+01	.807	82.06	63.33
6000.00	-23.1	.16872E+00	-.27086E+01	.16872E+00	-.27086E+01	.852	81.92	63.47
6200.00	-25.7	.17268E+00	-.27373E+01	.17268E+00	-.27373E+01	.896	81.84	63.55
6400.00	-28.2	.17547E+00	-.27638E+01	.17547E+00	-.27638E+01	.940	81.70	63.69
6600.00	-30.8	.17729E+00	-.27891E+01	.17729E+00	-.27891E+01	.991	81.53	63.87

6800.00	-31.0	.15216E+00	-.30967E+01	.10430E+00	-.28484E+01	1.040	76.66	68.73
7000.00	-24.1	.77416E-01	.26346E+01	.53064E-01	.28829E+01	1.095	70.54	74.85
7200.00	-17.3	.57140E-01	.29628E+01	.39166E-01	-.30721E+01	1.148	67.65	77.74
7400.00	-14.7	.77139E-01	-.29603E+01	.77139E-01	-.29603E+01	1.198	73.30	72.09
7600.00	-18.6	.94463E-01	-.28615E+01	.94463E-01	-.28615E+01	1.252	74.83	70.56
7800.00	-22.5	.10525E+00	-.28440E+01	.10525E+00	-.28440E+01	1.311	75.55	69.85
8000.00	-26.4	.11229E+00	-.28498E+01	.11229E+00	-.28498E+01	1.369	75.89	69.50
8200.00	-30.3	.11721E+00	-.28637E+01	.11721E+00	-.28637E+01	1.429	76.05	69.34
8400.00	-34.2	.12076E+00	-.28811E+01	.82772E-01	-.26328E+01	1.493	72.81	72.58
8600.00	-28.7	.70263E-01	.25926E+01	.48162E-01	.28408E+01	1.559	67.91	77.48
8800.00	-23.3	.42090E-01	.28495E+01	.28850E-01	.30977E+01	1.625	63.26	82.13
9000.00	-29.9	.39431E-01	.27085E+01	.27028E-01	.29568E+01	1.691	62.49	82.90
9200.00	-25.8	.52312E-01	-.30109E+01	.52312E-01	-.30109E+01	1.757	68.04	77.35
9400.00	-26.1	.67646E-01	-.28601E+01	.67646E-01	-.28601E+01	1.823	70.09	75.31
9600.00	-26.5	.77602E-01	-.28151E+01	.77602E-01	-.28151E+01	1.890	71.09	74.30
9800.00	-26.8	.84469E-01	-.28008E+01	.84469E-01	-.28008E+01	1.957	71.65	73.74
10000.00	-27.2	.89519E-01	-.27987E+01	.89519E-01	-.27987E+01	2.028	71.98	73.41
10200.00	-29.3	.92361E-01	-.28213E+01	.92361E-01	-.28213E+01	2.101	72.08	73.31
10400.00	-31.9	.94879E-01	-.28413E+01	.94879E-01	-.28413E+01	2.176	72.15	73.25
10600.00	-34.6	.97023E-01	-.28598E+01	.97023E-01	-.28598E+01	2.249	72.17	73.22
10800.00	-36.1	.82146E-01	.30995E+01	.56307E-01	-.29354E+01	2.328	67.29	78.11
11000.00	-31.3	.48113E-01	.27087E+01	.32979E-01	.29569E+01	2.405	62.48	82.91
11200.00	-26.5	.36071E-01	.28559E+01	.24725E-01	.31042E+01	2.485	59.82	85.57
11400.00	-34.1	.29497E-01	.26767E+01	.20218E-01	.29250E+01	2.566	57.92	87.47
11600.00	-54.1	.29257E-01	.26980E+01	.29257E-01	.26980E+01	2.651	60.98	84.41
11800.00	-109.6	.41025E-01	.28135E+01	.41025E-01	.28135E+01	2.736	63.77	81.62
12000.00	-117.4	.50568E-01	.27324E+01	.30863E-01	.27792E+01	2.829	61.15	84.24
12200.00	-111.8	.60090E-01	.25603E+01	.36718E-01	.26071E+01	2.917	62.51	82.88

12400.00	-106.2	.60312E-01	.24699E+01	.36854E-01	.25167E+01	3.010	62.40	82.99
12600.00	-100.7	.57596E-01	.24268E+01	.35194E-01	.24735E+01	3.104	61.86	83.53
12800.00	-95.1	.54015E-01	.24120E+01	.33006E-01	.24588E+01	3.199	61.17	84.22
13000.00	-92.0	.48090E-01	.28436E+01	.48090E-01	.28436E+01	3.290	64.31	81.09
13200.00	-88.8	.51298E-01	.30669E+01	.51298E-01	.30669E+01	3.388	64.73	80.66
13400.00	-85.4	.54421E-01	-.31002E+01	.54421E-01	-.31002E+01	3.485	65.12	80.27
13600.00	-82.1	.57395E-01	-.30231E+01	.57395E-01	-.30231E+01	3.582	65.45	79.94
13800.00	-86.7	.57735E-01	-.30421E+01	.57735E-01	-.30421E+01	3.680	65.37	80.02
14000.00	-91.3	.59633E-01	-.30404E+01	.59633E-01	-.30404E+01	3.780	65.53	79.86
14200.00	-92.4	.63549E-01	-.29966E+01	.63549E-01	-.29966E+01	3.881	65.96	79.43
14400.00	-90.0	.65927E-01	-.29654E+01	.65927E-01	-.29654E+01	3.984	66.16	79.23
14600.00	-87.5	.67604E-01	-.29451E+01	.67604E-01	-.29451E+01	4.089	66.26	79.14
14800.00	-85.1	.68990E-01	-.29299E+01	.68990E-01	-.29299E+01	4.195	66.31	79.08
15000.00	-82.7	.70156E-01	-.29181E+01	.70156E-01	-.29181E+01	4.309	66.34	79.05
15200.00	-80.3	.71142E-01	-.29090E+01	.71142E-01	-.29090E+01	4.420	66.35	79.04
15400.00	-77.8	.71975E-01	-.29021E+01	.71975E-01	-.29021E+01	4.533	66.34	79.05
15600.00	-73.5	.73454E-01	-.28798E+01	.73454E-01	-.28798E+01	4.647	66.40	78.99
15800.00	-69.2	.74194E-01	-.28677E+01	.74194E-01	-.28677E+01	4.763	66.38	79.01
16000.00	-64.8	.74749E-01	-.28582E+01	.74749E-01	-.28582E+01	4.881	66.33	79.06
16200.00	-60.5	.75178E-01	-.28503E+01	.75178E-01	-.28503E+01	5.002	66.27	79.12
16400.00	-57.4	.74993E-01	-.28543E+01	.74993E-01	-.28543E+01	5.125	66.15	79.24
16600.00	-54.3	.75126E-01	-.28539E+01	.75126E-01	-.28539E+01	5.248	66.06	79.33
16800.00	-51.2	.75237E-01	-.28536E+01	.75237E-01	-.28536E+01	5.381	65.97	79.43
17000.00	-48.1	.75303E-01	-.28536E+01	.75303E-01	-.28536E+01	5.520	65.87	79.52
17200.00	-45.0	.75321E-01	-.28541E+01	.75321E-01	-.28541E+01	5.655	65.77	79.62
17400.00	-44.7	.73846E-01	-.28844E+01	.73846E-01	-.28844E+01	5.790	65.50	79.89
17600.00	-45.4	.73163E-01	-.29049E+01	.73163E-01	-.29049E+01	5.927	65.32	80.07
17800.00	-46.1	.72862E-01	-.29205E+01	.72862E-01	-.29205E+01	6.068	65.18	80.21

18000.00	-36.9	.76974E-01	-.28453E+01	.76974E-01	-.28453E+01	6.213	65.56	79.83
18200.00	-34.9	.74429E-01	-.28794E+01	.74429E-01	-.28794E+01	6.358	65.18	80.21
18400.00	-33.0	.73960E-01	-.28877E+01	.73960E-01	-.28877E+01	6.503	65.03	80.36
18600.00	-31.1	.73614E-01	-.28943E+01	.73614E-01	-.28943E+01	6.650	64.89	80.50
18800.00	-29.8	.72319E-01	-.29149E+01	.72319E-01	-.29149E+01	6.799	64.64	80.75
19000.00	-30.5	.71841E-01	-.29336E+01	.71841E-01	-.29336E+01	6.946	64.50	80.90
19200.00	-61.3	.59964E-01	.30042E+01	.59964E-01	.30042E+01	7.097	62.83	82.56
19400.00	-92.0	.56632E-01	.28244E+01	.56632E-01	.28244E+01	7.248	62.25	83.14
19600.00	-74.2	.39896E-01	.25546E+01	.27347E-01	.28029E+01	7.397	55.84	89.55
19800.00	-54.8	.30739E-01	.27634E+01	.21070E-01	.30117E+01	7.549	53.48	91.91
20000.00	-65.4	.22500E-01	.24181E+01	.15423E-01	.26664E+01	7.702	50.69	94.71
20200.00	-76.0	.17484E-01	.24390E+01	.11985E-01	.26873E+01	7.859	48.41	96.98
20400.00	-75.0	.30223E-01	.31044E+01	.30223E-01	.31044E+01	8.015	56.36	89.03
20600.00	-66.3	.37819E-01	-.29864E+01	.37819E-01	-.29864E+01	8.174	58.22	87.17
20800.00	-57.6	.43304E-01	-.28921E+01	.43304E-01	-.28921E+01	8.332	59.31	86.08
21000.00	-59.0	.44663E-01	-.29266E+01	.44663E-01	-.29266E+01	8.495	59.50	85.89
21200.00	-60.3	.46822E-01	-.29335E+01	.46822E-01	-.29335E+01	8.663	59.83	85.57
21400.00	-61.7	.48567E-01	-.29418E+01	.48567E-01	-.29418E+01	8.831	60.06	85.33
21600.00	-63.0	.49968E-01	-.29512E+01	.49968E-01	-.29512E+01	8.998	60.23	85.16
21800.00	-64.4	.51097E-01	-.29614E+01	.51097E-01	-.29614E+01	9.171	60.34	85.05
22000.00	-65.7	.52013E-01	-.29720E+01	.52013E-01	-.29720E+01	9.343	60.42	84.97
22200.00	-61.4	.54526E-01	-.29304E+01	.54526E-01	-.29304E+01	9.519	60.75	84.64
22400.00	-57.0	.55575E-01	-.29157E+01	.55575E-01	-.29157E+01	9.697	60.84	84.56
22600.00	-52.7	.56334E-01	-.29055E+01	.56334E-01	-.29055E+01	9.879	60.88	84.51
22800.00	-45.5	.58617E-01	-.28621E+01	.58617E-01	-.28621E+01	10.060	61.14	84.25
23000.00	-35.4	.59792E-01	-.28291E+01	.59792E-01	-.28291E+01	10.246	61.24	84.15
23200.00	-14.0	.65409E-01	-.27069E+01	.65409E-01	-.27069E+01	10.437	61.95	83.44
23400.00	-15.3	.58231E-01	-.28381E+01	.58231E-01	-.28381E+01	10.625	60.86	84.53
23600.00	-16.7	.57064E-01	-.28754E+01	.57064E-01	-.28754E+01	10.819	60.61	84.78

23800.00	-34.8	.51270E-01	-.30799E+01	.51270E-01	-.30799E+01	11.008	59.61	85.78
24000.00	-52.9	.49700E-01	.30913E+01	.49700E-01	.30913E+01	11.193	59.27	86.12
24200.00	-39.1	.59676E-01	-.29300E+01	.59676E-01	-.29300E+01	11.382	60.78	84.61
24400.00	-22.4	.56104E-01	-.29510E+01	.56104E-01	-.29510E+01	11.582	60.17	85.22
24600.00	-23.8	.56769E-01	-.29637E+01	.56769E-01	-.29637E+01	11.783	60.21	85.18
24800.00	-25.2	.55907E-01	-.29871E+01	.55907E-01	-.29871E+01	11.988	60.00	85.39
25000.00	-36.6	.51712E-01	-.31181E+01	.51712E-01	-.31181E+01	12.189	59.26	86.13
25200.00	-56.9	.27254E-01	.21424E+01	.18681E-01	.23906E+01	12.391	50.34	95.05
25400.00	-98.9	.13637E-01	.16686E+01	.93474E-02	.19169E+01	12.597	44.26	101.13
25600.00	-140.8	.93912E-02	.16489E+01	.64372E-02	.18972E+01	12.805	40.95	104.44
25800.00	-182.8	.67559E-02	.15510E+01	.46308E-02	.17993E+01	13.018	38.02	107.37
26000.00	-203.4	.83452E-02	.18302E+01	.57202E-02	.20785E+01	13.229	39.79	105.60
26200.00	-122.8	.17777E-01	.29274E+01	.12185E-01	-.31075E+01	13.441	46.29	99.10
26400.00	-147.1	.13684E-01	.20048E+01	.93795E-02	.22530E+01	13.657	43.95	101.44
26600.00	-171.4	.86718E-02	.20497E+01	.59441E-02	.22979E+01	13.875	39.93	105.46
26800.00	-135.7	.13566E-01	.27915E+01	.92988E-02	.30397E+01	14.095	43.75	101.64
27000.00	-191.7	.89612E-02	.17616E+01	.61425E-02	.20098E+01	14.318	40.08	105.31
27200.00	-179.4	.11855E-01	.25377E+01	.81260E-02	.27860E+01	14.547	42.45	102.94
27400.00	-163.7	.77466E-02	.24867E+01	.53099E-02	.27349E+01	14.774	38.69	106.70
27600.00	-213.1	.77114E-02	.21376E+01	.52858E-02	.23858E+01	15.003	38.59	106.80
27800.00	-250.7	.63031E-02	.20770E+01	.43205E-02	.23253E+01	15.237	36.77	108.62
28000.00	-276.8	.59706E-02	.21557E+01	.40925E-02	.24040E+01	15.470	36.24	109.15
28200.00	-304.8	.79709E-02	.26066E+01	.79709E-02	.26066E+01	15.707	41.97	103.42
28400.00	-326.6	.11526E-01	.28127E+01	.11526E-01	.28127E+01	15.946	45.11	100.28
28600.00	-340.1	.14183E-01	.28515E+01	.14183E-01	.28515E+01	16.187	46.85	98.54
28800.00	-355.2	.15929E-01	.28586E+01	.15929E-01	.28586E+01	16.428	47.80	97.59
29000.00	-372.0	.17266E-01	.28654E+01	.17266E-01	.28654E+01	16.684	48.44	96.95
29200.00	-375.4	.20393E-01	.29207E+01	.20393E-01	.29207E+01	16.941	49.82	95.57
29400.00	-358.9	.22641E-01	.29387E+01	.22641E-01	.29387E+01	17.199	50.67	94.72

29600.00	-360.2	.17763E-01	.24697E+01	.12176E-01	.27180E+01	17.461	45.23	100.16
29800.00	-356.6	.11842E-01	.23492E+01	.81173E-02	.25974E+01	17.725	41.65	103.74
30000.00	-352.9	.10303E-01	.24282E+01	.70619E-02	.26765E+01	18.000	40.38	105.01
30200.00	-409.3	.48429E-02	.18389E+01	.33195E-02	.20872E+01	18.280	33.76	111.63
30400.00	-405.7	.81564E-02	.24272E+01	.55908E-02	.26755E+01	18.552	38.23	107.16
30600.00	-406.4	.13785E-01	.29139E+01	.13785E-01	.29139E+01	18.831	46.02	99.37
30800.00	-424.9	.15103E-01	.29110E+01	.15103E-01	.29110E+01	19.108	46.75	98.64
31000.00	-437.5	.17637E-01	.29658E+01	.17637E-01	.29658E+01	19.383	48.04	97.35
31200.00	-448.1	.19509E-01	.29816E+01	.19509E-01	.29816E+01	19.658	48.86	96.53
31400.00	-456.7	.21809E-01	.30202E+01	.21809E-01	.30202E+01	19.935	49.78	95.61
31600.00	-459.2	.23330E-01	.30310E+01	.23330E-01	.30310E+01	20.219	50.31	95.08
31800.00	-461.8	.24786E-01	.30411E+01	.24786E-01	.30411E+01	20.509	50.78	94.61
32000.00	-464.4	.26024E-01	.30472E+01	.26024E-01	.30472E+01	20.793	51.15	94.24
32200.00	-467.0	.27110E-01	.30513E+01	.27110E-01	.30513E+01	21.083	51.45	93.94
32400.00	-483.0	.24299E-01	.28990E+01	.24299E-01	.28990E+01	21.382	50.44	94.95
32600.00	-492.2	.27830E-01	.29945E+01	.27830E-01	.29945E+01	21.671	51.57	93.82
32800.00	-490.0	.17844E-01	.23092E+01	.12231E-01	.25575E+01	21.963	44.37	101.02
33000.00	-487.0	.10583E-01	.23618E+01	.72538E-02	.26101E+01	22.259	39.78	105.61
33200.00	-484.0	.10253E-01	.24901E+01	.70281E-02	.27383E+01	22.556	39.46	105.93
33400.00	-481.0	.93677E-02	.25273E+01	.64211E-02	.27756E+01	22.858	38.62	106.77
33600.00	-477.9	.89150E-02	.26018E+01	.61107E-02	.28501E+01	23.165	38.14	107.25
33800.00	-486.6	.13038E-01	.30128E+01	.13038E-01	.30128E+01	23.470	44.67	100.72
34000.00	-506.9	.16906E-01	.30725E+01	.16906E-01	.30725E+01	23.777	46.87	98.52
34200.00	-515.4	.19460E-01	.30990E+01	.19460E-01	.30990E+01	24.087	48.05	97.35
34400.00	-523.9	.21253E-01	.31025E+01	.21253E-01	.31025E+01	24.412	48.76	96.63
34600.00	-530.4	.19207E-01	.28049E+01	.13165E-01	.30531E+01	24.742	44.55	100.84
34800.00	-530.9	.10767E-01	.22847E+01	.73800E-02	.25329E+01	25.070	39.47	105.92
35000.00	-531.5	.86496E-02	.25662E+01	.59289E-02	.28145E+01	25.394	37.52	107.87
35200.00	-532.1	.86171E-02	.25710E+01	.59066E-02	.28193E+01	25.719	37.44	107.95

35400.00	-529.5	.81962E-02	.26559E+01	.56181E-02	.29042E+01	26.052	36.95	108.44
35600.00	-527.1	.81033E-02	.27115E+01	.55544E-02	.29598E+01	26.379	36.81	108.58
35800.00	-525.8	.98853E-02	.28194E+01	.60404E-02	.28662E+01	26.727	37.49	107.90
36000.00	-528.4	.16204E-01	.28456E+01	.99017E-02	.28924E+01	27.069	41.73	103.66
36200.00	-530.9	.18553E-01	.27014E+01	.11337E-01	.27482E+01	27.407	42.86	102.53
36400.00	-533.5	.19348E-01	.25896E+01	.11822E-01	.26363E+01	27.745	43.17	102.22
36600.00	-536.1	.19463E-01	.25030E+01	.11893E-01	.25498E+01	28.097	43.18	102.21
36800.00	-538.6	.19194E-01	.24364E+01	.11729E-01	.24832E+01	28.453	43.01	102.38
37000.00	-521.6	.16678E-01	.28537E+01	.16678E-01	.28537E+01	28.806	46.02	99.37
37200.00	-525.0	.17671E-01	.30541E+01	.17671E-01	.30541E+01	29.157	46.48	98.91
37400.00	-528.4	.19355E-01	-.31317E+01	.19355E-01	-.31317E+01	29.510	47.22	98.17
37600.00	-531.9	.20922E-01	-.30813E+01	.20922E-01	-.30813E+01	29.869	47.85	97.54
37800.00	-517.1	.26615E-01	.30745E+01	.16263E-01	.31213E+01	30.237	45.62	99.77
38000.00	-512.1	.26217E-01	.27941E+01	.16020E-01	.28409E+01	30.607	45.44	99.95
38200.00	-516.1	.23695E-01	.25565E+01	.14479E-01	.26032E+01	30.979	44.52	100.87
38400.00	-525.1	.22495E-01	.24032E+01	.13746E-01	.24500E+01	31.360	44.02	101.37
38600.00	-542.4	.19490E-01	.21641E+01	.11910E-01	.22109E+01	31.744	42.73	102.66
38800.00	-569.4	.19279E-01	.22233E+01	.19279E-01	.22233E+01	32.133	46.87	98.52
39000.00	-573.6	.18124E-01	.26169E+01	.18124E-01	.26169E+01	32.529	46.29	99.10
39200.00	-577.8	.19172E-01	.27734E+01	.19172E-01	.27734E+01	32.924	46.73	98.66
39400.00	-549.9	.22825E-01	.28221E+01	.15646E-01	.30704E+01	33.314	44.92	100.47
39600.00	-500.3	.86163E-02	.28301E+01	.59060E-02	.30784E+01	33.709	36.41	108.98
39800.00	-467.5	.10286E-01	-.28503E+01	.70504E-02	-.26021E+01	34.110	37.91	107.48
40000.00	-464.9	.12820E-01	-.27125E+01	.12820E-01	-.27125E+01	34.513	43.06	102.33
40200.00	-467.8	.16334E-01	-.26283E+01	.16334E-01	-.26283E+01	34.924	45.12	100.27
40400.00	-470.7	.18970E-01	-.26236E+01	.18970E-01	-.26236E+01	35.331	46.38	99.01
40600.00	-473.6	.21022E-01	-.26387E+01	.21022E-01	-.26387E+01	35.742	47.23	98.16
40800.00	-476.5	.22709E-01	-.26589E+01	.22709E-01	-.26589E+01	36.161	47.85	97.54
41000.00	-479.5	.24138E-01	-.26806E+01	.24138E-01	-.26806E+01	36.584	48.34	97.05

41200.00	-478.1	.26013E-01	-.26595E+01	.26013E-01	-.26595E+01	37.001	48.95	96.44
41400.00	-476.7	.27315E-01	-.26586E+01	.27315E-01	-.26586E+01	37.429	49.33	96.06
41600.00	-475.4	.28446E-01	-.26610E+01	.28446E-01	-.26610E+01	37.854	49.64	95.75
41800.00	-474.0	.29451E-01	-.26649E+01	.29451E-01	-.26649E+01	38.283	49.90	95.49
42000.00	-473.6	.24631E-01	-.30076E+01	.16883E-01	-.27594E+01	38.713	45.03	100.36
42200.00	-473.9	.14484E-01	.28155E+01	.99278E-02	.30638E+01	39.153	40.37	105.02
42400.00	-474.2	.10807E-01	.29277E+01	.74074E-02	-.31072E+01	39.592	37.79	107.60
42600.00	-474.4	.99962E-02	.29261E+01	.68518E-02	-.31088E+01	40.033	37.07	108.32
42800.00	-474.7	.90377E-02	.29486E+01	.61948E-02	-.30863E+01	40.474	36.15	109.24
43000.00	-475.0	.85773E-02	.29811E+01	.58793E-02	-.30539E+01	40.918	35.66	109.73
43200.00	-475.3	.82490E-02	.30025E+01	.56542E-02	-.30324E+01	41.370	35.28	110.11
43400.00	-475.6	.80050E-02	.30227E+01	.54870E-02	-.30122E+01	41.818	34.98	110.41
43600.00	-475.9	.78234E-02	.30396E+01	.53626E-02	-.29953E+01	42.277	34.74	110.65
43800.00	-473.3	.80599E-02	.31154E+01	.55246E-02	-.29195E+01	42.733	34.96	110.43
44000.00	-462.2	.81053E-02	-.30090E+01	.55557E-02	-.27607E+01	43.203	34.97	110.42
44200.00	-450.2	.86204E-02	-.29027E+01	.59089E-02	-.26544E+01	43.675	35.46	109.93
44400.00	-437.2	.89364E-02	-.28186E+01	.61254E-02	-.25703E+01	44.156	35.74	109.65
44600.00	-437.5	.84127E-02	-.29897E+01	.57665E-02	-.27414E+01	44.636	35.17	110.22
44800.00	-433.8	.85747E-02	-.29154E+01	.58775E-02	-.26671E+01	45.123	35.30	110.09
45000.00	-418.1	.98609E-02	-.27268E+01	.60737E-02	-.24785E+01	45.601	35.55	109.84
45200.00	-418.5	.84711E-02	-.29240E+01	.58065E-02	-.26757E+01	46.092	35.12	110.27
45400.00	-425.5	.70369E-02	-.30998E+01	.48234E-02	-.28515E+01	46.578	33.47	111.92
45600.00	-452.5	.68037E-02	.28180E+01	.46636E-02	.30662E+01	47.061	33.14	112.25
45800.00	-489.5	.56022E-02	.24319E+01	.38400E-02	.26802E+01	47.542	31.41	113.98
46000.00	-529.9	.47198E-02	.22652E+01	.32351E-02	.25135E+01	48.022	29.89	115.51
46200.00	-536.2	.61546E-02	.25801E+01	.42186E-02	.28283E+01	48.509	32.15	113.24
46400.00	-508.6	.63192E-02	.31038E+01	.43315E-02	-.29311E+01	48.997	32.35	113.05
46600.00	-481.0	.76039E-02	-.28813E+01	.52121E-02	-.26330E+01	49.502	33.92	111.48
46800.00	-490.3	.68306E-02	.29794E+01	.46820E-02	-.30555E+01	50.012	32.95	112.44

47000.00	-499.5	.60995E-02	.29446E+01	.41809E-02	-.30903E+01	50.519	31.93	113.46
47200.00	-487.1	.69749E-02	-.30069E+01	.47809E-02	-.27587E+01	51.026	33.05	112.34
47400.00	-472.5	.74183E-02	-.29032E+01	.50849E-02	-.26550E+01	51.527	33.55	111.84
47600.00	-464.8	.10588E-01	-.25033E+01	.10588E-01	-.25033E+01	52.045	39.89	105.50
47800.00	-469.0	.14304E-01	-.24566E+01	.14304E-01	-.24566E+01	52.560	42.46	102.93
48000.00	-473.2	.16729E-01	-.24773E+01	.16729E-01	-.24773E+01	53.077	43.79	101.60
48200.00	-477.4	.18576E-01	-.25088E+01	.18576E-01	-.25088E+01	53.601	44.66	100.73
48400.00	-481.6	.20073E-01	-.25417E+01	.20073E-01	-.25417E+01	54.133	45.30	100.09
48600.00	-485.9	.21328E-01	-.25737E+01	.21328E-01	-.25737E+01	54.672	45.79	99.60
48800.00	-523.9	.19467E-01	-.29310E+01	.13344E-01	-.26827E+01	55.206	41.68	103.71
49000.00	-542.1	.11726E-01	.24653E+01	.80376E-02	.27135E+01	55.747	37.24	108.15
49200.00	-560.4	.71305E-02	.25131E+01	.48876E-02	.27613E+01	56.293	32.89	112.51
49400.00	-559.4	.82806E-02	.27917E+01	.56760E-02	.30399E+01	56.835	34.15	111.24
49600.00	-545.8	.73072E-02	.29994E+01	.50087E-02	-.30355E+01	57.386	33.03	112.36
49800.00	-538.9	.75413E-02	.30802E+01	.51692E-02	-.29547E+01	57.938	33.27	112.12
50000.00	-535.8	.69509E-02	.30608E+01	.47645E-02	-.29741E+01	58.488	32.52	112.87
50200.00	-544.2	.68220E-02	.29416E+01	.46761E-02	-.30933E+01	59.044	32.33	113.06
50400.00	-556.3	.61536E-02	.28169E+01	.42180E-02	.30651E+01	59.604	31.40	113.99
50600.00	-568.1	.62598E-02	.28045E+01	.42907E-02	.30527E+01	60.168	31.51	113.88
50800.00	-562.9	.64888E-02	.30162E+01	.44477E-02	-.30187E+01	60.737	31.79	113.60
51000.00	-547.7	.62678E-02	-.30613E+01	.42963E-02	-.28130E+01	61.312	31.45	113.94
51200.00	-547.5	.67368E-02	-.31389E+01	.46177E-02	-.28906E+01	61.883	32.05	113.34
51400.00	-547.3	.64555E-02	.31291E+01	.44249E-02	-.29058E+01	62.459	31.64	113.75
51600.00	-547.1	.64212E-02	.31408E+01	.44014E-02	-.28941E+01	63.040	31.56	113.83
51800.00	-574.2	.10582E-01	-.29091E+01	.10582E-01	-.29091E+01	63.641	39.15	106.24
52000.00	-585.2	.11940E-01	-.29123E+01	.11940E-01	-.29123E+01	64.243	40.16	105.23
52200.00	-589.8	.84068E-02	.27481E+01	.57624E-02	.29964E+01	64.842	33.80	111.59
52400.00	-562.1	.78770E-02	-.29239E+01	.53993E-02	-.26757E+01	65.445	33.20	112.19
52600.00	-550.5	.76233E-02	-.30599E+01	.52254E-02	-.28116E+01	66.068	32.89	112.51

52800.00	-550.8	.69808E-02	-.31102E+01	.47850E-02	-.28620E+01	66.680	32.09	113.30
53000.00	-551.2	.66578E-02	-.31169E+01	.45636E-02	-.28686E+01	67.298	31.64	113.75
53200.00	-551.6	.64807E-02	-.31169E+01	.44422E-02	-.28687E+01	67.916	31.38	114.01
53400.00	-551.9	.63608E-02	-.31130E+01	.43600E-02	-.28647E+01	68.539	31.18	114.21
53600.00	-552.3	.62785E-02	-.31079E+01	.43036E-02	-.28596E+01	69.152	31.04	114.35
53800.00	-561.3	.59005E-02	.30246E+01	.40445E-02	-.30103E+01	69.772	30.46	114.93
54000.00	-573.1	.55647E-02	.29382E+01	.38143E-02	-.30967E+01	70.391	29.92	115.47
54200.00	-573.5	.57237E-02	.30724E+01	.39233E-02	-.29625E+01	71.011	30.14	115.25
54400.00	-571.9	.59913E-02	.31302E+01	.41068E-02	-.29047E+01	71.650	30.50	114.89
54600.00	-564.3	.60340E-02	-.30252E+01	.41360E-02	-.27769E+01	72.290	30.53	114.86
54800.00	-556.7	.63213E-02	-.29506E+01	.43329E-02	-.27023E+01	72.930	30.90	114.49
55000.00	-535.1	.72965E-02	-.26513E+01	.50014E-02	-.24030E+01	73.570	32.12	113.27
55200.00	-541.0	.69970E-02	-.30257E+01	.45904E-02	-.27775E+01	74.202	31.34	114.05
55400.00	-546.9	.60005E-02	-.30678E+01	.41130E-02	-.28195E+01	74.837	30.36	115.03
55600.00	-549.2	.62957E-02	-.30385E+01	.43153E-02	-.27902E+01	75.483	30.74	114.65
55800.00	-541.1	.62499E-02	-.28948E+01	.42840E-02	-.26465E+01	76.136	30.65	114.74
56000.00	-529.2	.68740E-02	-.27521E+01	.47118E-02	-.25038E+01	76.791	31.44	113.95
56200.00	-517.2	.68867E-02	-.27053E+01	.47205E-02	-.24570E+01	77.444	31.43	113.96
56400.00	-515.5	.70053E-02	-.27980E+01	.48017E-02	-.25498E+01	78.100	31.55	113.85
56600.00	-513.9	.67364E-02	-.28272E+01	.45174E-02	-.25789E+01	78.768	31.17	114.22
56630.00	-513.6	.67268E-02	-.28281E+01	.46109E-02	-.25798E+01	79.437	31.16	114.23

FORM **NTIA-29**
(4-80)

U.S. DEPARTMENT OF COMMERCE
NAT'L. TELECOMMUNICATIONS AND INFORMATION ADMINISTRATION

BIBLIOGRAPHIC DATA SHEET

	1. PUBLICATION NO.	2. Gov't Accession No.	3. Recipient's Accession No.
	NTIA Report 82-114		

4. TITLE AND SUBTITLE

HF Ground Wave Propagation over Forested and Built-up Terrain

5. Publication Date
November 1982

6. Performing Organization Code

7. AUTHOR(S)
D. A. Hill

9. Project/Task/Work Unit No.
9104493

8. PERFORMING ORGANIZATION NAME AND ADDRESS
U.S. Department of Commerce
National Telecommunications and Information Administration
Institute for Telecommunication Sciences
325 Broadway, Boulder, CO 80303

10. Contract/Grant No.

11. Sponsoring Organization Name and Address

Defense Nuclear Agency
Washington, DC 20305

12. Type of Report and Period Covered
NTIA Report

13.

14. SUPPLEMENTARY NOTES

15. ABSTRACT *(A 200-word or less factual summary of most significant information. If document includes a significant bibliography or literature survey, mention it here.)*

An integral equation method is presented for computing the vertically polarized field strength over irregular terrain which is covered with forest, buildings, or snow. The terrain cover is modeled as an equivalent slab, and a general computer code, WAGSLAB, is developed. Numerous special cases are treated analytically, and comparisons are made with numerical results from WAGSLAB.

16. Key Words *(Alphabetical order, separated by semicolons)*

flat earth; HF ground wave propagation; irregular terrain; mixed path; lateral wave, slab model; spherical earth; vertical polarization

17. AVAILABILITY STATEMENT

☒ UNLIMITED.

☐ FOR OFFICIAL DISTRIBUTION.

18. Security Class. *(This report)*
Unclassified

20. Number of pages
100

19. Security Class. *(This page)*
Unclassified

21. Price:

☆U.S. GOVERNMENT PRINTING OFFICE:1983—677-389 / 93